AFRPL-TR-66-330

HALOGEN PASSIVATION STUDIES

Contract No. AF 04(611)-10932

W. A. Cannon, W. D. English, S. K. Asunmaa, S. M. Toy, and N. A. Tiner

Astropower Laboratory, Missile & Space Systems Division
A Division of Douglas Aircraft Company, Inc.

TECHNICAL REPORT AFRPL-TR-66-330

January 1967

Air Force Rocket Propulsion Laboratory
Research and Technology Division
Air Force Systems Command
Edwards Air Force Base, California

NOTICES

When Government drawings, specifications, or other data are used for any purpose other than in connection with a definitely related Government procurement operation, the United States Government thereby incurs no responsibility nor any obligation whatsoever; and the fact that the Government may have formulated, furnished, or in any way supplied the said drawings, specifications, or other data, is not to be regarded by implication or otherwise as in any manner licensing the holder or any other person or corporation, or conveying any rights or permission to manufacture, use, or sell any patented invention that may in any way be related thereto.

AFRPL-TR-66-330

HALOGEN PASSIVATION STUDIES

Contract No. AF 04(611)-10932

W. A. Cannon, W. D. English, S. K. Asunmaa, S. M. Toy, and N. A. Tiner

Astropower Laboratory, Missile & Space Systems Division
A Division of Douglas Aircraft Company, Inc.

TECHNICAL REPORT AFRPL-TR-66-330

January 1967

Air Force Rocket Propulsion Laboratory
Research and Technology Division
Air Force Systems Command
Edwards Air Force Base, California

FOREWORD

This report was prepared by Astropower Laboratory, Advance Systems and Technology, Missile and Space Systems Division, Douglas Aircraft Company under Air Force Contract AF04(611)-10932. The contract was administered by the Air Force Rocket Propulsion Laboratory, Research and Technology Division, Air Force Systems Command, Edwards Air Force Base, California, with Lt. Ralph Fargnoli as Project Engineer.

This report covers work done on the halogen passivation studies during the period from 1 November 1965 to 31 October 1966. The report was prepared by W. A. Cannon and W. D. English, with S. K. Asunmaa and S. M. Toy contributing, under the supervision of N. A. Tiner. In addition to the authors, A. Pinkul, S. W. Sanders and A. Muller have made contributions to the work.

Manuscript released by authors November 1966 for publication as an AFRPL Technical Report.

This technical report has been reviewed and is approved.

W. H. Ebelke, Colonel, USAF
Chief, Propellant Division

ABSTRACT

This report includes data on the nature of passivation of metal surfaces with fluorine and fluorine compounds, the composition of passive films formed, and the deleterious effect of atmospheric moisture on passive surfaces. Fluorination reactions reach completion on stainless steel, nickel and aluminum alloy surfaces very rapidly. The surface films formed range from 5 to 20 Å in thickness and grow at the expense of the oxide films. The apparent film thickness on copper and Monel surfaces continues to increase slowly over an extended period of time. Exposure of passive films to a humid atmosphere produces hydrated metal fluorides which cause secondary fluorination reactions upon reexposure of the surfaces to fluorine. The passive films formed by exposure to chlorine trifluoride and chlorine pentafluoride were comparable in thickness to the films formed by fluorine gas, contained metal chloride species, and were less resistant to humid air attack. Fluorine gas appears to be the most effective agent for passivation of metals. Adequate passive films are formed at all pressures within 0.1 to 1.4 atmosphere for a period of 15 to 30 minutes. Stepwise increase in concentration is unnecessary for passivation of metals, and slight deformation of metal surfaces does not destroy the passive films.

TABLE OF CONTENTS

LIST OF ILLUSTRATIONS

LIST OF TABLES

SECTION I

INTRODUCTION

A propellant system is usually thoroughly passivated before it is used with fluorine containing oxidizers. The passivation procedures employed in general involve lengthy (2 to 4 hours) fluorination of metal surfaces by passing a gas, such as fluorine or chlorine trifluoride at low concentrations, over the metal until the heat of reaction subsides. The resultant passivation is not permanent. Each time a passivated system is exposed to the atmosphere, mechanical shock or flexing, or is cleaned, it is repassivated.

There is no definitive knowledge concerning the nature of passivation. The procedures used are developed by rule-of-thumb. It is generally known that when a system is suddenly exposed to high concentrations of fluorine, portions of the system may ignite; and that pre-exposure to low concentrations of fluorine develops thin passive fluoride films on the metal surface and renders this ignition much less likely.

The major objectives of the present program are to obtain information on the nature of passivation of metal surfaces by fluorine-containing oxidizers, the conditions of destruction of passive surfaces, and to improve the present passivation procedures by utilization of the information developed. The oxidizers considered include fluorine (F_2), chlorine trifluoride (ClF_3), chlorine pentafluoride (ClF_5) and bromine pentafluoride (BrF_5). The metal surfaces include technically important alloys used at cryogenic temperatures for tankage and plumbing hardware in present propellant systems: namely, stainless steels, aluminum alloys, copper and nickel alloys. These objectives constitute a part of the technological goals of the Air Force Rocket Propulsion Laboratory for developing the technology of fluorine oxidizers to the point where these oxidizers can be effectively, efficiently and safely used in rocket propulsion systems.

SECTION II

SURVEY OF PREVIOUS WORK

1. GENERAL CHARACTERISTICS OF GAS-SOLID REACTIONS

All metals react when exposed to gaseous fluorine at room temperature. The reaction usually results in formation of a metal fluoride film on the metal surface. The rate of reaction is largely determined by the extent to which films formed are protective.

The majority of investigations of the manner and rate of growth of protective films on metals have dealt with protective oxide coatings. A great deal of theory and empirical observations have been accumulated over the years for various oxygen-metal systems. Most of this information is applicable to fluorine gas-metal interactions and is briefly reviewed.

In general, the crystal structure of a surface layer tends to conform to the structure of the underlying metal. If the volume ratio of the compound is appreciably different from the basis metal, stresses will be developed in the surface layer. This is particularly true at low temperatures where the lack of lattice mobility impedes recrystallization. The stresses can lead to the formation of pores, cracks, and blisters which can have a profound effect on reaction kinetics, or in the extreme case can result in complete failure of the protective qualities of the film.

The first stage of a reaction between a metal surface and a gas is the formation of a chemisorbed monolayer on the surface. Measurements at low pressures have shown that rates of chemisorption are logarithmic. Landsberg[1] thus suggested that the rate controlling step in thin film growth is chemisorption.

Nucleation phenomena have been considered as playing a part in film growth. In general, the formation of a solid solution of gas in solid is followed by a rapid growth of product film.[2] This implies an induction period followed by a rapid acceleration in reaction rate. Finally as the nuclei coalesce, further reaction becomes controlled by one of the rate laws discussed below. Such a stepwise growth has been observed experimentally.

The effect of gas pressure on the reaction rate is of great importance for determining the reaction mechanism. If, for example, the rate determining step involves the dissociation of a bimolecular gas, the oxidation rate would be expected to increase as the square root of the gas pressure. If a diffusion process in a film controls the overall reactions, various oxidation rate-pressure relationships may be found. If a parabolic rate law applies, the pressure dependance of reaction rate is usually smaller than the square root relationship.

2. KINETIC LAWS OF GAS-SOLID REACTIONS

A number of empirical relations have been recognized in the kinetic study of gas-solid reactions. Usually their relations are expressed in terms of weight increase as a function of time or, film thickness as a function of time. For convenience, they will be expressed here in terms of weight increase, Δm, and time, t.

The linear relationship

$$\Delta m = K_L t \qquad (1)$$

where K_L is the rate constant

states that the weight increase is a linear function of time. Linear oxidation kinetics are frequently observed for metals when the volume ratio of the oxide is either appreciably less than unity or substantially greater than unity. In the former case the oxide is unable to form a coherent surface film and thus fresh metal is continuously exposed. In the case of high volume ratios, porosity of the films develops due to splitting and cracking set up by development of stresses. The existence of linear relations does not, however, require the absence of a non-porous layer. A thin non-porous layer may exist next to the metal. When this layer reaches a critical thickness, stresses may cause cracking. An experimentally determined linear reaction rate may then be controlled by diffusion across a non-porous layer of essentially constant thickness.

The parabolic relationship

$$(\Delta m)^2 = K_p t \qquad (2)$$

has been found to express reaction rates for practically all metal-oxygen systems, at least within certain temperature ranges. The parabolic reaction rate implies that the rate of increase of film thickness is inversely proportional to the film thickness. Parabolic kinetics are expected to occur whenever the reaction product forms an adherent, non-porous film across which one or both of the reactants must diffuse.

Some experimental reaction rate data have been found to agree with a cubic relationship

$$(\Delta m)^3 = K_C t \qquad (3)$$

although such examples are fairly rare.

The logarithmic (or exponential) rate law is frequently encountered in low-temperature oxidation reactions. The integral form of equation

expressing this is

$$\Delta m = K_E \log (at + t_o) \qquad (4)$$

which contains three constants, K_E, a and t_o. The alternative inverse logarithmic form is

$$\frac{1}{\Delta m} = A - K_I \log t \qquad (5)$$

where A and K_I are constants.

The logarithmic reaction rate law describes a reaction which decreases very rapidly with time. Such rates are generally applicable to formation of protective films which are very thin and formed at low temperature. Thus, the formation of oxide films on metals at room temperature frequently follow exponential rate laws. One possible explanation of the logarithmic rate was advanced by Evans[3] who postulated the formation of cavities in the oxide film due to compressive stresses. Such cavities block the diffusion paths in the film which leads to a rapid decrease in reaction rate. This explanation assumes that diffusion of metal ions through the coating is the rate controlling step for the reaction.

In the mechanism proposed by Cabrera and Mott[4] the electrons are supposed to pass from the metal to the adsorbed oxygen on the surface by a quantum mechanical tunneling effect, thereby producing a strong electric field across the oxide film which is responsible for pulling metal ions through the film. A certain interpretation of the Cabrera-Mott theory leads to exponential oxidation kinetics for the tunneling mechanism.

3. FLUORINE-METAL REACTIONS

Although there is an enormous amount of literature on reactions of oxygen with metals, there are very few investigations reported concerning fluorine-metal reactions. In view of the fact that most metals, and this applies to all of the metals under investigation in this contract, have naturally-occurring oxide films, it is appropriate to also review literature data which involve reactions of fluorine with metallic oxides.

Brown, Crabtree, and Duncan[5] have investigated the kinetics of reaction of fluorine with copper metal freshly reduced in hydrogen before exposure to the gaseous fluorine. They found the reaction rate to be independent of pressure over the range from 6 to 60 torr at 100°C. The reaction rate in the temperature range from 25°C to 300°C was logarithmic. There was some deviation at higher temperatures which could have been the onset of a parabolic law. The calculated film thicknesses ranged from about two molecular layers (~10Å) for 5 hours exposure at room temperature to 35 molecular layer for 5 hours exposure at 200°C. The authors concluded that no single mechanism could explain all the observations. The quantum mechanical tunneling

effect could explain the growth rate for the thin film region below about 10 molecular layers, say 50 Å, but at greater film thickness the tunneling effect becomes inefficient. But their data showed that the logarithmic growth law was obeyed up to much greater film thickness. The Evans mechanical breakdown mechanism[6] leads to a logarithmic rate and could explain in part the mechanism for thick films. It is difficult to see, however, how the same kinetic law can hold no matter whether the film is one or two molecular layers thick or up to 35 layers thick. Evidently a logarithmic expression holds for corrosion kinetics in which more than one process is occurring.

O'Donnell and Spatkowski[7] have investigated the reaction of fluorine and copper at 450°C and at pressures from 10 to 133 torr. The reaction was found to be pressure dependent and followed a logarithmic rate law. The reaction did not seem to be entirely diffusion controlled and fluorine was thought to be the migrating species in the reaction.

Miscellaneous metal-fluorine reactions were investigated by Haendler, et al[8]. Reaction products were identified but no rate data were determined.

Air Products and Chemicals, Inc.[9] have conducted an investigation of reactions between fluorine and various metal powders at room temperature and 185°F. Fluoride film thickness as a function of time of exposure was reported assuming that the reaction takes place between fluorine and metal to form the normal metal fluoride. Surface areas of the powders were only approximate so relative film thicknesses may not be exact. The data show rates of reaction generally logarithmic in character, the rate of film growth virtually ceasing after a few hours time for some alloy powders. The effect of moisture on fluoride films was also investigated by measuring additional reaction with fluorine after exposure of passivated powders to atmosphere moisture.

The fluorination of iron was studied by O'Donnell[10] at temperatures from 225°C to 525°C and at pressures ranging from 20 to 200 torr fluorine pressure. In all ranges the reaction followed a logarithmic rate law and was dependent on the square root of the gas pressure. The author concluded that fluorine gas passed through pores in the film. As the film grows the blocking of pores leads to a rapid decrease in reaction rate, hence a logarithmic rate law is observed.

Jarry, Fischer and Gunther[11] investigated the mechanism of the reaction of fluorine with nickel at about 600 - 700°C. On the basis of the metallographic examination of fluoride scales growing on the nickel and from separate radioautographic data, it was proven that fluorine is the migrating species in the reaction. This is in sharp contrast to the growth of oxide films on nickel where it has been shown that nickel ions migrate through the scale to the gas-solid interface to react with oxygen.

Relatively few investigations have been reported of the reaction of fluorine with metal oxides. Such investigations should be of great significance

for a better understanding of passivation in view of the ubiquitous oxide films on technical alloys. It is one matter to understand the reaction mechanism and kinetic laws for interaction of fluorine with a freshly reduced metal surface but quite another set of circumstances prevail for the reaction with a commercial alloy. The key to understanding the reaction mechanisms on the latter may well be in a detailed study of reaction of fluorine with bulk metal oxides. One must proceed cautiously in this direction, though, because of the tendency of oxide films to be pseudomorphic with the underlying solid.

Haendler et al[8] studied the reaction of fluorine with oxides of copper, tin, titanium, zirconium, and vanadium. Copper (I) oxide reacted between 150° and 300°C as follows:

$$Cu_2O + F_2 \longrightarrow CuF_2 + CuO \qquad (6)$$

A higher temperature (above 300°C) was required for the CuO to react to form additional copper fluoride.

Ritter and Smith[12] investigated the reaction of fluorine with copper (II) oxide. A fairly high surface area oxide powder comprised of spherical particles was reacted with fluorine starting at room temperature and increasing to 100°C over a period of 3 or 4 hours. The initial reaction was slow until the fluoride film thickness reached about 10 or 15 Å at which time the reaction rate accelerated, then decreased again. Most of the kinetic data was obtained during this final phase of reaction. The authors conclude that the film grows slowly at first until the stresses developed in the distorted lattice are sufficient to rupture the initial film. This occurs at a film thickness of 10 - 15 Å and leads to an acceleration of reaction rate. At higher temperature the film grows with normal lattice parameters and obeys a parabolic rate law. It is further concluded that the reaction, at the latter stage, is fluorine diffusion controlled. The reaction rate was directly proportional to the square root of fluorine pressure.

Very few quantitative investigations have been reported in the literature involving reactions of halogen fluorides with metals or metal oxides. Emeleus and Woolf[13] demonstrated that bromine trifluoride reacted with several metal oxides, including copper (II) oxide, to quantitatively release oxygen forming the metal fluoride in the process.

The kinetics of the reaction between nickel oxide and chlorine trifluoride was investigated by Farrar and Smith[14]. It was found that the initial thin film of fluoride increased in thickness due to a diffusion process as indicated by a parabolic reaction rate. After the fluoride film reached a critical thickness, a recrystallization occurred which led to a major change in corrosion mechanism. Now a linear kinetic law took over in which the chlorine trifluoride migrated down grain boundary paths and the rate controlling reaction was diffusion across a transition zone of relatively constant thickness. The nickel fluoride film contained a large excess of chlorine trifluoride.

Farrar and Smith also found that of the two most likely reactions between nickel oxide and chlorine trifluoride, namely:

$$3NiO + 2ClF_3 \longrightarrow 3NiF_2 + Cl_2 + 3/2O_2 \qquad (7)$$

and

$$NiO + ClF_3 \longrightarrow NiF_2 + ClF + 1/2O_2 ; \qquad (8)$$

the former appears to predominate as evidenced by a large proportion of chlorine in the reaction product. Only very small amounts of ClF were found by mass spectrographic and infrared analyses.

Thus it appears that in fluorination reactions of solids, the species which diffuses to the reaction site is the fluorinating agent. This may have some relation to particle size of the reactive species. The oxide ion, O_2^{-2}, is about 3.2 Å in diameter while the fluoride ion is about 2.7 Å. Other considerations might suggest diffusion of neutral species. Since F_2 dissociates easily (bond energy = 39 Kcal/mole), it would probably migrate in atomic form; its atomic radius is 0.7 Å. The much more stable oxygen molecule (bond energy = 117 Kcal/mole) does not dissociate readily; the molecular radius is about 1.4 Å.

The formation of the fluoride ion would depend on a supply of electrons from the metal surface under the oxide film. Quantum mechanical tunneling would provide a path for these to reach the surface, then the potential gradient from positive metal to negative fluoride will attract the fluoride ions into the film until they react with a metal oxide bond and release oxygen.

SECTION III

MATERIALS AND EXPERIMENTAL METHODS

1. MATERIALS

The fluorinating agents considered in this program included fluorine (F_2), chlorine trifluoride (ClF_3), chlorine pentafluoride (ClF_5), and bromine pentafluoride (BrF_5).

Fluorine gas was obtained from Allied Chemical, chlorine pentafluoride was supplied by the Air Force, and the other interhalogens were obtained from the Matheson Company. Fluorine, chlorine pentafluoride, and chlorine trifluoride were passed over sodium fluoride pellets to remove HF. Bromine pentafluoride was subjected to a double batch distillation before use, while bromine trifluoride was used without further purification.

The sheet stock and powdered metals and alloys which were obtained for use in this program included technically important alloys used at cryogenic temperatures for tankage and plumbing hardware in present propellant systems. They are listed and described in Tables I and II.

2. EVALUATION OF GAS-SOLID REACTIONS

Of the various techniques employed for evaluating the extent of a gas-solid reaction, the two most generally applicable are the manometric and gravimetric methods.[15] The former experimental technique involves a measurement of the change in pressure during the course of the reaction taking place in a closed, isothermal system. In principle it is applicable to any reaction in which a net change in pressure occurs. For example, if a reaction takes place between a metal and fluorine as follows

$$M + F_2 \rightarrow MF_2 \tag{9}$$

there will be a change in pressure directly related to the number of moles of reactants consumed. However if a reaction were to take place between a metal oxide and fluorine as follows

$$MO + F_2 \rightarrow MF_2 + \frac{1}{2} O_2 \tag{10}$$

There is still a net change in pressure, but a calculation of the moles of fluorine reacted must take into account that one-half mole of gaseous reaction product is produced per mole of fluorine consumed. One must therefore know the nature of the reaction to convert pressure changes to quantitative rate data

TABLE I. SHEET STOCK FOR HALOGEN PASSIVATION STUDIES

Material	Supplier & Identification	Condition & Thickness	Composition
Al alloy 2014	Kaiser Aluminum	T_6 - 0.040	Cu 5.0-3.9, Mg 0.8-0.2, Mn 1.20-0.40, Fe 1.0 max, Si 1.20-0.50
Al alloy 2024	Alcoa Lot #418-731	T_{351}-0.040	Cu 4.9-3.8, Mg 1.8-1.2, Mn 0.9-0.3, Si 0.50 max, Fe 0.50 max, Cr 0.10 max, Zn 0.25 max
Al alloy 6061	Alcoa Lot # 703-771	T_6 - 0.040	Cu 0.4-0.15, Mg 1.2-0.8, Mn 0.15 max, Si 0.8-0.4, Fe 0.7 max, Cr 0.35-0.15, Zn 0.25 max
St. Steel 316	Republic Steel Heat #49298	Annealed - 0.025	0.06 C, 17.04 Cr, 13.12 Ni, 2.5 Mo, 1.52 Mn, 0.27 Si, 0.26 Cu
St. Steel 304	Republic Steel	Annealed - 0.020	0.063 C, 1.80 Mn, 0.022 P, 0.007 S, 0.69 Si, 18.23 Cr, 8.89 Ni
St. Steel 347	Republic Steel Heat #49088	Annealed - 0.025	0.07 C, 17.43 Cr, 10.9 Ni, 1.86 Mn, 0.64 Si, 2.34 Mo, 0.37 Cu, 0.75 (Cb + Ta)
AM 350	Allegheny Ludlum Steel Heat #89324	Annealed - 0.025	0.086 C, 16.51 Cr, 4.34 Ni, 2.72 Mo, 0.82 Mn, 0.30 Si, 0.09 N_2
AM 355	Alleheny Ludlum Steel	Annealed - 0.025	0.14 C, 15.53 Cr, 4.45 Ni, 2.75 Mo, 0.85 Mn, 0.27 Si, 0.12 N_2
Nickel 200	International Nickel Heat N9385A	Annealed - 0.025	99.55 Ni, 0.07 C, 0.26 Mn, 0.05 Fe, 0.03 Si, 0.01 Cu

(Continued)

TABLE I. SHEET STOCK FOR HALOGEN PASSIVATION STUDIES (CONTINUED)

Material	Supplier & Identification	Condition & Thickness	Composition
Monel 400	International Nickel Heat N9846	Annealed - 0.025	65.5 Ni, 31.7 Cu, 0.11 C, 0.92 Mn, 1.54 Fe, 0.16 Si
Inconel X	International Nickel	Annealed - 0.025	0.07 C, 0.05 Mn, 0.25 Si, 0.90 Cb + Ta, 2.62 Ti, 6.45 Fe, 15.00 Cr, Balance Ni
Copper	American Brass	Annealed - 0.037	99.46 Cu, 0.01 Fe
Nickel 211	Wilbur B. Driver	Annealed - 0.003	95.2 Ni, 4.5 Mn, 1 Ca, 0.05 Cu, 0.15 Fe, 0.05 Si (Nominal)

TABLE II. POWDERS FOR HALOGEN PASSIVATION STUDIES

Material	Supplier & Identification	Nominal Mesh Size	Composition
St. Steel 304	Plasmadyne Permalloy 213-F SO #5-4766 Lot #Q15415	-325/450	C 0.08 max, Mn 2 max, Si 1 max, P 0.04 max, S 0.030 max, Cr 18-20, Ni 8-11, (nominal)
St. Steel 316	Plasmadyne Plasmalloy #215-F SO #5-4766 Lot #Q10495	-325/450	C 0.08 max, Mn 2 max, Si 1 max, P 0.04 max, S 0.03 max, Cr 16, Ni 10-14, Mo 2-3 (nominal)
St. Steel 347L	Metals Disintegrating Corp. #N-2355	-325	C 0.03 max, Cr 17-19, Ni 9-12, Cb 10xC (nominal)
Nickel 200 A	Plasmadyne Plasmalloy 112-F SO #5-4657 Lot #M12308	-325/450	Ni 99.5, C 0.06, Mn 0.75, Fe 0.15, S 0.005, Si 0.05, Cu 0.05 (nominal)
Monel 400	Plasmadyne Permalloy 206-F Lot #Q-10435	-325/450	Ni 66.0, C 0.12, Mn 0.90, Fe 1.35, S 0.005, Si 0.15, Cu 31.5 (nominal)
Copper	Metals Disintegrating Corp. MD 301 Lot #3137	Atomized Powder	99.9% Cu
Al 6061	Reynolds Metals LS-701 Atomized Powder	-100/325	Mg 0.8-1.2, Si 0.4-0.8, Cr 0.15-0.35, Cu 0.15-0.40 (nominal)
Al 2014	Reynolds Metals LS 863 Atomized Powder	-100/325	Cu 3.9-5.0, Si 0.5-1.2, Mn 0.4-1.2, Mg 0.2-0.8 (nominal)
Al 2024	Reynolds Metals	-100/325	Cu 3.8-4.9, Mn 0.3-0.9, Mg 1.2-1.8 (nominal)
AM 350	Hoeganes Sponge Iron Co.	-325	C 0.10, Mn 0.80, Si 0.25, Cr 16.5, Ni 4.3, Mo 2.75, N 0.10, Fe balance (nominal)

The main disadvantages of the manometric method are that initial reactant gas may become contaminated with byproduct gas and that there will be a pressure change during the course of the reaction. The effect of the decreasing partial pressure of the reactant gas may have a profound effect on the reaction rate, particularly for those reactions which are pressure dependent. Some of these problems can be overcome by incrementally restoring the initial pressure as the reaction proceeds or operating under conditions where the net pressure change is a very small part of the total pressure.

The gravimetric method requires the measurement of the weight change of a solid during the course of a reaction. If the films formed are extremely thin, then the weight changes taking place may be very small, requiring the use of extremely sensitive microbalances. If one uses a metal powder with large surface to weight ratio then the weight changes may be great enough so that ordinary analytical balance weighing will suffice. However, the use of powders is open to the criticism that the surfaces may not be representative of bulk metals and due to the large surface to volume ratio the reaction may not be isothermal.

Preliminary investigations demonstrated that passive films formed on metals by exposure to fluorine or halogen fluorides are extremely thin. It was calculated that it would be very difficult to determine by conventional analytical weighing techniques, the uptake of gas or increase in weight of a bulk metal specimen of reasonable proportions. Powdered metal specimens were used therefore in all kinetic studies.

a. Manometric Method

A manometric system, or as it will be referred to here, a constant volume system, was constructed for determining rates of fluoride film formation in metal powders exposed to fluorine gas. The essential parts of the system are depicted schematically in Figure 1. The necessary manometer shown to the right of the drawing is included only for calibration of the sensitive gauge and is valved off during all routine operations in the system.

The volumes of the ballast chamber and sample chamber are approximately equal – 150 ml each – therefore if the ballast chamber is initially pressurized with gas to about two atmospheres, the final pressure after opening the valves to the evacuated sample chamber will be approximately one atmosphere. The principle of operation is the determination of the change in pressure of fluorine in a constant, known volume as a function of time, as the fluorine reacts with a metal powder contained in the sample chamber.

The procedure is outlined as follows:

1. The apparatus is first passivated without a sample being present.

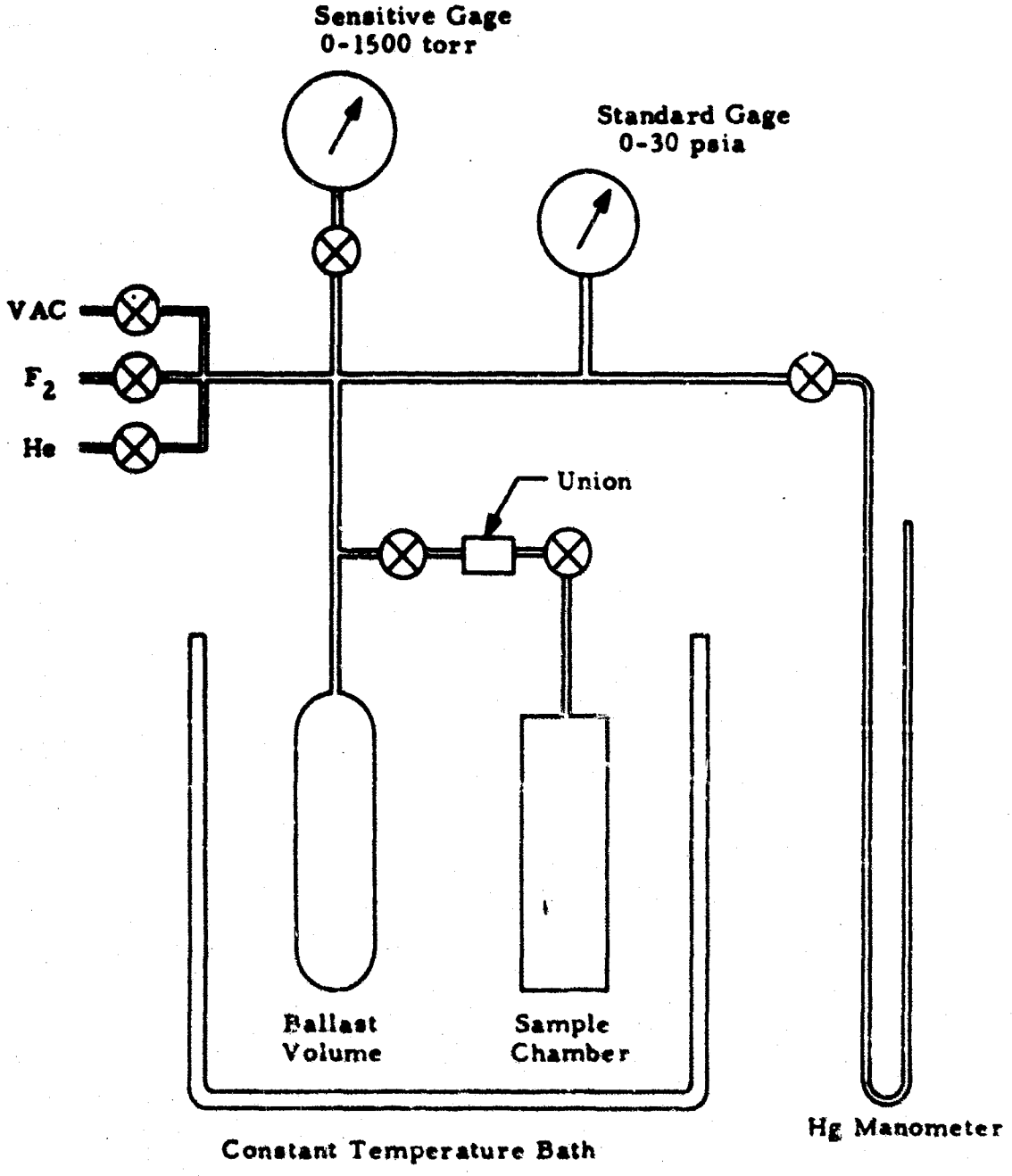

Figure 1. Constant Volume Apparatus for Measuring Reaction Rates of Fluorine with Metal Powders

2. The entire system is purged and evacuated.

3. A metal powder sample of known surface area is weighed into the sample chamber, after which the system is again evacuated.

4. Helium gas is introduced into the system, except the sample chamber, at about two atmospheres pressure. The valves to the sample chamber are opened and the gas expanded into the entire system. If the initial and final pressure is measured accurately with the sensitive pressure gauge, this step serves to calibrate the volume of the sample chamber, and to indicate the "zero time" pressure for the fluorine gas.

5. The system is again evacuated.

6. Fluorine gas is admitted and step 4 repeated.

7. Pressure in the system is measured as a function of time using the sensitive pressure gauge. (This gauge is sensitive to $\pm$ 1 torr.)

The weight of fluorine, W_F, removed from the gas phase by virtue of reaction with the metal powder, can be computed at any specific reaction time by

$$W_F = 38 \frac{\Delta P V_T}{RT} \qquad (11)$$

where ΔP is the total change in pressure at the given time and V_T is the total system volume, exclusive of the volume of the powder. The use of this expression requires the assumption that the reaction takes place exclusively between fluorine and metal without the formation of any volatile reaction products (i.e., reaction equation 9). The probable consequence of this assumption will be discussed later.

The mean film thickness can be related to W_F as follows:

$$d = \frac{X \cdot W_F}{A\rho} 10^8 \qquad (12)$$

where

d = film thickness in Angstrom units

X = ratio of molecular weights of metal fluoride and fluorine

A = total area of powder specimen in square centimeters

ρ = density of metal fluoride in g/ml.

b. Gravimetric Method

The volumetric method for determining rate of reaction of fluorine with metal powders cannot be used with halogen fluorides because the

reaction does not necessarily lead to a net change of pressure in the gas phase. Therefore, a gravimetric method was used for these oxidizers. The flow system is shown schematically in Figure 2.

The halogen fluoride vapor is passed slowly through a glass U-tube which contains a quantity of the metal powder under investigation. The weight change of the tube is determined for various periods of time of exposure from which a plot of mean film thickness as a function of time can be made.

In the system described, four reaction tubes are manifolded in parallel to cover a range of exposure times. Each tube is detachable from the system, and the flow of halogen fluoride through a given tube can be interrupted at any time and the tube purged with nitrogen to arrest further reaction. The detail of the glass reaction tubes is given in Figure 3. The weight gain of the tube is related to the film thickness by equation 12 above.

3. ELECTROCHEMICAL MEASUREMENTS

a. Electrode Polarization

Studies on the anodic polarization of nickel in bromine trifluoride have been previously carried out in this Laboratory.[16] This method of investigation has now been expanded and applied to this contract. The experimental approach involves the study of the anodic polarization behavior of test electrodes in bromine trifluoride. The electrodes under investigation are subjected to a variety of passivation treatments and environmental effects. The ultimate aim was to define the relationship between the anodic behavior and the nature of the passive films.

Aside from the reactivity of bromine trifluoride, the experimental methods are handicapped by a lack of any suitable reference electrode compatible with this material, and by the fact that it is a passivating medium. Therefore, passivation by exposure to the bromine trifluoride may be superimposed on the passivation produced by exposures to other passivating gases. If these experimental difficulties can be overcome, or compensated for, the electrochemical approach may prove to be a very valuable indication of the quality of passive films.

The polarization cell used in the control experiment with pure nickel electrodes is shown in Figure 4. The working electrode and platinum counter electrode (10 x 10 mm in size) are disposed 5 mm apart. A platinum wire reference electrode is spaced 1 mm away from the working electrode. The cell is constructed of Pyrex glass and requires approximately 20 ml of bromine trifluoride to fill it above the level of the top of the electrodes. The cell is filled by suction from the electrolyte reservoir which communicates with the cell by way of the Teflon plug stopcock. The cell can also be drained when desired by opening the stopcock and allowing the electrolyte to flow back to the reservoir.

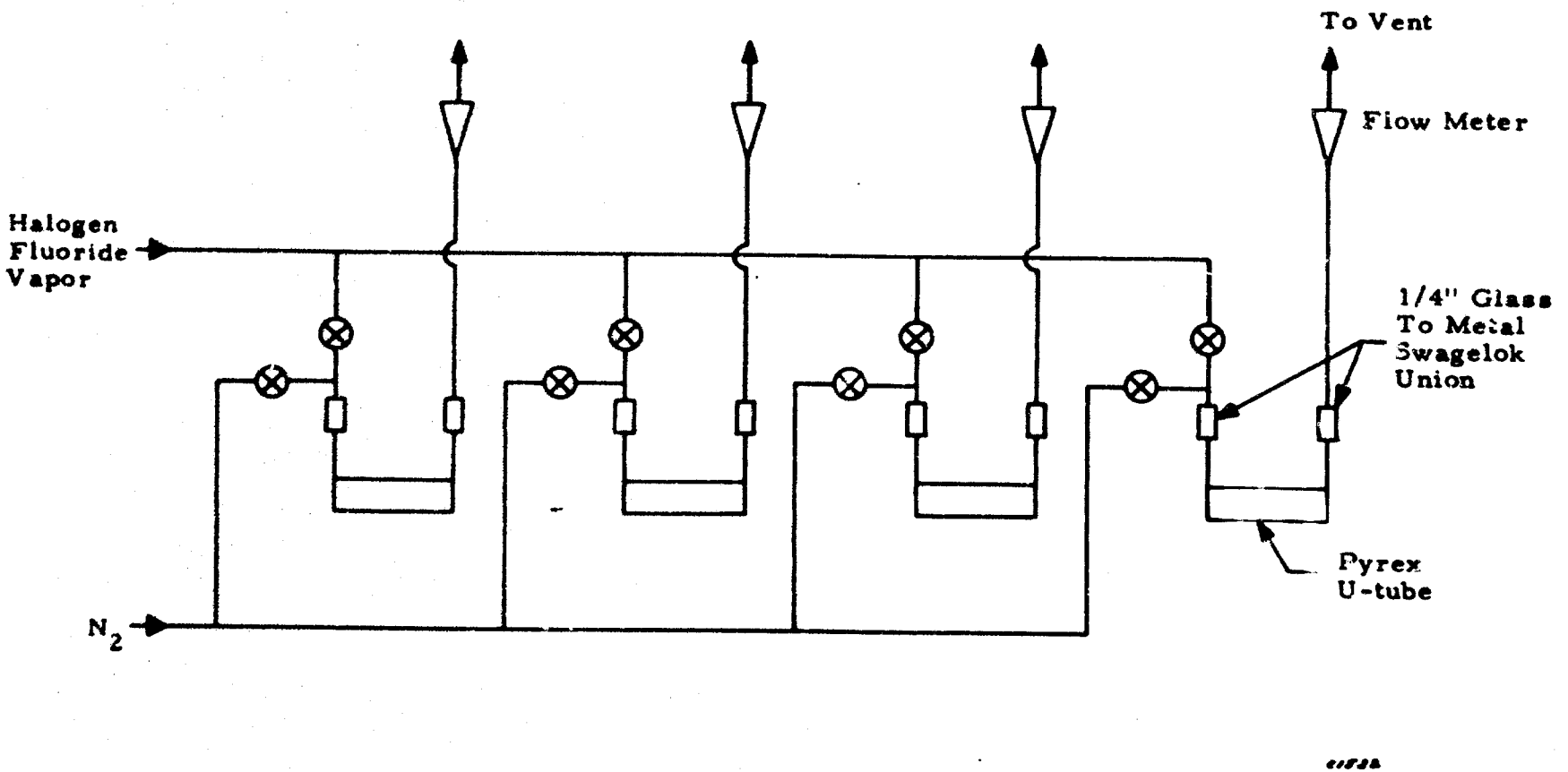

Figure 2. Apparatus for Gravimetric Determination of Rate of Reaction of Halogen Fluorides with Metal Powders

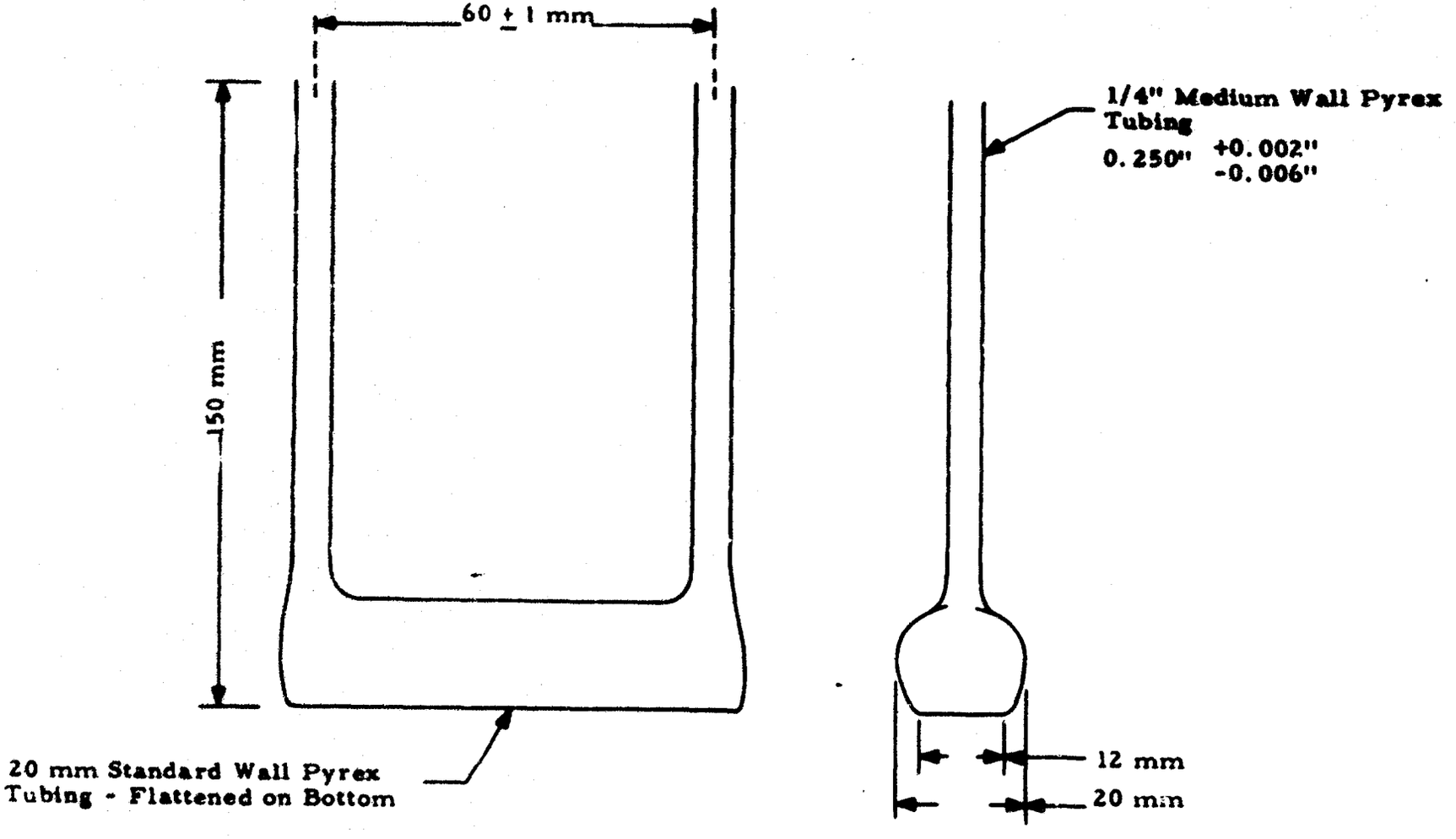

Figure 3. Detail of U-Tubes for Gravimetric Apparatus

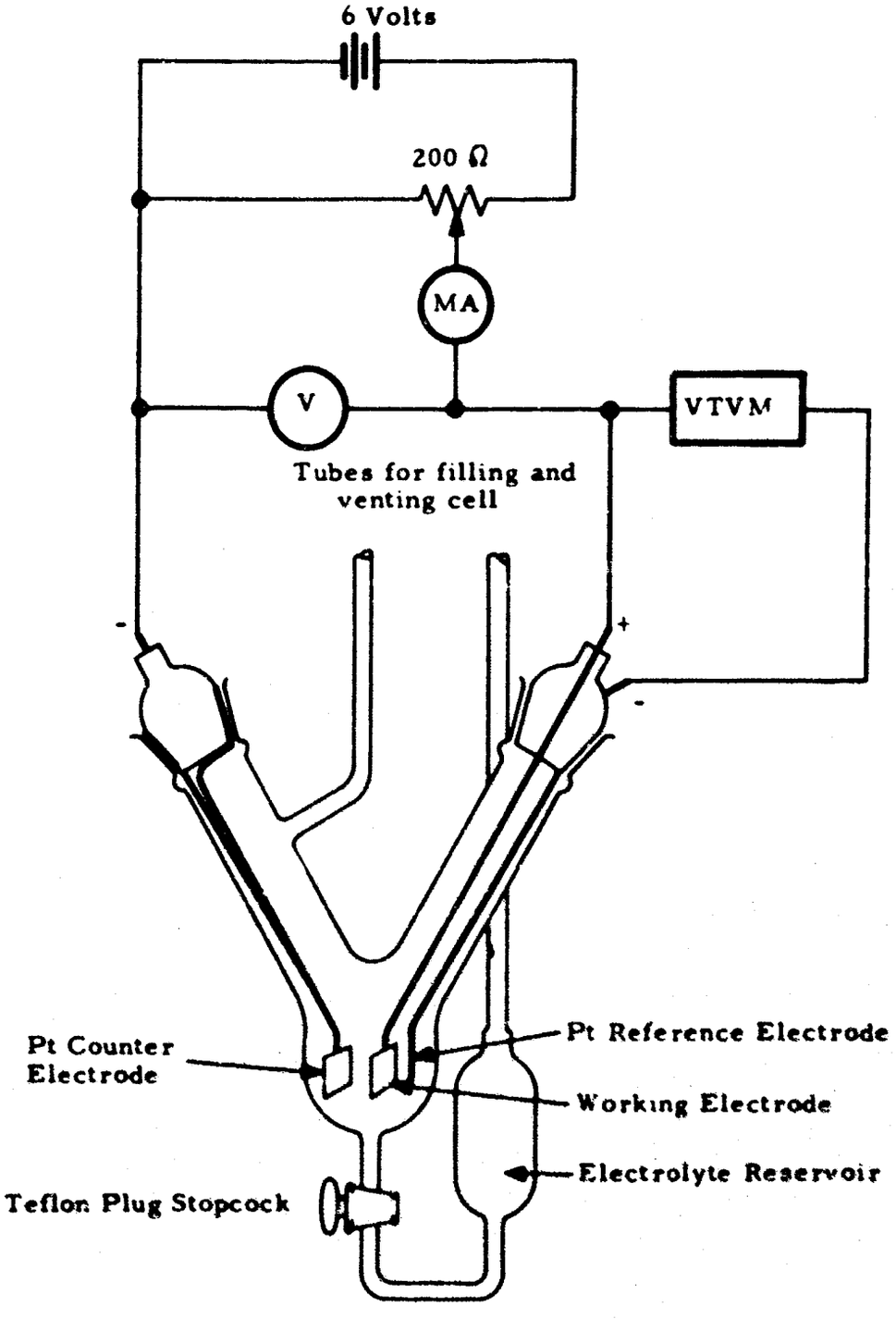

Figure 4. Polarization Cell and Circuit

b. Electrode Flexing

The apparatus used for anodic polarization of convoluted electrodes is shown in Figure 5. Nickel 200 and other electrodes formed into a sharply convoluted form were anodically polarized in bromine trifluoride at +3.00 volts until a nearly steady state anodic current was achieved. At this time the electrode was extended in the electrolyte so as to flex the electrode convolutions and hence to impose a stress on any passive film on the electrode. At the same time the anodic current was observed for any increase which would indicate rupture of the protective film over any part of the surface and re-establishment of the higher anodic current characteristic of an unpassivated nickel surface.

4. ELECTRON DIFFRACTION ANALYSIS

Attempts were made to characterize the fluoride films formed on metal surfaces by means of reflection diffraction techniques. The metal samples were cut from sheet stock in the form of rectangular coupons, 7 x 8 mm in size. Surface preparation before passivating in fluorine consisted of wet grinding on 600 silicon carbide paper followed by etching in cold concentrated HCl. This was followed by rinsing, drying and final degreasing in Freon 11. Samples were then exposed to fluorine.

An Hitachi HU-11 electron microscope with a reflection diffraction attachment RDA was used with 75kv acceleration voltage and a charge neutralizer Type SG-B electron spray gun. The purpose of the charge neutralizer is to produce a low voltage electron spray from a helicoidal filament, and to eliminate surface charge in the specimen area. A collected surface charge, particularly in insulating and semiconducting materials, may cause a distortion or instability of the diffraction pattern.

A dry box (see Figure 6) was attached to the reflection diffraction stage for specimen manipulation in a dry argon atmosphere. The microscope column was purged by dry argon and maintained under positive pressure during change of specimens and introduction of the diffraction stage. The reflection diffraction attachment (RDA) also carried a reference sample: deposited aluminum film on a specimen grid. The known d-spacings, (d) of the reference sample, were used for determining the camera length (L) and thus for calculating the crystallographic d-spacings of the specimen under examination. The distances R (in millimeters) of observed electron diffraction spots from the non-diffracted beam or the radii of the diffraction rings were measured and converted to d-values (in Angstroms) using the calibrated camera constant $L\lambda$ (λ = wavelength) by means of the relation

$$d = \frac{L\lambda}{R} \qquad (13)$$

From d-values so obtained, an identification may be made using the ASTM X-ray standard card file.

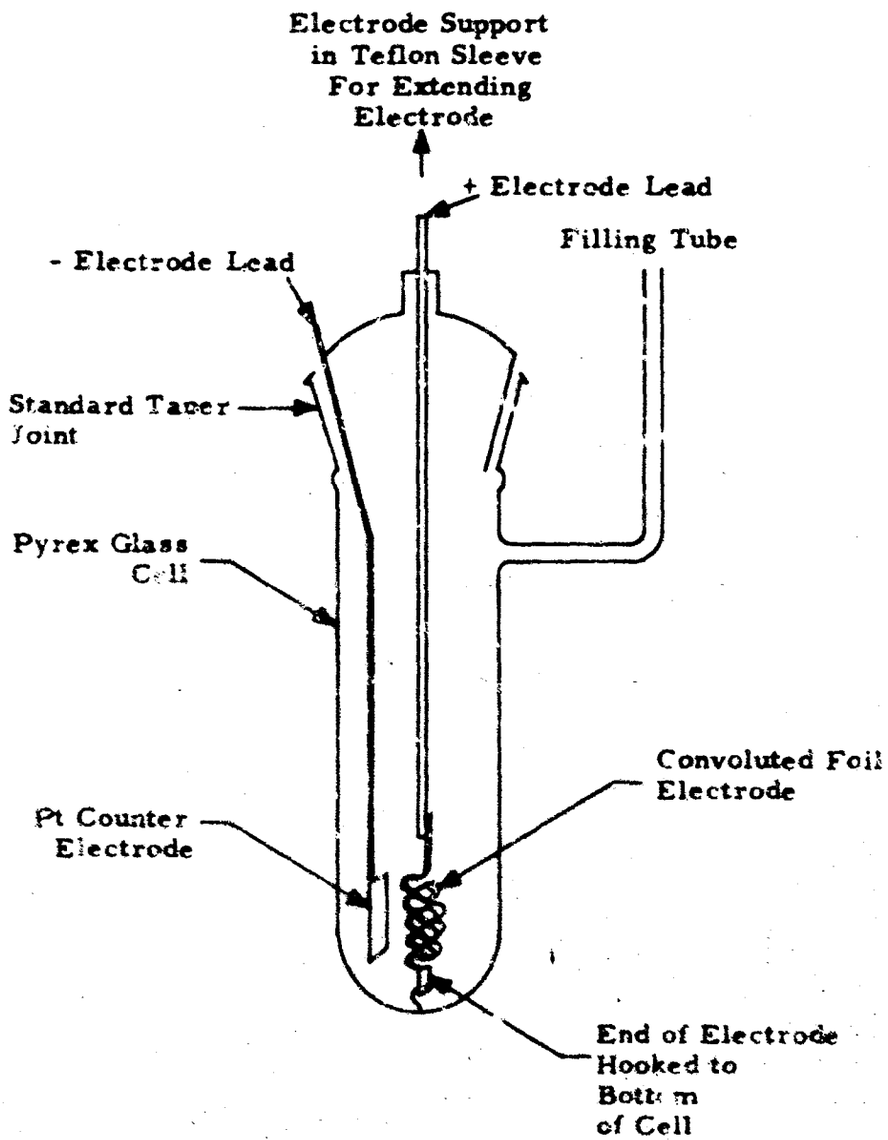

Figure 5. Electrochemical Cell for Electrode Flexing Experiment.

Figure 6. Hitachi HU-11 Electron Microscope and Argon Filled Dry Box Attachment

5. SURFACE AREA MEASUREMENTS

Knowledge of the specific surface area of the metal powders is basic to kinetic studies where an effort is being made to relate weight gain to thickness of the fluoride film. The B.E.T. method using krypton gas adsorption at 77°K is a most satisfactory means of determining the specific areas of powder of the type being used in this investigation.[17]

The krypton-gas B.E.T. method makes use of the following adsorption isotherm equation:

$$\frac{P}{V(P_o - P)} = \frac{1}{V_m C} + \frac{(C-1)}{V_m C} \cdot P/P_o \qquad (14)$$

where V is the volume of gas adsorbed by a surface at the equilibrium pressure P, P_o is the saturation pressure of the adsorbate, V_m is the volume of adsorbate required to form a monolayer on the surface, and C is a constant for a given adsorbate-adsorbent system.

On typical heterogeneous adsorbents, this two-constant equation can be used with considerable confidence over a limited range of pressures preceding and following the buildup of a monomolecular layer. For any isotherm, or portion of an isotherm, which obeys this relationship, a plot of $P/V(P_o - P)$ against P/P_o will yield a straight line with intercept equal to $1/V_m C$ and slope $(C - 1)/V_m C$. This is the so-called B.E.T. plot. From the slope and intercept, V_m can be calculated; it is equal to the reciprocal of the sum of the slope and intercept.

The total area accessible to adsorption is the product of the total number of gas molecules in V_m and the effective cross-sectional area of each molecule, σ. Therefore:

$$S = \frac{V_m N}{M} \cdot \sigma \qquad (15)$$

where S is the total surface area of the absorbent, N is Avogadro's number, and M is the molar volume of the adsorbate. The foregoing equations are the basis of the determination of surface areas by gas adsorption.

Surface area measurements were made on the powders before and after passivation in fluorine gas. The passivations were carried out by exposing the previously evacuated powder samples to a fluorine pressure of 50 torr for five minutes, then pumping off the residual gas, thereupon admitting increasingly higher pressures of fluorine. The alternate five-minute exposures and evacuations were repeated at increments of 100, 200, and 400 torr fluorine pressure with a final exposure of one hour at one atmosphere. The exposures were at a temperature of 25°C. Weighed quantities of the metal powders were individually exposed in the tubes shown in Figure 7. This allows passivation, evacuation and subsequent introduction of the powder specimen to the krypton adsorption apparatus without exposure

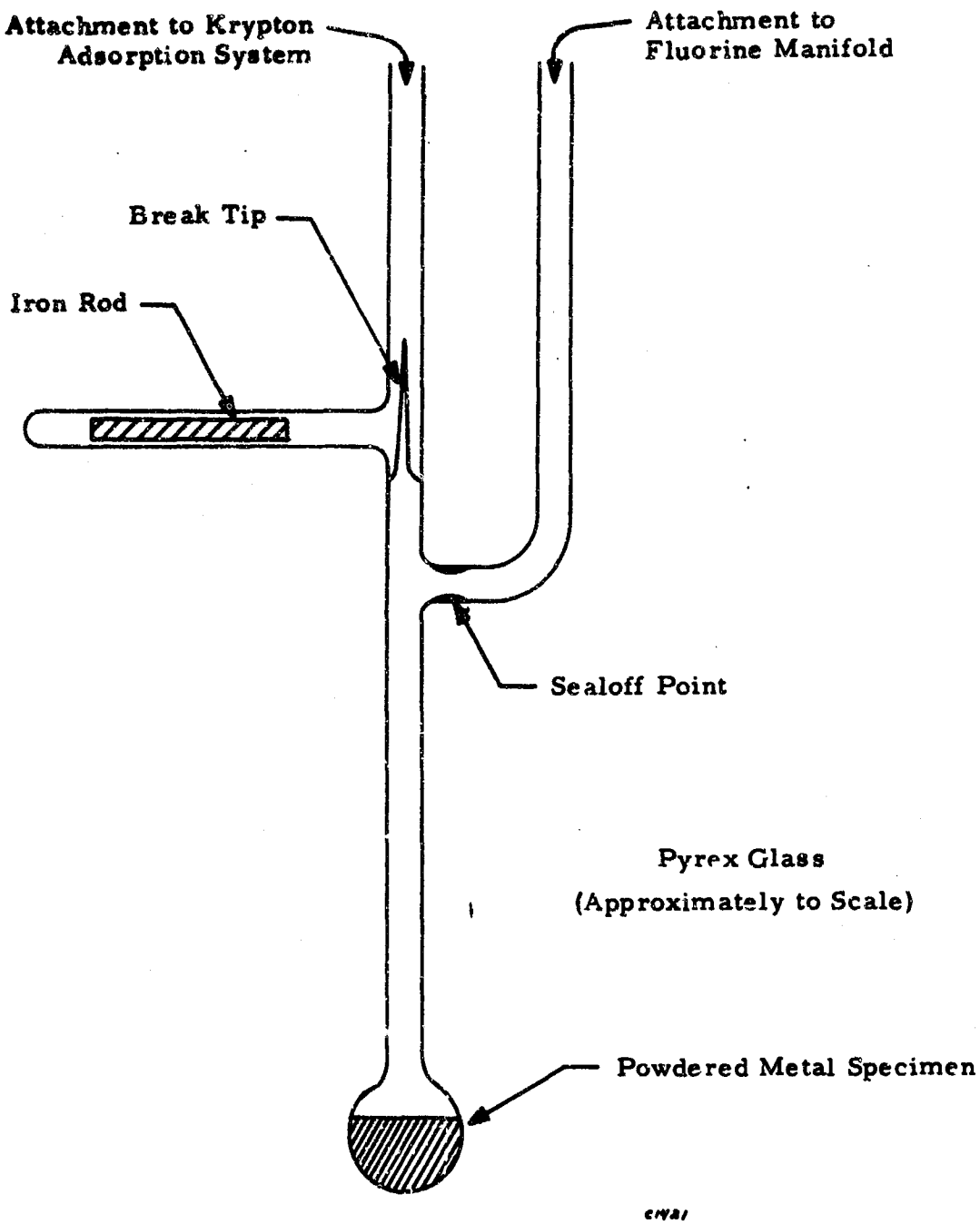

Figure 7. Apparatus for Determining Surface Area of Metal Powders After Passivation in Fluorine

to air. This procedure serves to prevent alteration of the freshly-formed passive film by exposure to moisture in the air.

6. EVALUATION OF ENVIRONMENTAL EFFECTS

The effects of atmosphere moisture on passive films were investigated by passivating samples of metal powders by various techniques. After pumping off the passivating gas or vapor, the powdered sample, enclosed in a stainless steel bomb, was exposed to air at 50% relative humidity for 48 hours. The bomb was then closed, evacuated, and the amount of fluorine reacting with the powder measured manometrically in the constant volume passivation system.

SECTION IV

RESULTS AND DISCUSSION

1. REACTION OF FLUORINE WITH METAL POWDERS

The design and operation of the constant volume apparatus used for measuring the rate of uptake of gaseous fluorine by metal powder has been described in Section III. The volume of the sample bomb is calibrated in each experiment by expanding helium from the fixed volume portion of the system (Figure 1) to the evacuated sample container and measuring the pressure difference. The helium is pumped out and this operation is repeated with fluorine gas. The initial pressure of fluorine gas is calculated from the helium calibration, because the initial reaction is so rapid that it is impractical to measure the initial fluorine pressure directly.

The very rapid initial reaction of fluorine with metal powders indicates that the oxide films are involved in the fluorination reaction, since an induction period for diffusion through the film is not found. If this is true, the weight of fluorine reacted as calculated by Equation 11 will be in error as the derivation implies that the gas solid reaction is as follows:

$$M + F_2 \rightarrow MF_2 \tag{9}$$

whereas in reality the following reaction is to be expected:

$$MO + F_2 \rightarrow MF_2 + \frac{1}{2} O_2 \tag{10}$$

If the latter equation correctly expresses the fluorination reaction, it can be seen that one-half mole of oxygen is released for each mole of fluorine consumed. The pressure change determined manometrically therefore is only one-half that predicted by Equation 11. Another modification of Equation 11 is required because it is impractical to thermostat the entire volume of the system. The equation which relates the weight of fluorine (W_F) removed from the gas phase through reaction with the metal powder with the pressure change is

$$W_F = 38 \frac{2(\Delta P)}{R} \left[\frac{V_1}{T_1} + \frac{V_2}{T_2} \right] \tag{16}$$

where ΔP is the total change in pressure, V_1 is the volume of the system thermostatically controlled at temperature T_1, and V_2 is the smaller volume of the system outside the constant temperature bath at ambient temperature T_2. The ambient temperature T_2 may vary from one run to another and

indeed may change during a prolonged run, in which case corrections to the data are required.

The mean film thickness as a function of time of reaction can be calculated using Equation 12. The use of this equation requires data for the specific surface area of the powder and an estimate of the density of the film, as well as knowledge of the molecular weight ratios of the metal fluoride and fluorine. The fluoride film is assumed to consist of the normal fluoride of the same alloy constituent for nickel, copper, and aluminum alloys, while the Monel and stainless steels are assumed to be mixed fluorides of the major alloy constituents in approximately the composition ratio found in the corresponding alloy.

The experimental values of surface areas are taken from Table III. The calculated values of density and molecular weight ratios necessary for use of Equation 12 are given in Table IV.

It may be advisable to exclude copper from the foregoing analysis. Evidence is that the normal thin oxide film in copper consists of copper (I) oxide.[18] On the basis of observations due to Haendler,[8] which are reinforced by evidence to be presented in the next section, the initial oxidation of the oxide-covered copper may proceed as follows:

$$Cu_2O + F_2 \rightarrow CuF_2 + CuO \qquad (6)$$

a reaction which would not produce any gaseous reaction products and the weight of fluorine reacting would therefore be correctly expressed by Equation 11. It can be stated that, in general, correct calculation of thickness of fluoride films requires detailed knowledge of surface composition and the nature of surface reactions. These factors are not precisely known at this time.

Table V gives data covering film thickness calculated from pressure changes for ten alloy powders for one hour exposure at 27°C (80°F). The experiments have shown that most of the film-forming reactions for all the materials studied is completed in less than one hour.

Figures 8, 9, and 10 are plots of calculated fluoride film thickness as a function of time for ten alloy powders at initial fluorine pressure near one atmosphere.

The general shape of the rate curves for fluorination of the metal powders suggests conformity to a logarithmic rate law at least in the early stages of the reaction. Such a rate law is not unexpected for the early stages of an oxidation reaction at low temperatures. When the data are tested by plotting the calculated fluoride film thickness against the logarithm of time, it is seen that generally good agreement is obtained in every case for conformity to a logarithmic rate law. Deviations are noted for copper and Monel at longer reaction times when the rate of reaction tends

TABLE III. SPECIFIC SURFACE AREAS OF METAL POWDERS USED IN CALCULATION OF FLUORIDE FILM THICKNESSES

Alloy	Specific Surface Area (cm^2/g)
Nickel - 112 F Lot M-12308	2330
Monel 206 F Lot Q - 10435	2020
Copper DM 301 Lot 3137	2500
Stainless Steel 347 L Lot N-2355	1490
Stainless Steel 304 213 F	1010
Stainless Steel 316 215 F	1040
Aluminum 6061	3460
Aluminum 2014	7050
Aluminum 2024	4830
Stainless Steel AM 350	3230

TABLE IV. VALUES OF DENSITIES AND MOLECULAR WEIGHTS USED FOR CALCULATION OF FLUORIDE FILM THICKNESSES

Metal or Alloy	Fluoride Composition	ρ(g/ml)	MW_M	Ratio MW_M/MW_F
Ni	NiF_2	4.63	96.7	2.54
Cu	CuF_2	4.23	101.5	2.68
Cr	CrF_3	3.8	109.0	1.91
Fe	FeF_3	3.53	112.8	1.98
Al	AlF_3	2.88	84.0	1.48
Monel	$(70NiF_2+30CuF_2)$	4.51	98.2	2.58
SS304	$(18CrF_3+8NiF_2+74FeF_3)$	3.67	110.7	1.99
SS347 and SS316	$(17CrF_3+12NiF_2+71FeF_3)$	3.72	110.0	2.01
AM350	$(15CrF_3+5NiF_2+80FeF_3)$	3.64	111.5	2.00

TABLE V. FILM THICKNESS MEASUREMENTS – CONSTANT VOLUME METHOD – 27°C (80°F)

Run No.	Alloy	Sample Wt (g)	Total Surface Area (cm^2)	$\frac{V_1}{T_1} + \frac{V_2}{T_2}$	Initial F_2 Pressure (torr)	ΔP 1 Hr (torr)	Calc. Fluoride Film Thickness 1 Hr (Å)	Remarks
2	Copper	101.7	2.54×10^5	1.450	783.6	59.5	13.1	ΔP value interpolated
3	Monel	100.5	2.03×10^5	1.448	756.9	26.7	13.4	
4	SS347	102.0	1.52×10^5	1.440	784.9	16.5	10.8	
5	SS316	101.7	1.06×10^5	1.447	781.0	16.5	14.2	
6	SS304	100.5	1.02×10^5	1.443	787.4	15.4	14.0	
7	Al6061	31.8	1.1×10^5	1.589	789.9	12.7	11.4	
8	Al2014	31.0	2.18×10^5	1.448	760.7	12.7	5.2	
9	Al2024	31.0	1.5×10^5	1.445	756.9	14.0	8.4	
10	Nickel	100.6	2.34×10^5	1.453	767.1	48.6	21.4	
11	Nickel	100.4	2.34×10^5	1.449	787.4	49.5	21.8	Duplicate ran to check reproducibility
12	Nickel	107.5	2.50×10^5	1.445	101.0	32.4	12.6	Low pressure run
13	Nickel	90.9	2.12×10^5	1.440	755.6	6.6	–	Previously passivated powder exposed to 50% RH before run
14	Nickel	102.9	2.40×10^5	1.427	1090	57.0	22.8	High pressure run

(Continued)

TABLE V. FILM THICKNESS MEASUREMENTS – CONSTANT VOLUME METHOD – 27°C (80°F) (CONTINUED)

Run No.	Alloy	Sample Wt (g)	Total Surface Area (cm^2)	$\frac{V_1}{T_1} + \frac{V_2}{T_2}$	Initial F_2 Pressure (torr)	ΔP 1 Hr (torr)	Calc. Fluoride Film Thickness 1 Hr (Å)	Remarks
15	AM350	92.3	3.0×10^5	1.445	788.9	18.5	9.8	
16	Monel	74.5	1.51×10^5	1.482	755.6	21.6	16.4	
17	Monel	74.5	1.51×10^5	1.482	755.6	6.3	–	Sample from Run 16 – exposed to 50% RH
18	Monel	101.7	2.06×10^5	1.450	773.4	26.7	13.2	
19	Monel	101.7	2.06×10^5	1.450	773.4	5.1	–	Sample from Run 18 – evacuates 30 min – repassivated
20	Nickel	101.0	2.35×10^5	1.444	729.0	33.1	12.9	Powder heated under vacuum for 65 hours at 105°C (221°F)
21	Copper	102.3	2.56×10^5	1.448	751.0	55.8	12.3	Powder heated under vacuum for 22 hours at 105°C (221°F)

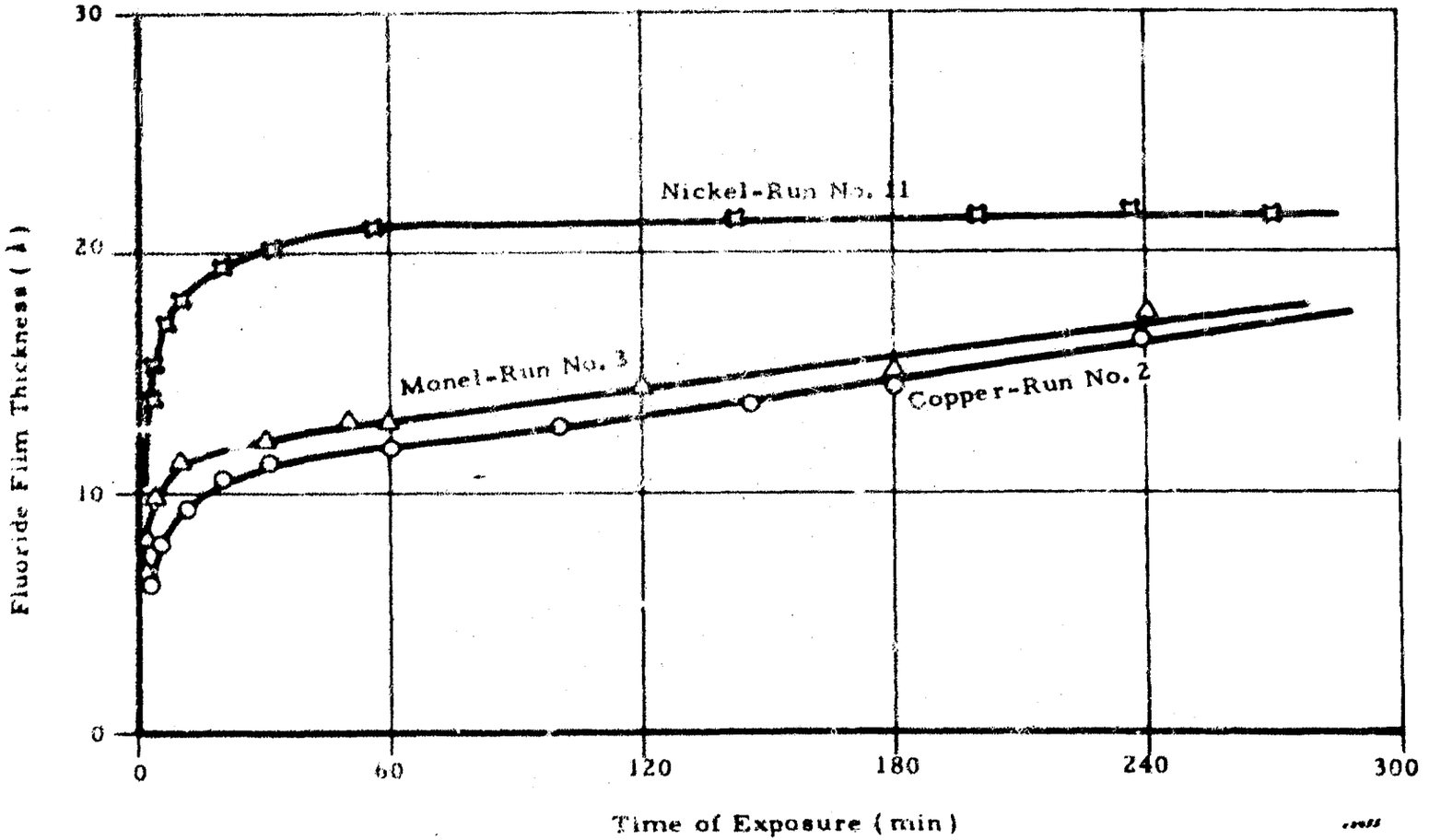

Figure 8. Fluoride Film Thickness vs. Exposure Time
Copper, Nickel and Monel - 27°C (80°F)

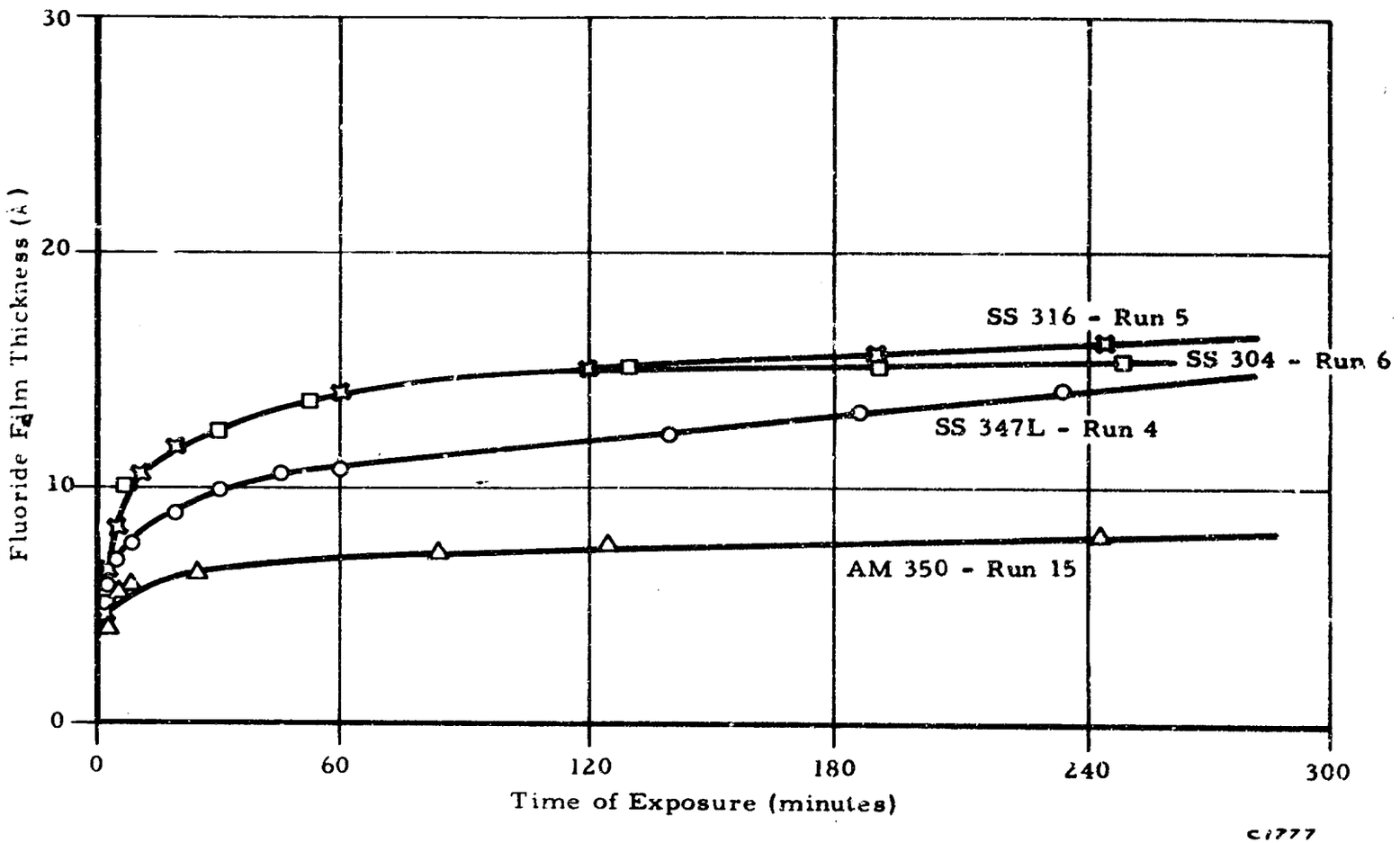

Figure 9. Fluoride Film Thickness vs. Exposure Time — Fluorine, 27°C (80°F) — Stainless Steels

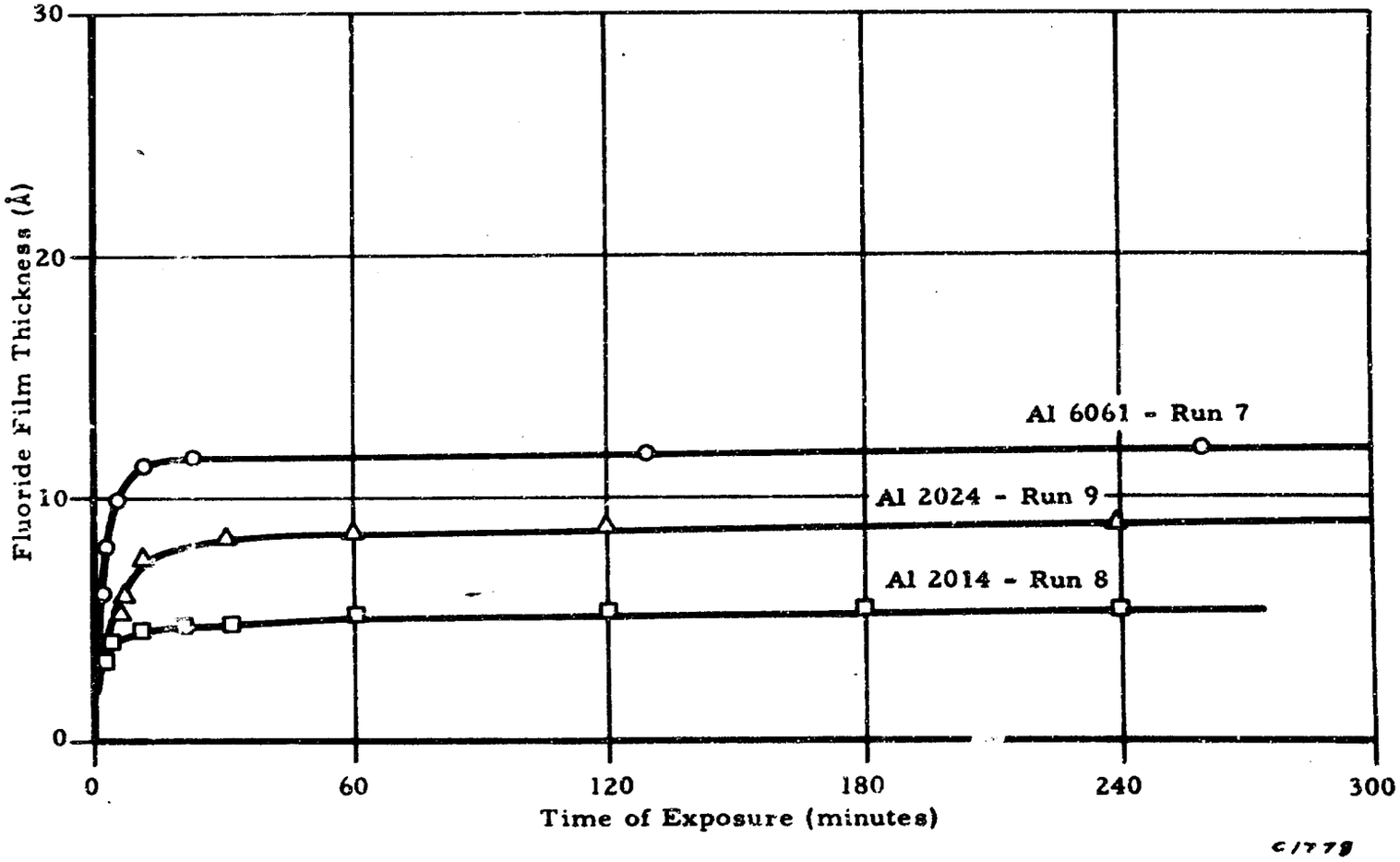

Figure 10. Fluoride Film Thickness vs. Exposure Time — Fluorine, 27°C (80°F) — Aluminum Alloys

to exceed a logarithmic rate. The aluminum alloys do not follow the logarithmic rate law at longer times because the film appears to cease growing after a relatively short period of time. Plots of the fluoride film thicknesses as a function of the logarithm of time are given in Figures 11, 12, and 13 for the various alloys. Calculated logarithmic rate constants based on Equation 4 are listed in Table VI.

The pressure dependence of the reaction rate has been investigated for one material – namely, nickel 200. Rate curves were determined for three different pressures ranging from an initial pressure of 101 torr to 1090 torr. The rate curves are given in Figure 14. Logarithmic rate constants were determined by plotting the data of Table VII. The plots are shown in Figure 15.

The logarithm of the rate constant is plotted against the logarithm of pressure in Figure 16 to show the effect of pressure on the rate. In the equation

$$\log K_E = S \log P + C \qquad (17)$$

the slope S is the order of the reaction with respect to fluorine pressure. The experimental value of S is 0.33, which indicates a reaction rate determined by approximately the cube root of fluorine pressure.

From the rate of growth of the fluoride films some speculations can be made concerning the possible mechanisms of growth. Logarithmic rate laws are generally attributed to two mechanisms: (1) the growth rate is controlled by tunneling of electrons through the film; or (2) growth rate is controlled by a pore structure or defects in the film. In the latter case two slightly different diffusion processes may be involved. In one case it may be assumed that compressive stresses set up in the product film results in formation of blisters or cavities in the protective film. Such cavities interrupt diffusive paths of ions and halt reaction in the area of the cavity. The result is a rapid decrease in reaction rate due to decrease in the effective reaction area. A slightly different view is held by others. It may also be argued that a pore structure exists in the film from the onset of growth and that the rate controlling step is passage of gas through the pores. As the film grows in thickness, blocking of pores takes place due to the compression of the film, thus preventing passage of the gas. The latter mechanism is obviously pressure dependent.

The mechanism based on pore structure or defects is rejected because it is difficult to see how a film only a few molecular diameters thick can develop sufficient compressive stresses or indeed even act as a distinct phase. A mechanism based on the tunneling effect is proposed as consistent with the observed facts. In all cases within the range where the logarithmic law holds, the total film thickness, even including the oxide film, is well within the limit for quantum-mechanical tunneling, viz., about 50 Å. The low pressure dependence is also consistent with a tunneling mechanism.

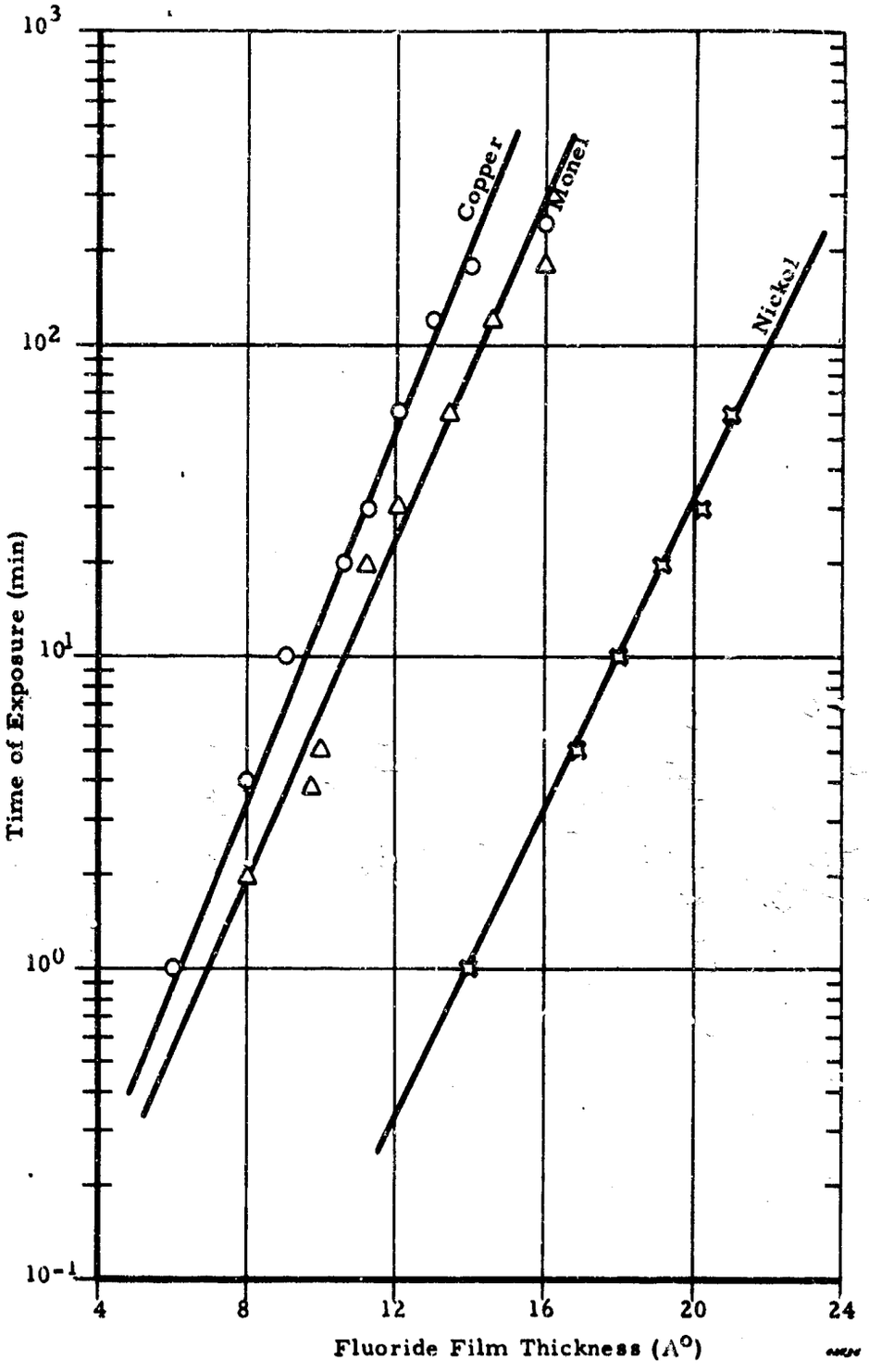

Figure 11. Plot of Fluoride Film Thickness vs. Logarithm of Time. 27°C (80°F)

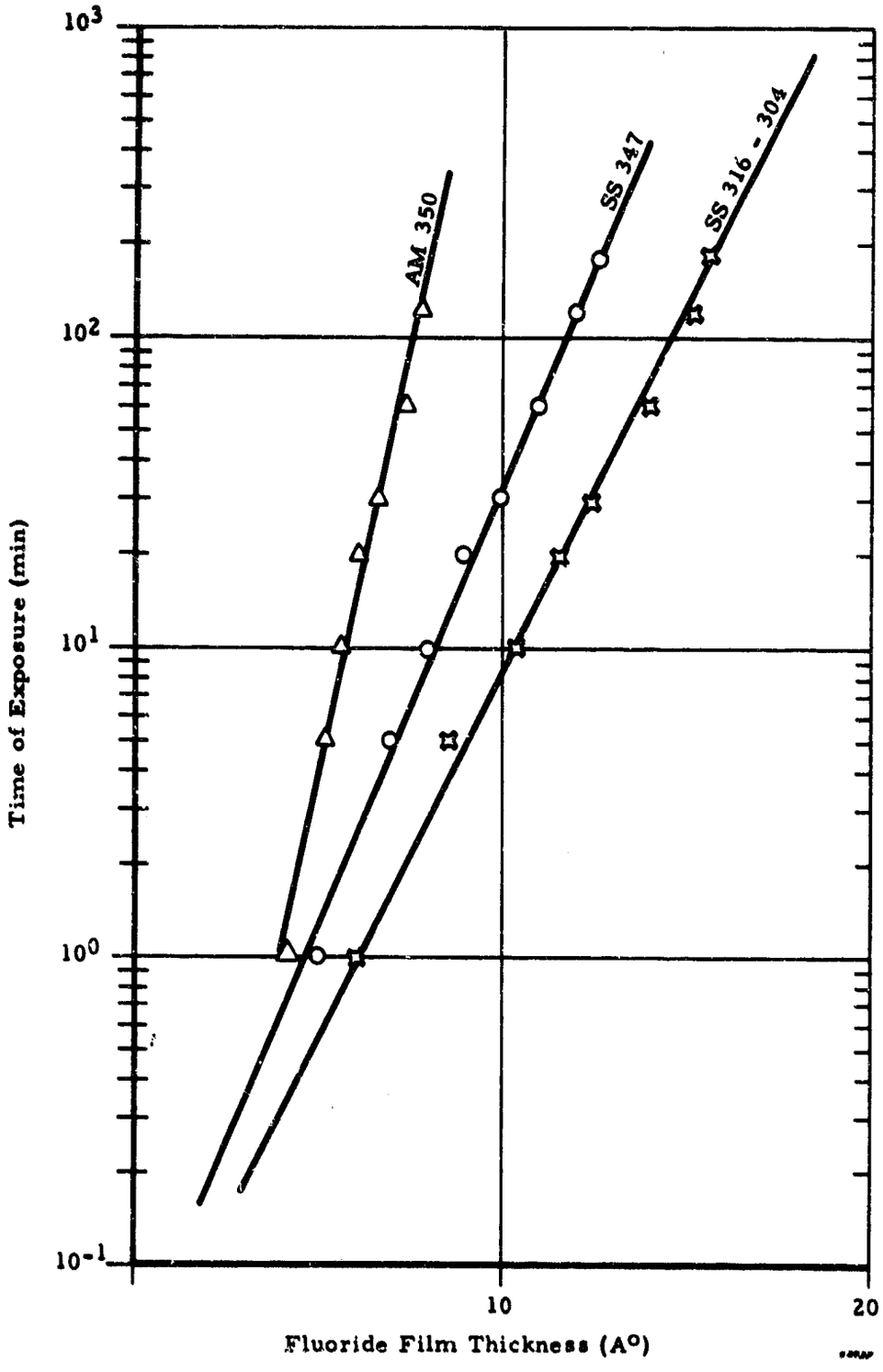

Figure 12. Plot of Fluoride Film Thickness vs Logarithm of Time. 27°C (80°F)

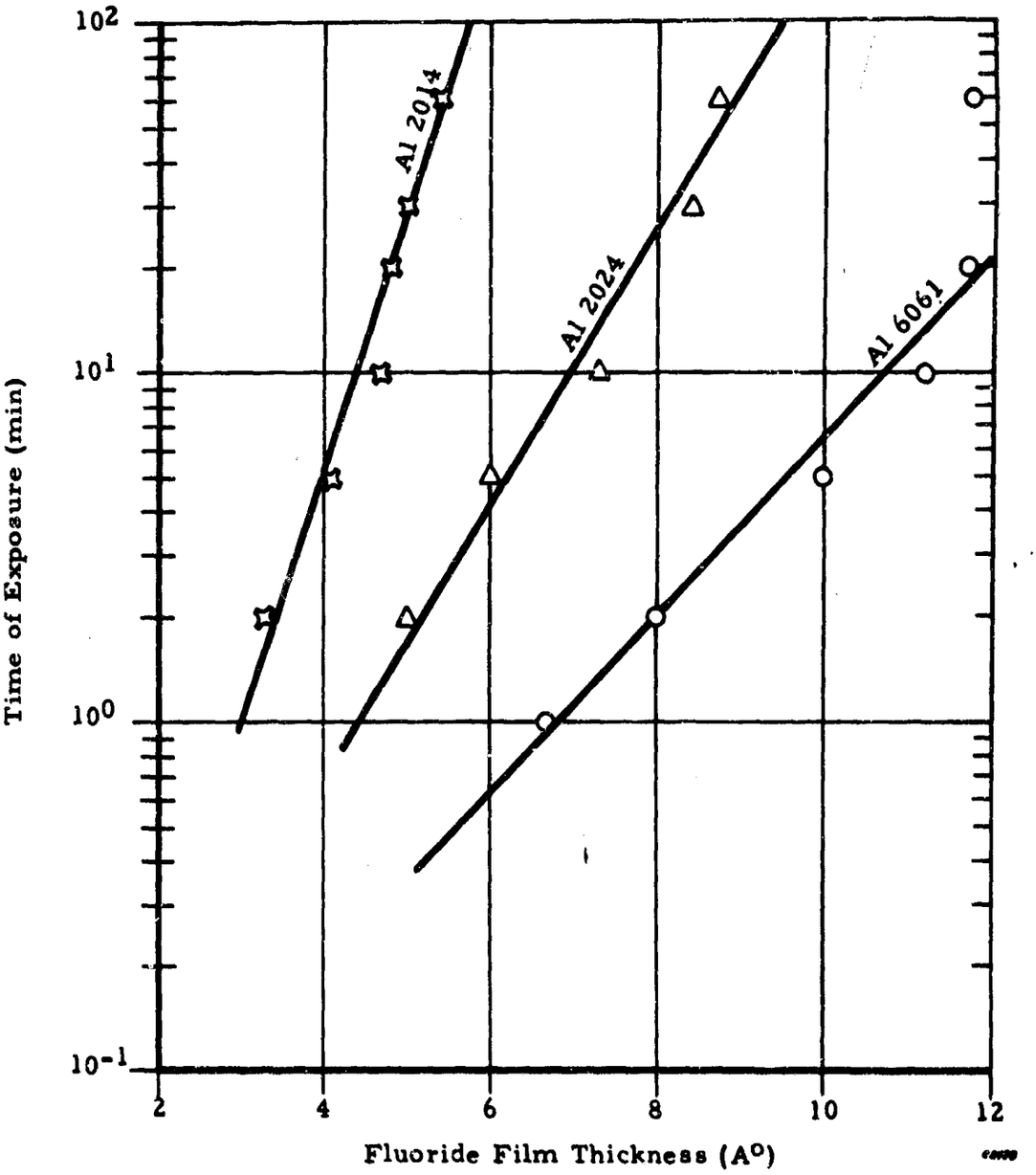

Figure 13. Plot of Fluoride Film Thickness vs. Logarithm of Time. 27°C (80°F)

TABLE VI. LOGARITHMIC RATE CONSTANTS FOR INITIAL FLUORIDE FILM FORMATION ON METAL POWDERS 27°C (80°F)

Fluorine Pressure Near One Atm.

$$\Delta m = K_E \log (at + t_o)$$

Metal or Alloy	Logarithmic Rate Constant K_E
Copper	3.3 Å-min^{-1}
Monel	3.6
Nickel	4.0
AM 350	1.7
SS 347	3.5
SS 316	4.2
SS 304	4.2
Al 2014	1.3
Al 2024	2.4
Al 6061	3.8

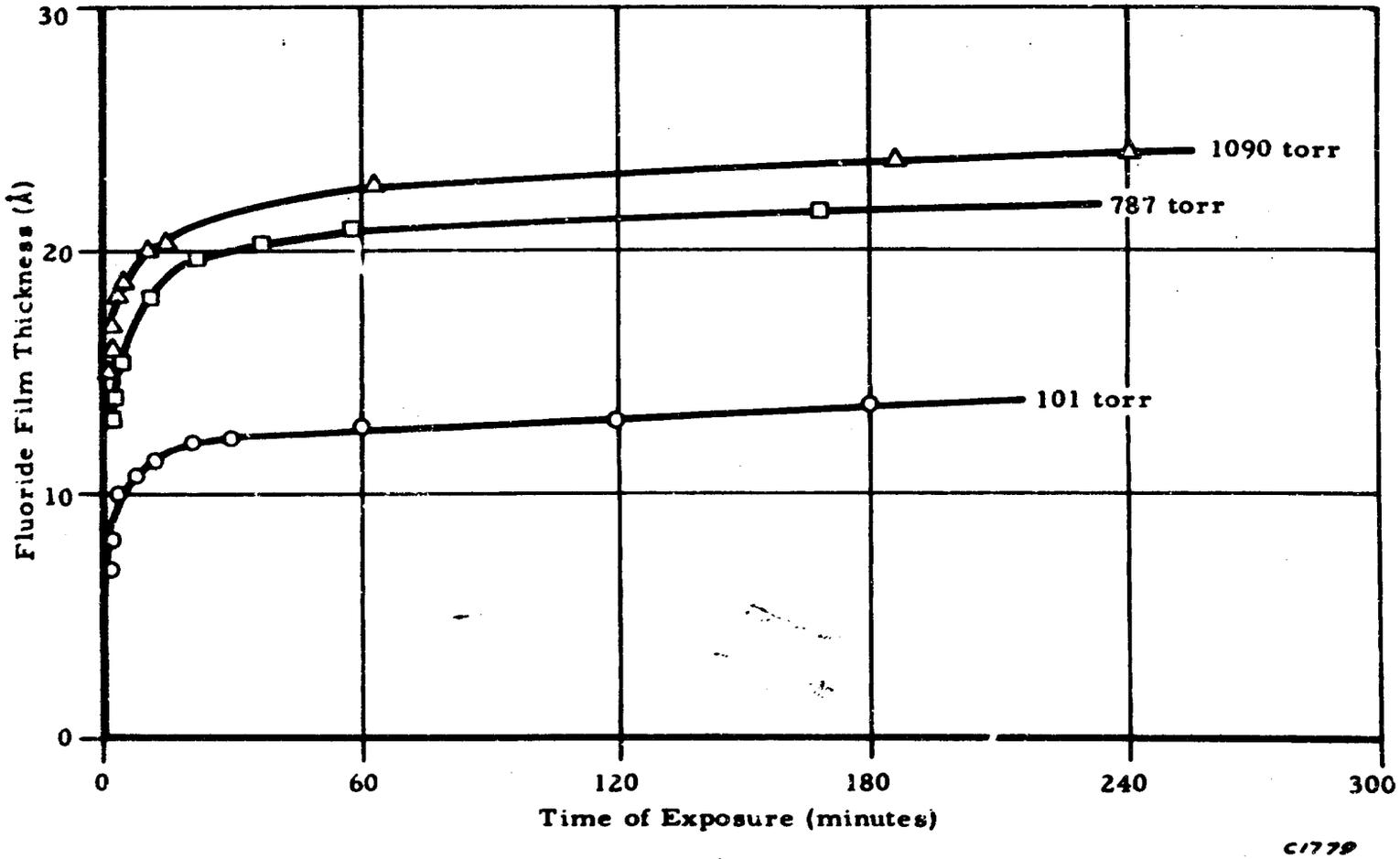

Figure 14 Effect of Pressure on Apparent Fluoride Film Thickness — Nickel, 27°C (80°F)

TABLE VII. EFFECT OF PRESSURE ON LOGARITHMIC RATE CONSTANT – NICKEL POWDER 27°C (80°F)

Time (min)	Fluoride Film Thickness (Å)		
	101 torr	787 torr	1090 torr
1	8.2	14.2	16.4
2	10.0	15.2	17.4
3	10.4	16.0	18.0
5	11.0	17.0	18.4
10	11.6	18.0	19.8
20	12.0	19.4	21.0
30	12.2	20.2	21.6
60	12.4	20.8	22.6
120	12.6	21.2	23.4
180	13.2	21.4	23.8
Logarithmic Rate Constant (K_E)	1.7	3.2	3.5

From plot of $\log K_E = S \log P + C$,

$S = 0.33$

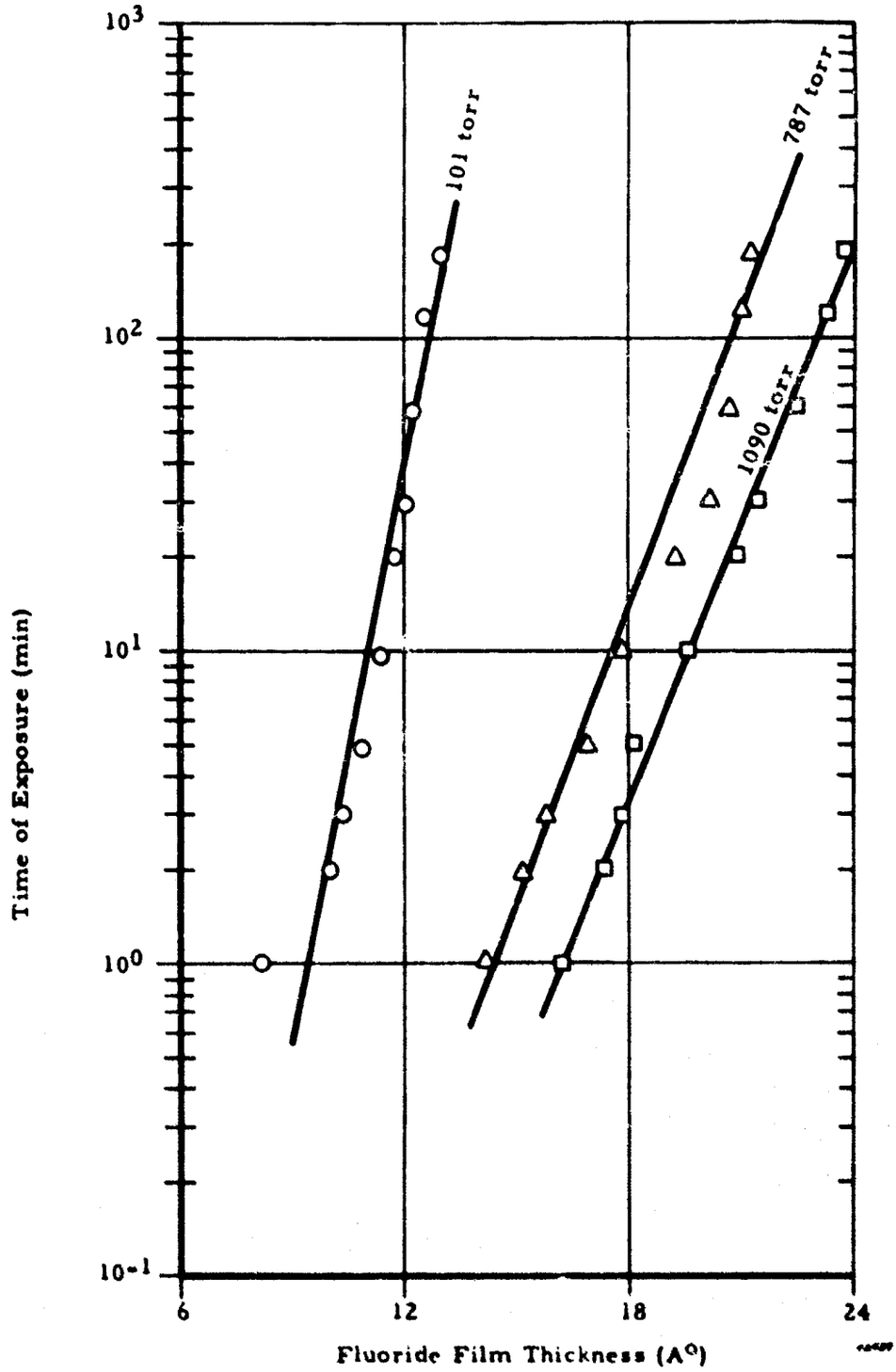

Figure 15. Effect of Pressure on Logarithmic Rate, Constant 27°C (80°F) Nickel Powder

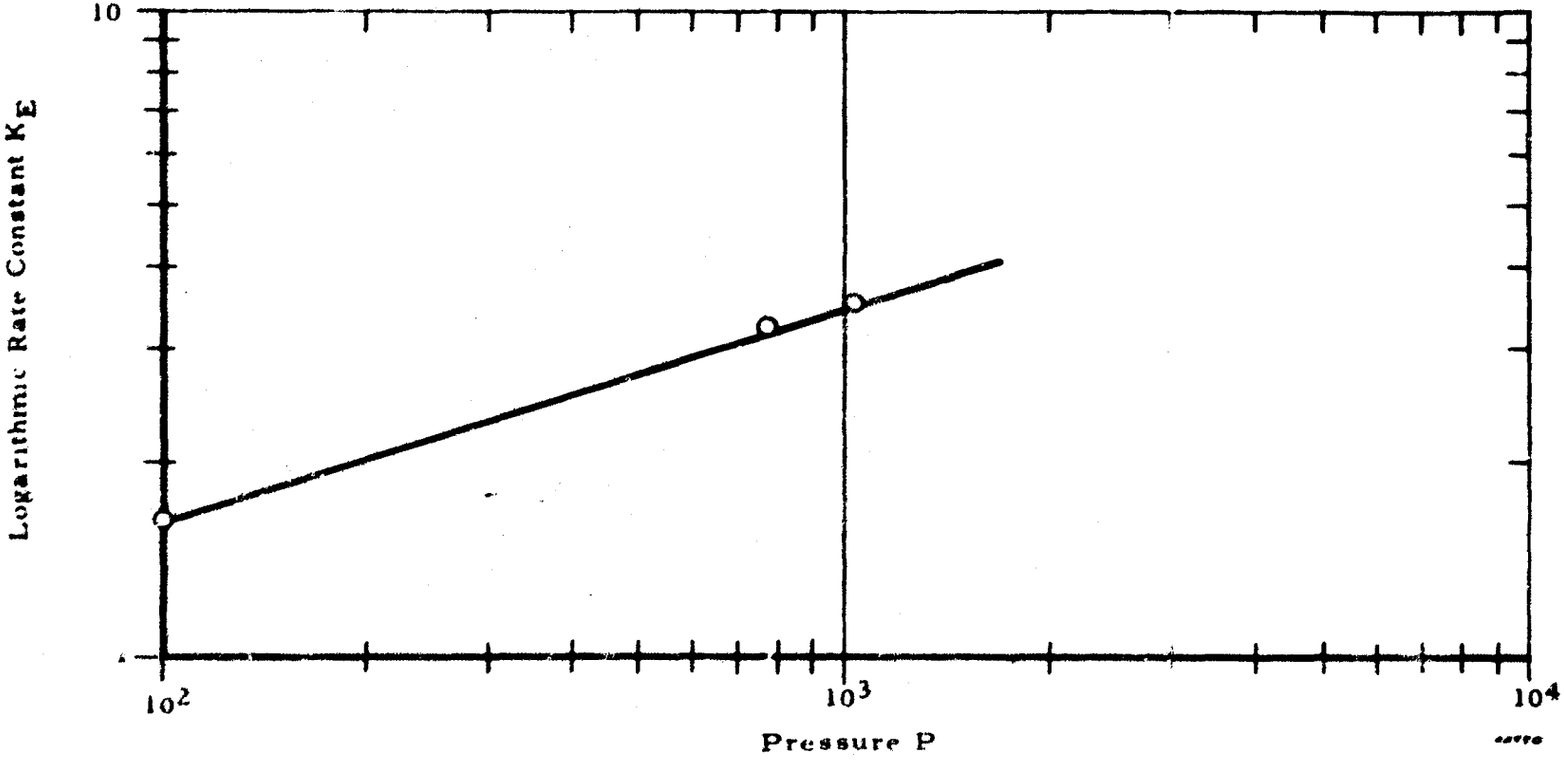

Figure 16. Plot of Logarithmic Rate Constant vs. Pressure
Nickel Powder - 27°C (80°F)

2. REACTION OF GASEOUS FLUORINE WITH METAL OXIDES

Most metals generally have oxide films on the surface which are probably at least 20 to 50 Å or more in thickness.[18] This is considerably thicker than the apparent fluoride film thickness produced by short exposure to gaseous fluorine and in view of the rapid reaction with fluorine, it is evident that the oxide film is largely, if not exclusively, involved in the reaction. This implies that the method of calculation of fluoride film thickness based on the following reaction may not be correct:

$$M + F_2 \rightarrow MF_2 \tag{9}$$

Instead, film thickness calculation should be based on the following general reaction.

$$MO + F_2 \rightarrow MF_2 + \tfrac{1}{2} O_2 \tag{10}$$

Methods of calculation of fluoride film thickness based on the first equation will yield results which are too low. This applies where a gravimetric method is employed, or if a pressure change is determined in a closed system, i.e., a volumetric method. If a particular metallic oxide exists in an intermediate oxidation state, for example Cu_2O, other reactions are possible:

$$Cu_2O + F_2 \rightarrow CuF_2 + CuO \tag{6}$$

$$\text{or} \quad Cu_2O + 2F_2 \rightarrow 2CuF_2 + \tfrac{1}{2} O_2 \tag{18}$$

It becomes apparent that detailed knowledge of the nature of reaction of fluorine with surface oxide films is important before any accurate estimation of fluoride film thickness can be made.

The relative rates of reaction of fluorine with both thin and thick oxide films on copper and nickel as well as with copper and nickel oxides were determined, using the constant volume passivation apparatus. Samples of copper and nickel powders were used (1) as received, (2) after hydrogen reduction followed by exposure to ambient air, and (3) after air oxidation at elevated temperature. Reagent grade CuO and NiO were also used. Surface areas of all these materials were measured in order to express the amount of fluorine reacted on an equivalent area basis. The surface areas are given in Table VIII.

Weighed samples of each of the materials listed in Table VIII were introduced into the constant volume apparatus, and the amounts of fluorine reacting at approximately one atmosphere initial pressure and 80°F were determined. Figure 17 is a plot of the amount of fluorine in milligrams reacting per 10^5 cm^2 of surface as a function of time on the copper derivatives. A similar plot is given in Figure 18 for the nickel materials.

TABLE VIII. SURFACE AREAS OF METALS AND METAL OXIDES

Material and Description	Surface Air (cm^2/g)
1. Copper Powder – MD-301	2500
2. Copper Powder – MD-301 (oxidized at 400°F)	5690
3. Copper Powder – MD-301 (H_2 reduced at 350°F, then exposed to ambient air)	2150
4. Copper Oxide – Reagent Powder	3540
5. Nickel Powder – 112F	2330
6. Nickel Powder – 112F (oxidized at 750°F)	1540
7. Nickel Powder – 112F (H_2 reduced at 650°F, then exposed to ambient air)	1080
8. Nickel Oxide (NiO) – Reagent Powder	4030

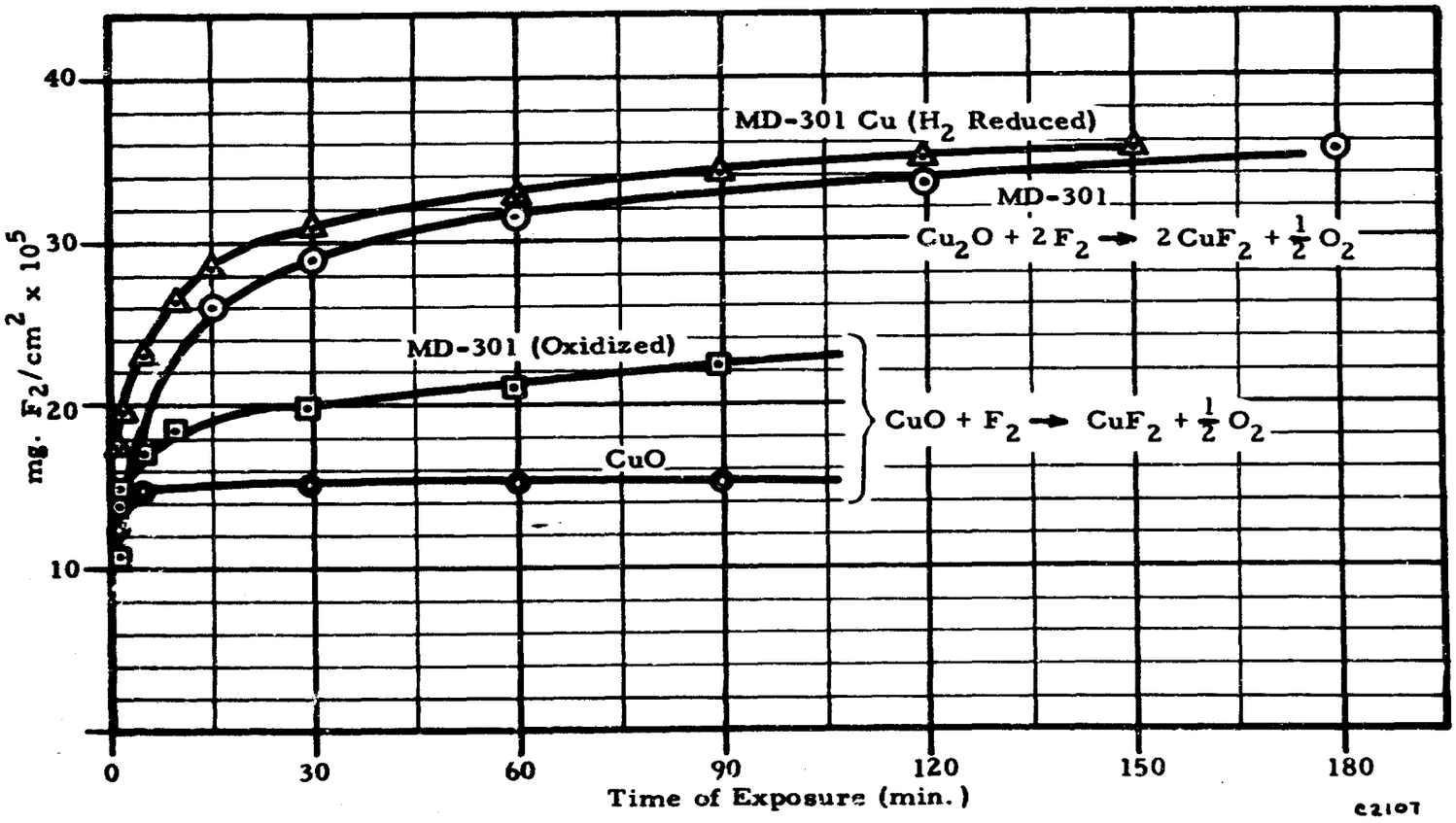

Figure 17. Reaction of Fluorine With Copper Oxides – One Atmosphere F_2 Pressure – 27°C (80°F)

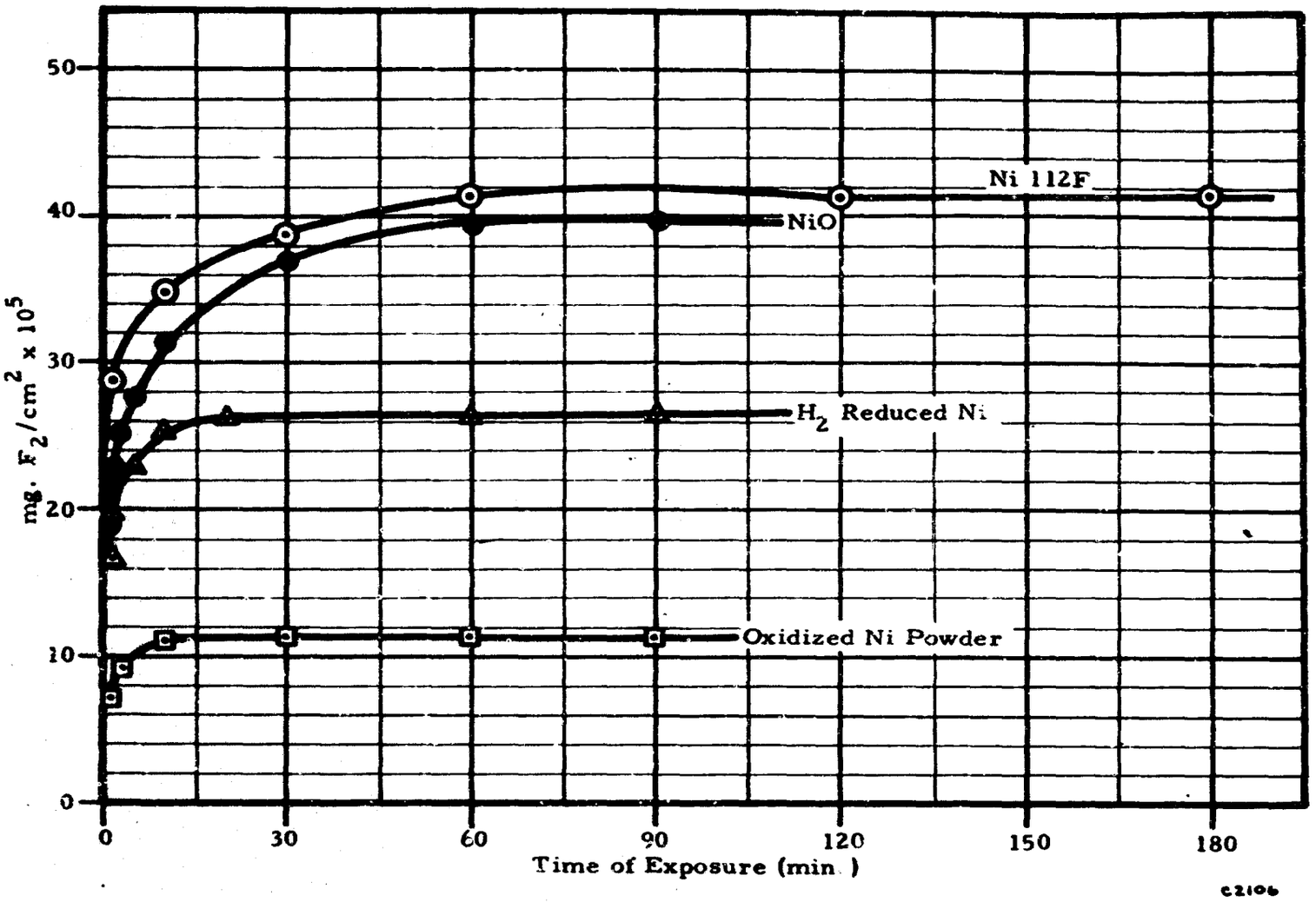

Figure 18 Reaction of Fluorine With Nickel Oxide Surfaces – One Atmosphere F_2 Pressure – 27°C (80°F)

The rate of reaction of fluorine with the as received copper and hydrogen-reduced copper are nearly identical. When expressed in terms of the amount of fluorine reacting for equivalent surface, the curves in Figure 16 are almost superimposable. It may be assumed here that the reacting surface is Cu_2O. There is considerable evidence that the thin oxide on copper is Cu_2O.[18] This film would be expected also to have reformed on the hydrogen-reduced sample when exposed to air.

The MD-301 copper powder which was oxidized in air until a black oxide film of CuO covered the particles, reacts more nearly like the reagent CuO (bottom two curves of Figure 17). The reacting oxide, CuO, attains a limiting fluoride film very rapidly which impedes further oxidation. It appears that the reaction between fluorine and CuO nearly ceases after about ten minutes. With a Cu_2O surface, the reaction is still continuing at an appreciable rate for 30 to 60 minutes. Obviously, a different mechanism is involved.

No simple explanation can be advanced at this time for the widely different reaction rates of fluorine with the nickel oxide surfaces as shown in Figure 18. The similar curve for the nickel powder and NiO lends support to the belief that the reactive film on the nickel is NiO, but this is not supported by the curve for the ignited nickel powder which was obviously covered with a heavy film of NiO (bottom curve of Figure 18). The decreased oxidation of the hydrogen-reduced nickel and oxidized nickel powder may be related to the high temperature each was exposed to which may have caused changes in the defect structure of the surfaces. The shape of the reaction rate curves implies a different reaction mechanism for these two materials.

3. REACTION OF GASEOUS CHLORINE TRIFLUORIDE WITH METAL POWDERS

a. Procedure

The flow system for the gravimetric determination of the reactions between halogen fluorides and metal powders was discussed in Section III. In the preliminary experiments in which chlorine trifluoride vapor was passed over 304 stainless steel powder, small weight losses were observed rather than the anticipated weight gains. The weight losses were traced to HF attack of the glass which more than offset weight gains due to reaction of chlorine trifluoride with the metal. Some of the HF attack may be caused by traces of HF left in the chlorine trifluoride but it is most likely that most of the attack is due to diffusion of the oxidizer through the Teflon Swagelok ferrules where the glass arms of the U-tubes connect to the stainless steel manifold. Visible etching takes place on the outside of the glass tubes at the junctures with the Teflon ferrules.

The original experimental procedure was altered to compensate for the loss of weight of the glass tubes. The metal powder is weighed into the tubes by difference, i.e., the empty tube is first weighed precisely on the analytical balance to the nearest 0.1 mg, then the metal powder sample is

placed in the tube and the tube and contents reweighed. After exposure to the flowing chlorine trifluoride vapor for the desired period of time, followed by purging with nitrogen, the tube and contents are weighed again. Finally, the contents of the tube are removed, the tube rinsed and dried, then reweighed to determine the weight of glass lost due to HF attack. The weight change of the powder is taken as the algebraic difference between the weight change of the tube and powder, and the weight change of the glass tube.

If it is assumed that the weight gain of the metal powder is due exclusively to reaction between chlorine trifluoride and metal to form a metallic fluoride of normal composition and density, then the mean film thickness can be approximated from

$$d = \frac{W_F \left[MW_{MF}/MW_F\right]}{A \cdot \rho} 10^8 \qquad (19)$$

where d = fluoride film thickness in Angstrom units

W_F = weight increase of metal powder during exposure to chlorine trifluoride (g)

MW_{MF} = molecular weight of metal fluoride

MW_F = molecular weight of fluorine in metal fluoride

A = total area of metal powder (cm^2)

ρ = density of metal fluoride (g/ml)

The fluoride film is assumed to consist of the normal fluoride of the main alloy constituent for nickel, copper, and aluminum alloys, while for the Monel and stainless steel the film is assumed to be a mixed fluoride of the major alloy constituents in approximately the composition ratio found in the alloy.

For reasons cited in foregoing discussions, the weight gain of the powder upon exposure to chlorine trifluoride is due to the conversion of the metal oxide to the fluoride, hence the film thickness calculated by Equation 19 would be low by approximately 50%.

This is because in the reaction of chlorine trifluoride with a metal oxide, oxygen is evolved. The reaction is as follows:

$$3MO + ClF_3 \rightarrow 3MF_2 + Cl_2 + \frac{3}{2}O_2 \qquad (7)$$

The equation for film thickness thus becomes

$$d = \frac{W_F \left[MW_{MF}/MW_F - MW_O\right]}{A \cdot \rho} 10^8 \qquad (20)$$

where MW_{MF} = molecular weight of metal fluoride

MW_F = molecular weight of fluorine in metal fluoride

MW_O = molecular weight of oxygen in metal oxide converted to metal fluoride

The situation of copper is even more complicated. Assume for the moment that the reaction takes place at the surface with copper (I) oxide converting it to copper (II) fluoride and copper (II) oxide in equal molar proportions. This reaction releases no oxygen, hence Equation 19 may be used to calculate the mean equivalent fluoride film thickness. This treatment neglects the fate of the copper (II) oxide.

The powders used in these experiments were initially dried; however, traces of moisture can be readsorbed during weighing and handling. The presence of chemisorbed moisture in the metal oxides also cannot be excluded. Any adsorbed moisture present in the metal powder samples will react with chlorine trifluoride and cause an apparent weight loss if the reaction products are swept out of the bed of powder. Another possible source of error is adsorption of the chlorine trifluoride on the powder. It is suggested that because of the fairly high boiling point of chlorine trifluoride, removal of adsorbed vapor by sweeping with nitrogen may be incomplete. Adsorbed chlorine trifluoride remaining on the metal powder would result in a positive error in the weight gain, tending to offset errors due to removal of adsorbed moisture during exposure. Finally, electron diffraction studies (see below) have resulted in the identification of metal chlorides as well as fluorides in these reacting with chlorine fluorides. No correction has been made for this occurrence.

In view of the possible sources of error mentioned above, and the uncertainties concerning composition and density of fluoride films, it is obvious that calculated values of film thickness must be viewed with reservation. However, the data are presented as being useful from a comparison standpoint.

The calculated values of the density, molecular weights and molecular weight ratios are to be found in Table IV. The specific surface area values used in applying the above equation are given in Table III for each of the alloy powders.

b. Experimental Determinations

The experimental determinations covering exposure of nine different alloy powders to chlorine trifluoride vapor at one atmosphere are given in Table IX. The exposure times range from 15 minutes to 120 minutes or more. Sufficient heat is released on initial contact of the chlorine trifluoride and powder to raise the temperature slightly above the ambient temperature of 25°C (77°F); therefore the exact temperature cannot be specified and varies during the exposure period. The rate of displacement

TABLE IX. FILM THICKNESS MEASUREMENTS – GRAVIMETRIC METHOD, CHLORINE TRIFLUORIDE – 25°C (77°F)

Alloy	Wt. Powder (g)	Total Surface Area (cm^2)	Time of Exposure (min.)	Wt. Change Tube & Powder (mg.)	Wt. Change Glass Tube (mg.)	Wt. Change Powder (mg.)	Calculated Film Thickness (Å)
SS304	38.4800	3.90×10^4	15	-1.6	-2.3	+0.7	1.6
	38.6833	3.91×10^4	30	-0.4	-1.6	+1.2	2.8
	38.4755	3.89×10^4	60	-2.5	-5.0	+2.5	5.7
	38.3702	3.88×10^4	120	1.9	3.9	+2.0	4.8
SS316	38.6474	4.01×10^4	15	-2.3	-2.8	+0.5	1.2
	38.6150	4.01×10^4	30	-1.4	-4.3	+2.9	6.6
	38.4453	4.00×10^4	60	-0.6	-3.1	+2.5	5.7
	38.7894	4.05×10^4	120	-1.2	-3.1	+1.9	4.3
SS316	39.1675	4.07×10^4	15	-4.9	-5.1	+0.2	0.5
	39.2587	4.08×10^4	30	-1.4	-3.2	+1.8	4.0
	39.2135	4.07×10^4	60	-1.8	-4.8	+3.0	6.5
	39.2100	4.07×10^4	120	+0.2	-3.2	+3.4	7.5
SS347L	39.1325	5.81×10^4	15	-3.6	-3.1	-0.5	Negative
	39.3051	5.85×10^4	30	-2.3	-3.0	+0.7	1.0
	39.3658	5.86×10^4	60	-5.4	-6.3	+0.9	1.4
	39.4315	5.87×10^4	120	-0.7	-3.3	+2.6	4.0
SS347L	39.3264	5.85×10^4	15	-7.6	-4.3	-3.3	Negative
	39.4906	5.89×10^4	30	-2.6	-3.5	+0.9	1.4
	39.3262	5.85×10^4	60	-1.9	-2.1	+0.2	0.4
	39.3094	5.85×10^4	180	-0.7	-9.5	+8.8	13.9
Al 2024	16.8114	8.11×10^4	15	+3.8	-29.2	+33.0	33.0
	16.6150	8.03×10^4	30	+4.0	-20.6	+24.6	26.9
	17.2948	8.34×10^4	60	+3.8	-19.7	+23.5	24.8
	18.2087	8.80×10^4	120	-0.2	-25.9	+25.7	25.6
Al 2014	16.9739	1.29×10^5	15	+4.2	-2.5	+6.7	5.0
	16.8527	1.19×10^5	30	+5.6	-14.3	+19.9	14.6
	17.0803	1.20×10^5	60	+4.9	-16.7	+21.6	15.9
	16.9815	1.20×10^5	120	+4.2	-14.3	+18.5	13.6
Al 6061	17.1355	5.94×10^4	15	-4.7	-21.5	+16.8	25.0
	17.1647	5.94×10^4	30	-1.3	-23.1	+21.8	32.6
	17.0553	5.90×10^4	60	-8.5	-38.1	+29.6	44.0
	17.0647	5.90×10^4	120	+3.7	-18.6	+22.3	33.2
Al 6061	17.0854	5.91×10^4	15	-12.8	-30.3	+17.5	26.0
	17.0774	5.90×10^4	30	-5.8	-30.1	+24.3	36.2
	17.1262	5.89×10^4	60	-11.5	-32.4	+20.9	31.2
	17.0092	5.89×10^4	120	-26.7	-42.8	+16.1	24.0
Monel	39.7001	8.03×10^4	15	-5.1	-10.9	+5.8	7.2
	39.7334	8.03×10^4	20	-6.7	-13.4	+6.7	8.3
	39.3392	7.95×10^4	30	-13.0	-17.7	+4.7	5.8
	39.7835	8.04×10^4	45	-6.9	-12.4	+5.5	6.7
	40.7109	8.24×10^4	60	-4.8	-12.7	+7.9	9.6
	39.8435	8.06×10^4	60	-8.3	-16.3	+8.0	9.8
	39.9329	8.07×10^4	120	-6.2	-12.3	+6.0	7.4
	39.8009	8.06×10^4	120	-7.3	-10.5	+3.2	4.0
Copper	39.9314	10.0×10^4	15	+36.2	-3.0	+39.2	24.8
	39.7806	9.9×10^4	30	+34.6	-4.0	+38.6	24.4
	39.9060	10.0×10^4	60	+33.7	-9.2	+42.9	27.0
	39.8869	10.0×10^4	120	+40.4	-3.8	+44.2	28.0
Nickel	39.7391	9.2×10^4	15	-5.9	-26.6	+20.7	21.2
	39.7346	9.2×10^4	30	-3.5	-25.6	+22.1	22.8
	39.7056	9.2×10^4	60	-10.5	-34.2	+23.7	24.3
	39.9434	9.3×10^4	120	-3.6	-27.9	+24.3	25.0

of the nitrogen in the relatively shallow bed of powder by the chlorine trifluoride should not be a limiting factor because both diffusion and convective mass transfer are expected to rapidly displace the inert gas.

The weight gains recorded for the stainless steels (SS304, SS316, and SS347L) are extremely small and hence the apparent film thicknesses calculated by this method are very small. The limiting film thicknesses for one or two hours exposure do not exceed about seven Å. The weighing errors involved result in scattered data from which it is difficult to plot any kind of curve. The results for the 347L stainless steel are so scattered as to be virtually worthless.

From the data for the apparent film thickness as a function of time of exposure for the aluminum alloys it is inferred that the limiting film thicknesses are on the order of 15, 25 and 35 Å for 2014, 2024, and 6061 alloy powders, respectively. Although the results are again scattered, it can be ascertained that much of the measurable weight gain takes place during the first 15 to 30 minutes of exposure. The apparent limiting film thicknesses for Monel, nickel and copper, respectively, are about 10, 25, and 25 Å.

Because of the scattered data, no attempt has been made to test conformity to any rate law. Qualitatively, the rates are similar to the rate data for fluorine reactions. The apparent limiting film thicknesses produced in chlorine trifluoride and fluorine do not agree very well for all alloys studied. In the case of nickel, for which the data were best, there is fair agreement. The limiting film thickness is approximately 25 Å and 21 Å, respectively, for chlorine trifluoride and fluorine at comparable pressure and temperature.

4. REACTION OF GASEOUS CHLORINE PENTAFLUORIDE WITH METAL POWDERS

The gravimetric method was applied to investigation of reaction between ClF_5 vapor and metal powders. As in the experiments with ClF_3, net weight losses of the sample tubes were observed and it was necessary to apply corrections to the data to compensate for weight losses of the glass.

The same procedure and methods of calculation were applied as described in Section IV, Paragraph 3 above.

The results for exposure of four metals and alloys to ClF_5 vapor at one atmosphere pressure for 60 minutes at 25°C (77°F) are given in Table X. The net weight changes obtained for 316 stainless steel and Monel 400 samples are so small that little significance can be attached to the calculated film thicknesses. Somewhat larger net weight changes were observed for nickel 200 and aluminum 2024. However, the calculated film thicknesses are less than those observed for chlorine trifluoride exposure under similar conditions. The disparities are so great for all other

TABLE X. GRAVIMETRIC FILM THICKNESS MEASUREMENT – COMPOUND A – 25°C (77°F) – ONE HOUR EXPOSURE

Metal or Alloy	Wt. Powder (g)	Total Surface Area (cm^2)	Wt. Change Tube & Powder (mg)	Wt. Change Glass Tube (mg)	Wt. Change Powder (mg)	Calculated Film Thickness (Å)
316 SS	39.4595	4.1×10^4	- 7.2	- 6.5	- 0.7	Negative
316 SS	39.5120	4.1×10^4	- 6.5	- 7.9	+ 1.4	1.8
316 SS	39.4907	4.1×10^4	-17.5	- 8.8	- 8.7	Negative
Monel 400	39.6179	8.0×10^4	- 5.1	- 6.4	+ 1.3	0.9
Monel 400	39.6764	8.0×10^4	-13.5	-15.8	+ 2.3	1.6
Monel 400	39.5393	8.0×10^4	-13.5	-12.1	- 1.4	Negative
Nickel 200	39.7704	9.3×10^4	-18.6	-31.0	+12.4	7.4
Nickel 200	39.4840	9.3×10^4	-13.0	-25.9	+12.9	7.7
Al 2024	16.9720	8.2×10^4	-13.5	-23.5	+10.0	6.1

materials investigated, that it was concluded that the gravimetric procedure, as practiced herein, could not be made to yield accurate results.

5. EFFECT OF ATMOSPHERIC MOISTURE ON PASSIVE FILMS

It is generally recognized that water vapor has a deleterious effect on fluoride films although the exact mechanism is not clearly understood. Many inorganic fluorides are hygroscopic, forming hydrates, hence it is not surprising that small amounts of moisture can alter and affect the protective character of a fluoride film. In addition to the possible loss of film integrity, the subsequent reaction of fluorine with adsorbed moisture, or with hydrates, can result in formation of HF which may be corrosive to certain metals and alloys in a system.

Very few quantitative data are available concerning interaction of water vapor and fluoride films. Kleinberg and Tompkins[9] reported on the amount of fluorine reacting with samples of fresh and passivated metal powders. The passivated powders were exposed to atmospheric moisture (condition and time of exposure were not stated) prior to a second passivation with fluorine at one atmosphere. The amount of fluorine taken up in the second passivation ranged from a low of 4 per cent of the first passivation (nickel powder) to 95 per cent of the first passivation (Monel). The results were somewhat erratic. Replicate analyses of Monel ranged from 30 to 95 per cent comparing the second passivation to the first.

The approach which has been used in this investigation is as follows: Samples of metal powders are passivated by various methods described below, then exposed to fluorine gas at near one atmosphere pressure and the pressure of fluorine gas is observed as a function of time in an isothermal system of constant volume. This procedure is repeated on a fresh sample of powder which has been passivated, then exposed to 50% relative humidity in air at room temperature. The pressure change is compared to that of an identical charge of fresh powder which has received no passivation treatment. These experiments were carried out in the constant volume passivation system.

In interpreting the results of the various experiments, the simple assumption is made that if a sample of metal powder does not take up any additional fluorine upon exposure to fluorine gas at one atmosphere and 80°F, it is completely passivated. On the other hand, if a sample of powder, following some specified pre-treatment, takes up an appreciable amount of fluorine when exposed, the passivation is not complete. Expressing the data as a pressure change, rather than a fluoride film thickness or weight of fluorine, does not require one to make any assumption as to the nature of the reaction.

a. Experimental Determinations

Three distinct operations were carried out to determine the efficacy of the various passivation procedures and the effect of moisture on them. These are described as follows.

(1) A 100 gram sample of metal powder was charged to the sample bomb of the constant volume passivation apparatus. The apparatus was evacuated for a minimum of 30 minutes, a volume calibration carried out with helium gas and the system again evacuated. Fluorine was then introduced to the system and the system pressure was measured as a function of time as fluorine reacted with the metal powder. The initial fluorine gas pressure was near one atmosphere and the sample bomb was thermostatted at 27°C (80°F).

(2) A fresh 100 gram sample of metal powder was charged to the bomb. After evacuation for a minimum of 30 minutes, the metal powder was subjected to one of the passivation treatments described in the later sections. The sample bomb is equipped with valve and coupling so that the passivation treatment can be conducted outside the constant volume apparatus. After completion of the prescribed passivation, the bomb was evacuated and introduced into the constant volume apparatus. The procedure under paragraph (1) above was repeated and the pressure change due to additional reaction of fluorine, if any, was recorded as a function of time.

(3) The operations under paragraph (2) were repeated using a fresh 100 gram charge of powder, except that before the sample bomb containing the passivated powder was placed in the constant volume apparatus, it was opened up to expose the bomb contents and placed in a constant humidity chamber at 50% relative humidity at 25°C (77°F) for 48 hours. After the exposure, the sample was evacuated in the constant volume system for 30 minutes before continuing the experiment.

The pressure changes plotted for the various experiments are directly comparable because the same sample size was always used and the system volume was always constant (430 ml total). Corrections to ΔP were applied for large variations in temperature of the unthermostatted parts of the constant volume apparatus. (It is impractical to thermostat the entire system, for example the gauge volume, hence minor corrections need to be applied for ambient temperature variations.)

b. Studies With Stainless Steel 316

The following results were obtained for stainless steel 316 alloy. Previous data indicate that a fluoride film of 14.2 Å thickness is formed in one hour exposure to fluorine at one atmosphere and at 27°C (80°F).

(1) Fluorine Passivation at One Atmosphere

The data are plotted in Figure 19. Curve 1 shows the change in pressure in the system due to uptake of fluorine by a fresh, unpassivated sample. Curve 2 is obtained after prior passivation for one hour at one atmosphere fluorine pressure at 27°C (80°F). On the basis of the criterion set forth above, the sample is completely passive by virtue of its lack of any further reaction with fluorine. After the same passivation, followed by exposure to 50% relative humidity in air, Curve 3 is obtained. The pressure

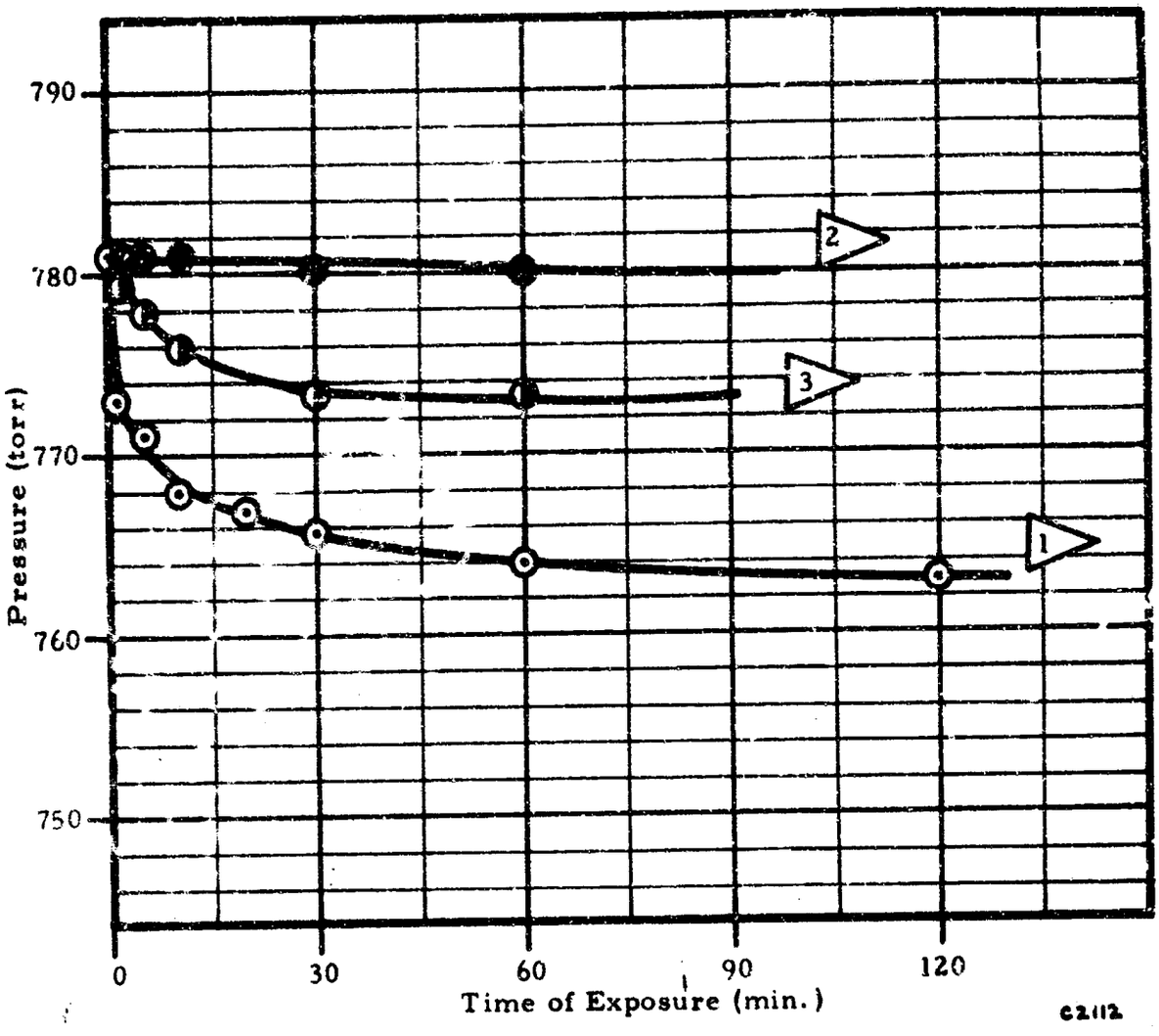

1 No prior passivation

2 Passivated in F_2 – 1 atm. – 1 hr. – 27°C (80°F)

3 Same as 2 plus exposure to 50% relative humidity at 25°C (77°F) for 48 hours

Figure 19. Exposure of Stainless Steel 316 Powder (100 g) to Fluorine – 27°C (80°F)

change after one hour is approximately 45% that of the unpassivated sample (Curve 1). The rate of reaction appears to be slower in the early stages as evidenced by the initially different negative slope of Curve 3 compared to Curve 1. This is a general observation for most of the later experiments and its significance will be discussed later.

(2) Fluorine Passivation at One Atmosphere With Incremental Build-Up of Pressure

This experiment is very similar to the one described in Paragraph (1) above except that instead of abruptly exposing the sample to fluorine at one atmosphere, the pressure is gradually built up in stages with evacuations between pressure increases. This is a common method of fluorine passivation. The technique is applied probably for two reasons: (1) it helps avoid runaway reaction caused by burning of organic contaminants, and (2) it helps avoid diffusion blocks in dead ends of systems or long runs of pipe or tubing. It is not known whether a better or more effective passive film is produced per se. The incremental pressure build-up was accomplished as follows:

Pump sample for 30 minutes

Pressurize with fluorine at 1 psia for 5 minutes – pump down

Pressurize with fluorine at 2 psia for 5 minutes – pump down

Pressurize with fluorine at 4 psia for 5 minutes – pump down

Pressurize with fluorine at 8 psia for 5 minutes – pump down

Pressurize with fluorine at 1 atmosphere for 60 minutes – pump down for 30 minutes

The results shown in Figure 20, Curve 2, indicate that the procedure results in complete passivation. Curve 3 shows a pressure change amounting to 65% of the first passivation after one hour. The somewhat greater sensitivity to moisture shown here perhaps reflects a slightly thicker fluoride film.

(3) Fluorine Passivation at Low Temperature

The data are plotted in Figure 21. The sample passivated at liquid nitrogen temperature (-195°C) in fluorine at 0.1 atmosphere for four hours continued to take up a small amount of fluorine as indicated by Curve 2. It is not conclusive that the passivation to the extent indicated took place at the low temperature. Adsorption of fluorine is expected to take place at liquid nitrogen temperature. The adsorbed fluorine may not have been completely removed by pumping, and as the sample warmed up, the adsorbed fluorine could have reacted with the metal surface. Curve 3 for the moisture exposed sample generally falls in line with the two previous experiments.

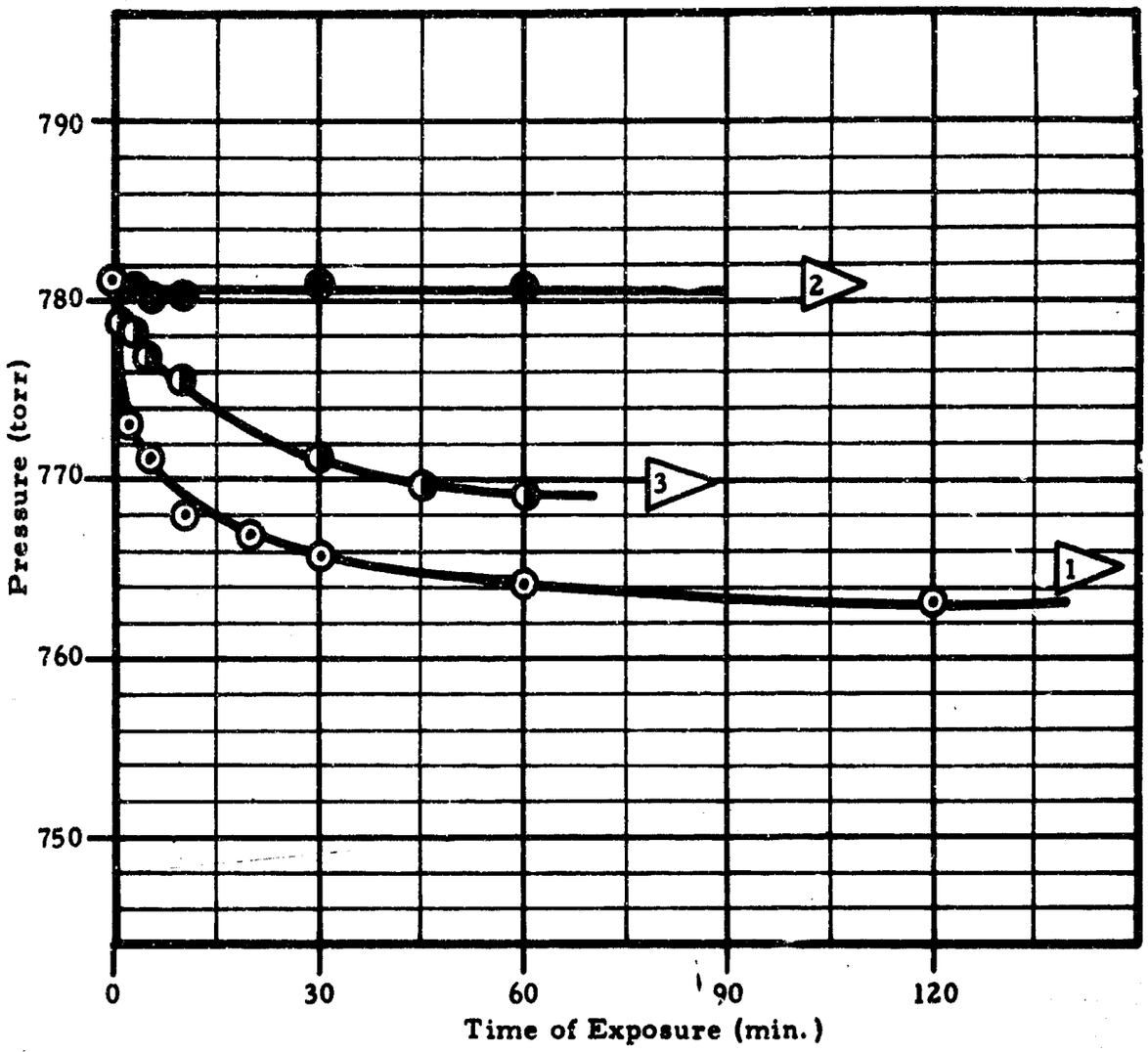

1 No prior passivation

2 Passivated in F_2 – 1 atm. – 1 hr. – 27°C (80°F) following incremental build-up of pressure (see text)

3 Same as 2 plus exposure to 50% relative humidity in air at 25°C (77°F) for 48 hours

Figure 20. Exposure of Stainless Steel 316 Powder (100 g) to Fluorine – 27°C (80°F)

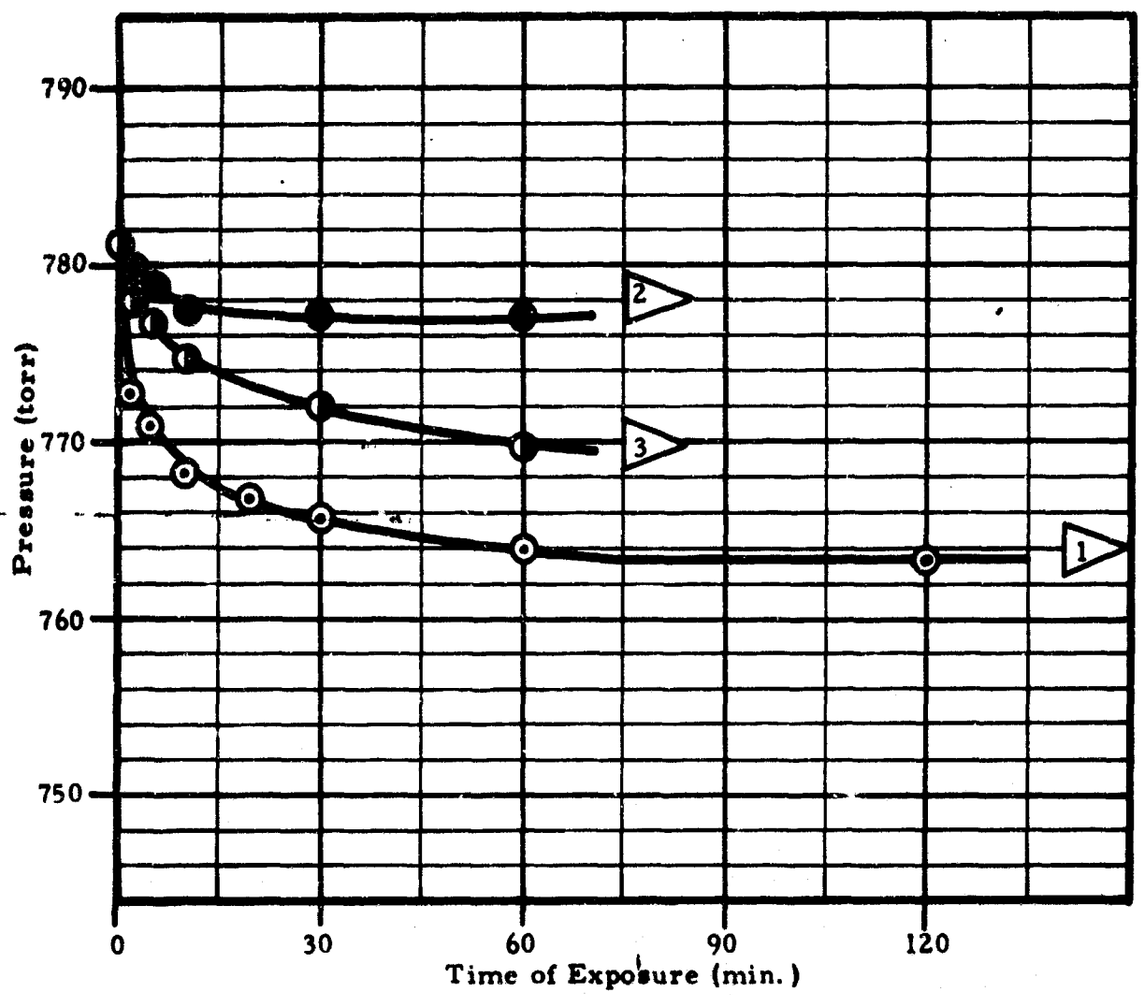

1 No prior passivation

2 Passivated in F_2 – 0.1 atm. – 4 hrs. – -195°C (-320°F)

3 Same as 2 except exposed to 50% relative humidity in air at 25°C (77°F) for 48 hours

Figure 21. Exposure of Stainless Steel 316 Powder (100 g) to Fluorine – 27°C (80°F)

(4) Passivation in Fluorine at High Pressure

Data for the samples passivated at 60 atmospheres (900 psi) in fluorine for one hour at 25°C (77°F) are presented in Figure 22. Curve 2 shows complete passivation and Curve 3 shows a relatively large pressure change for the humidity exposed sample. The pressure change amounts to 75% of that for a fresh sample after one hour exposure. This observation is in line with the belief that a thicker film would be formed at the high pressure. If the cube root dependence between pressure and apparent fluoride film thickness, as established for nickel, holds for stainless steel 316, a film approximately four times thicker should be formed at 60 atmospheres than at one atmosphere.

(5) Passivation by Chlorine Pentafluoride (ClF_5)

Figure 23 gives data for samples passivated in ClF_5 vapor at one atmosphere for one hour at 27°C (80°F). Curve 2 reveals that a sample so passivated takes up a small amount of fluorine but in a very peculiar manner. There is almost a linear decrease of pressure with time rather than the usual curve convex to the abscissa. Curve 3 is similar to Curve 2, indicating relatively little sensitivity of the passive film to moisture. It is unfortunate that technical difficulties prevented carrying these curves to longer intervals of time.

(6) Passivation by ClF_5 at Higher Temperature

In this set of experiments the ClF_5 passivation was carried out at 71°C (160°F). As the plots in Figure 24 show, the character of the passive film is completely changed. Complete passivation is indicated by Curve 2 while great sensitivity to moisture is revealed by Curve 3. The uptake of fluorine exceeds that for a fresh sample (Curve 1) by 50%.

(7) Passivation by Chlorine Trifluoride

The sample passivated in chlorine trifluoride vapor at one atmosphere for one hour at 27°C (80°F), appeared to be completely passivated as evidenced by the horizontal Curve 2 of Figure 25. The sample exposed to water vapor took up over 85% as much fluorine as a fresh sample indicating considerable sensitivity to water vapor. The passivation in chlorine trifluoride was in each case followed by pumping while the sample was heated to 71°C (160°F); therefore, retention of adsorbed chlorine trifluoride on the sample should not be excessive.

(8) Passivation in Bromine Pentafluoride

Passivation in bromine pentafluoride vapor was investigated. The data are presented in Figure 26. The rather unexpected observation was that the samples took up very large quantities of fluorine, both before and after exposure to humidity. Approximately three times as much fluorine is consumed as for the unpassivated sample. There is a strong

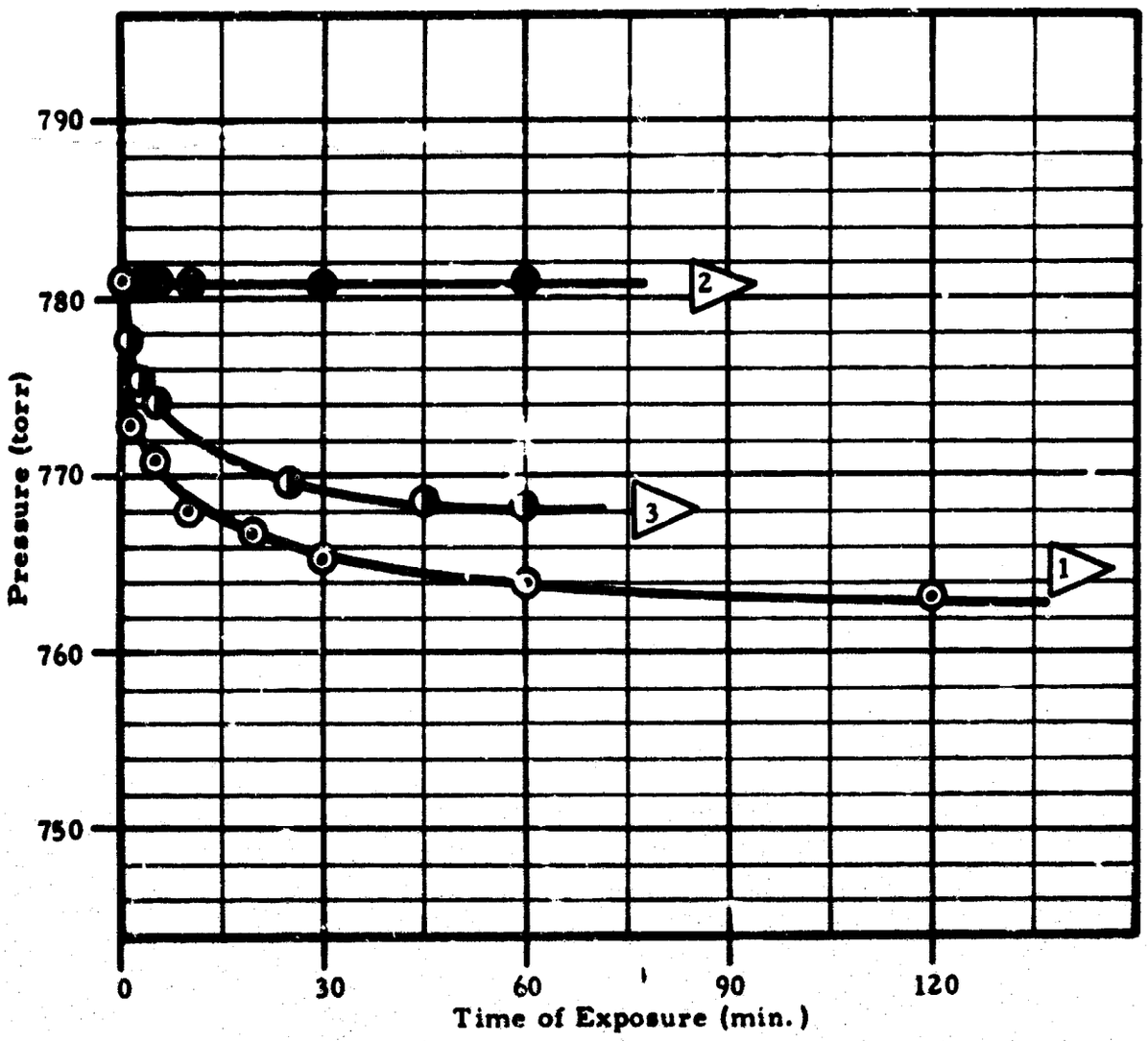

1 No prior passivation

2 Passivated in F_2 – 60 atm. – 1 hr. – 25°C (77°F)

3 Same as 2 except after passivation exposed to 50% relative humidity in air at 25°C (77°F) for 48 hours

Figure 22. Exposure of Stainless Steel 316 Powder (100 g) to Fluorine – 27°C (80°F)

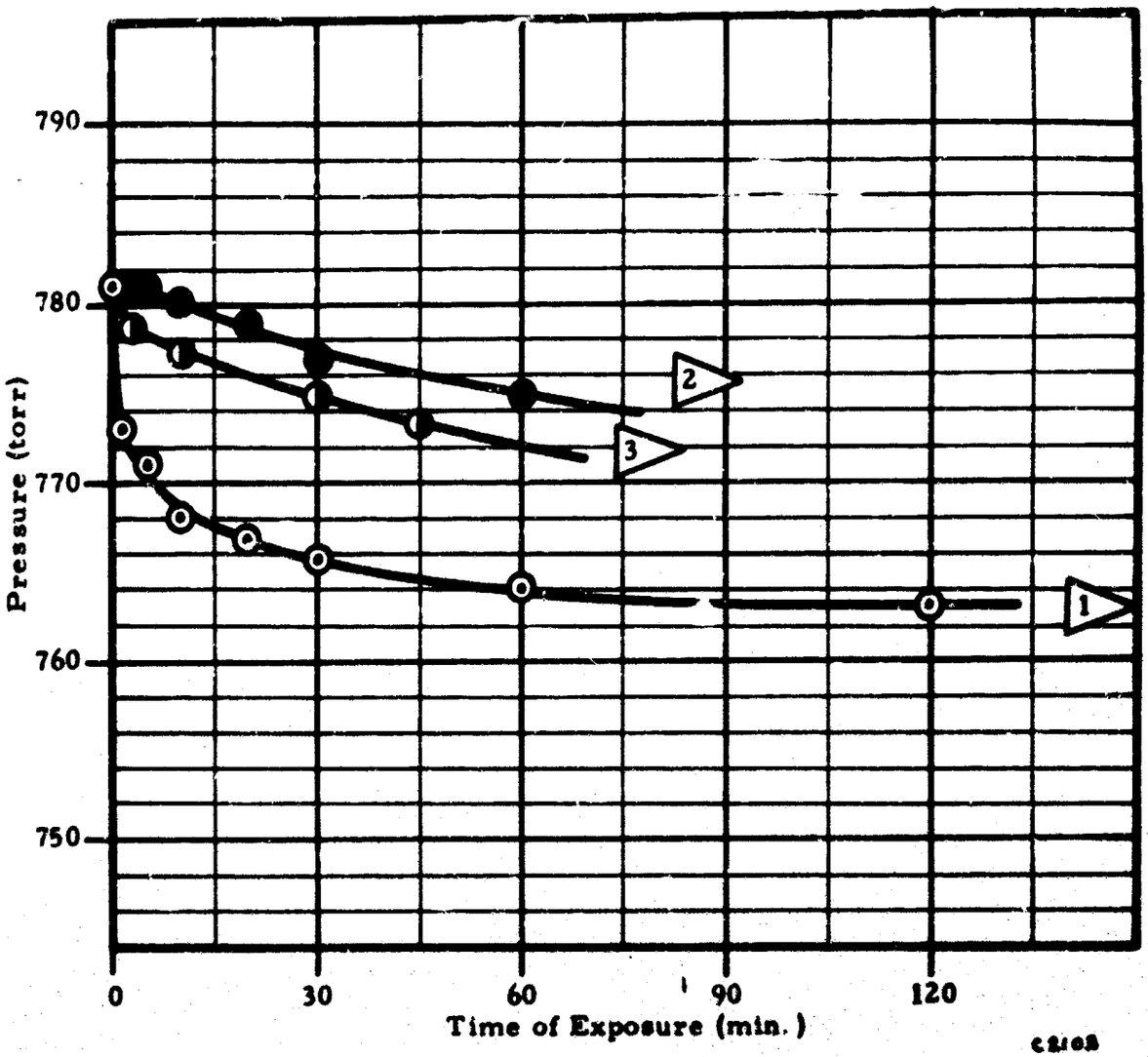

1 No prior passivation

2 Passivated in Compound A vapor – 1 atm. – 1 hr. – 27°C (80°F)

3 Same as 2 except followed by exposure to 50% relative humidity in air at 25°C (77°F) for 48 hours

Figure 23. Exposure of Stainless Steel 316 Powders (100 g) to Fluorine – 27°C (80°F)

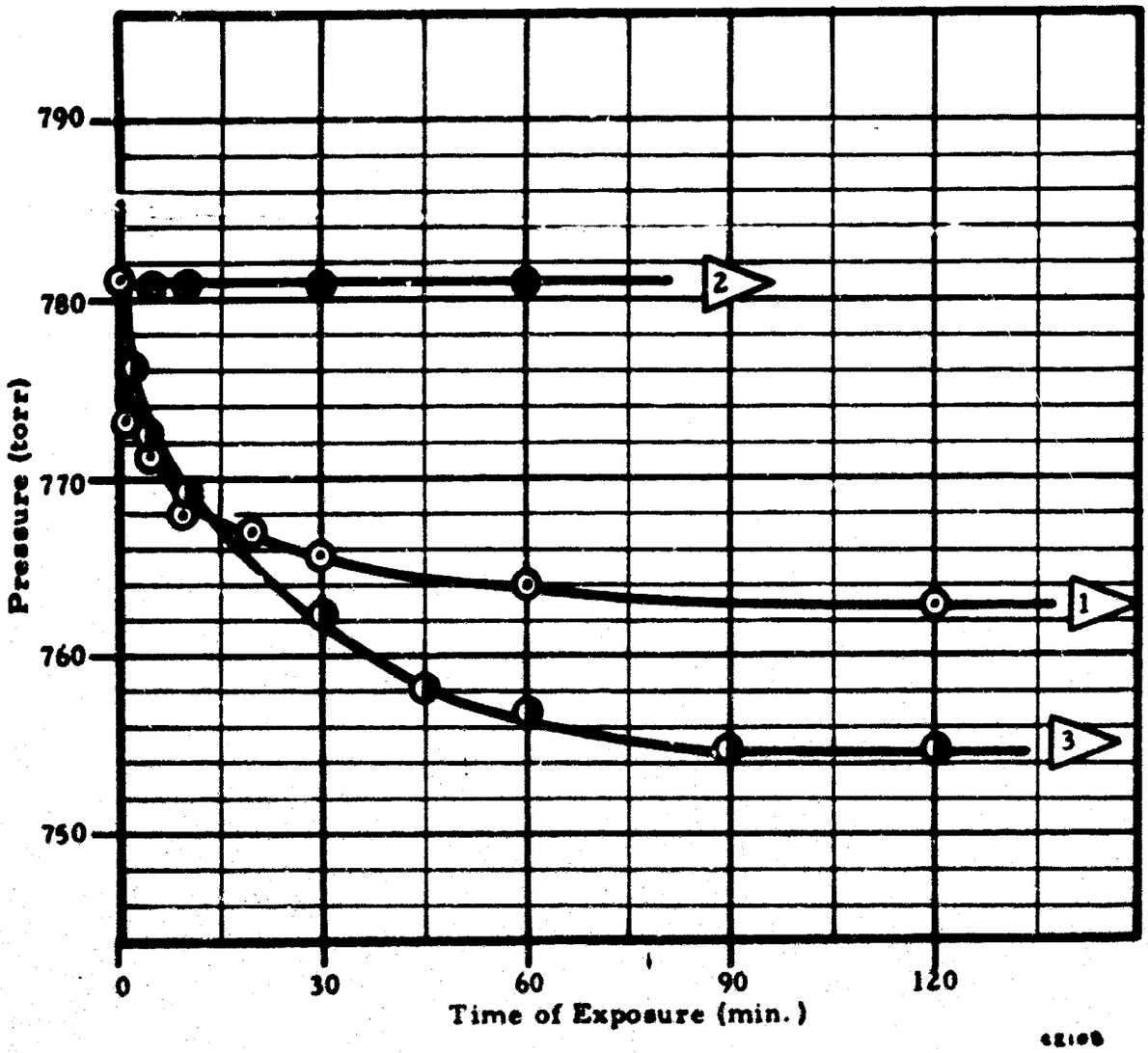

1 No prior passivation

2 Passivated in Compound A vapor – 1 atm. – 1 hr. – 71°C (160°F)

3 Same as 2 except followed by exposure to 50% relative humidity in air at 25°C (77°F) for 48 hours

Figure 24. Exposure of Stainless Steel 316 Powder (100 g) to Fluorine – 27°C (80°F)

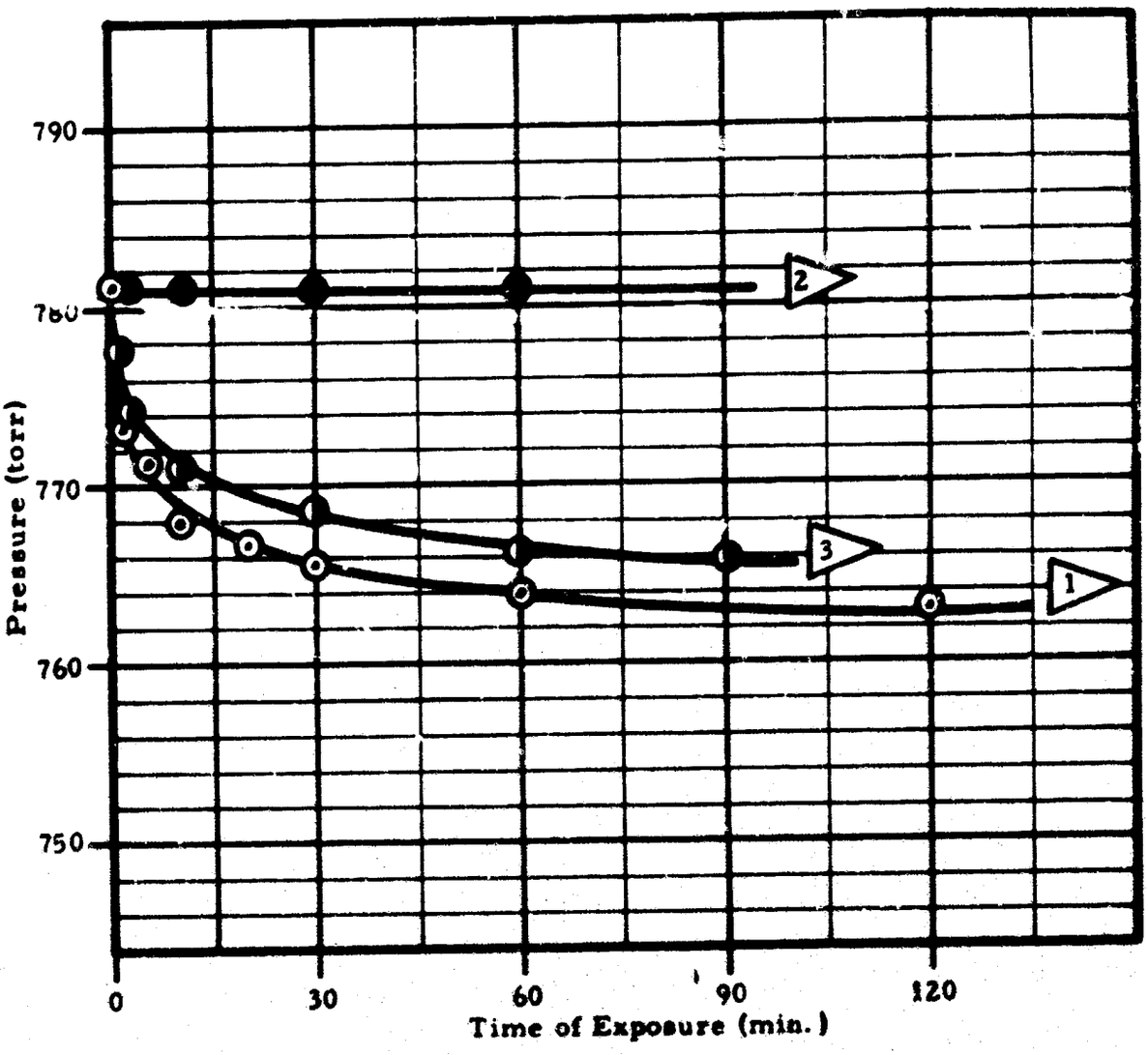

1 No prior passivation

2 Passivated in chlorine trifluoride vapor – 1 atm. – 1 hr. – 27°C (80°F)

3 Same as 2 except followed by exposure to 50% relative humidity in air at 25°C (77°F) for 48 hours

Figure 25. Exposure of Stainless Steel 316 Powder (100 g) to Fluorine – 27°C (80°F)

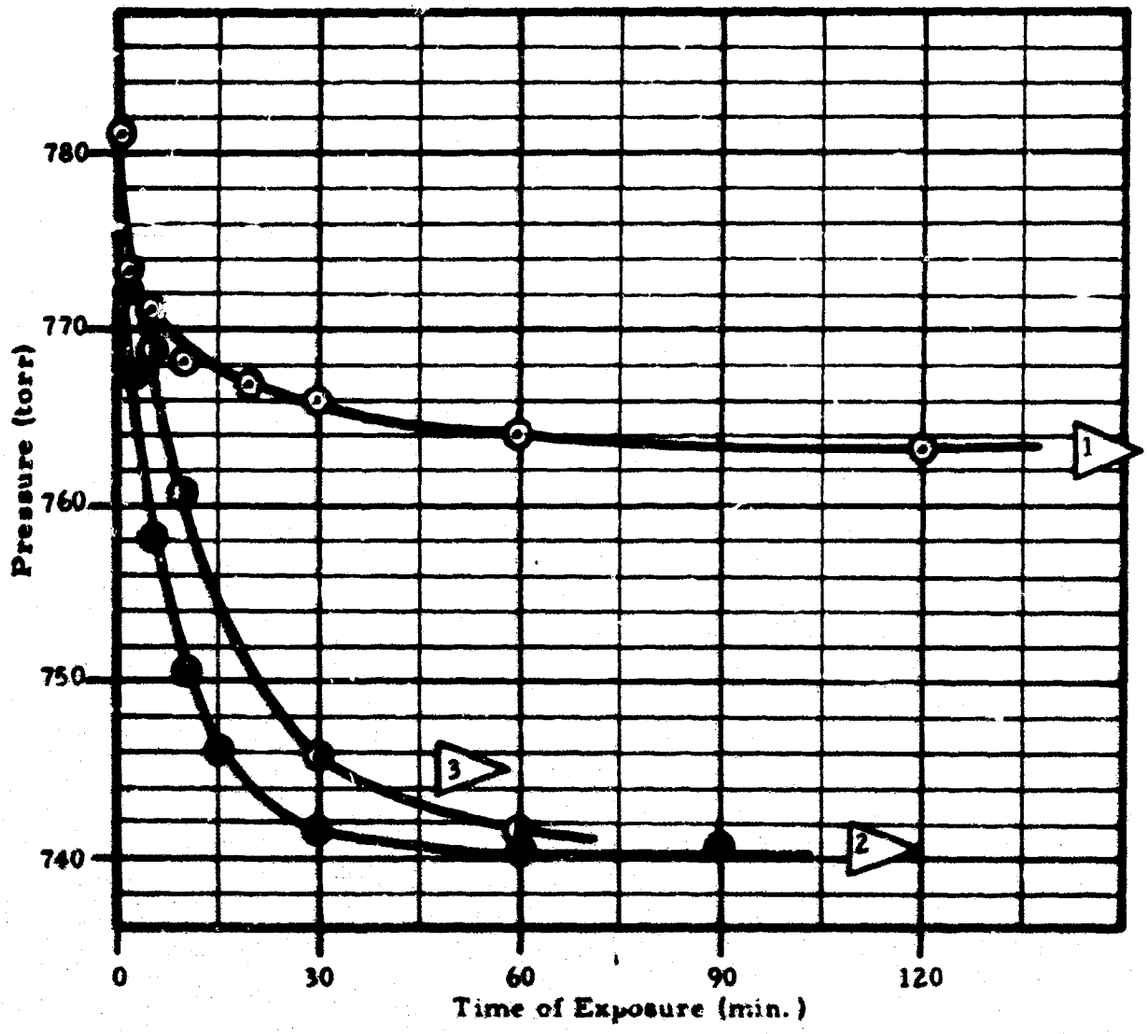

ca106

1 No prior passivation

2 Passivation in bromine pentafluoride vapor – 0.4 atm. – 1 hr. – 27°C (80°F)

3 Same as 2 except followed by exposure to 50% relative humidity in air at 25°C (77°F) for 48 hours

Figure 26. Exposure of Stainless Steel 316 Powder (100 g) to Fluorine – 27°C (80°F)

implication that by reaction with metal, or by dissociation, a relatively large amount of bromine trifluoride is left in the sample which subsequently reacts with fluorine. Bromine trifluoride, if present, would not be readily removed by pumping at 71°C (160°F) – the temperature employed here.

c. Studies With Monel

The results described in the following paragraphs were obtained with Plasmadyne Monel 206F. Previous results have shown that a fluoride film thickness of 13.4 Å is formed in one hour in fluorine at one atmosphere at 27°C (80°F).

(1) Fluorine Passivation at One Atmosphere

The curves are given in Figure 27. Curve 1 is the pressure change as a function of time for a fresh sample. After passivation in fluorine for one hour at one atmosphere, Curve 2 is obtained. There is a gradual, almost linear decrease in pressure with time but this seems to be normal for Monel. All previous work with Monel reveals that it continues to react with fluorine almost indefinitely so far as known. Unlike stainless steels and nickel, the pressure changes continuously with time. A fairly large moisture sensitivity is indicated by Curve 3.

(2) Fluorine Passivation With Incremental Build-Up of Pressure

The data are given in Figure 28 and are essentially identical to the results given in Paragraph (1) above.

(3) Fluorine Passivation at Low Pressure

Passivation was carried out in fluorine at 0.1 atmosphere for one hour at 27°C (80°F). This was the first time a low pressure passivation was attempted near room temperature. In view of the apparent complete passivation obtained (see Curve 2, Figure 29) and the lower sensitivity to moisture revealed by Curve 3, this passivation technique deserves further consideration.

(4) Passivation in ClF_5 Vapor

Passivation in ClF_5 vapor at one atmosphere for one hour at 27°C (80°F) yielded results shown in Figure 30. The results were very similar to those obtained by fluorine passivation under similar conditions.

(5) Passivation in Chlorine Trifluoride Vapor

The data are given in Figure 31. Somewhat lower moisture sensitivity was observed than for Compound A and fluorine under similar conditions of passivation.

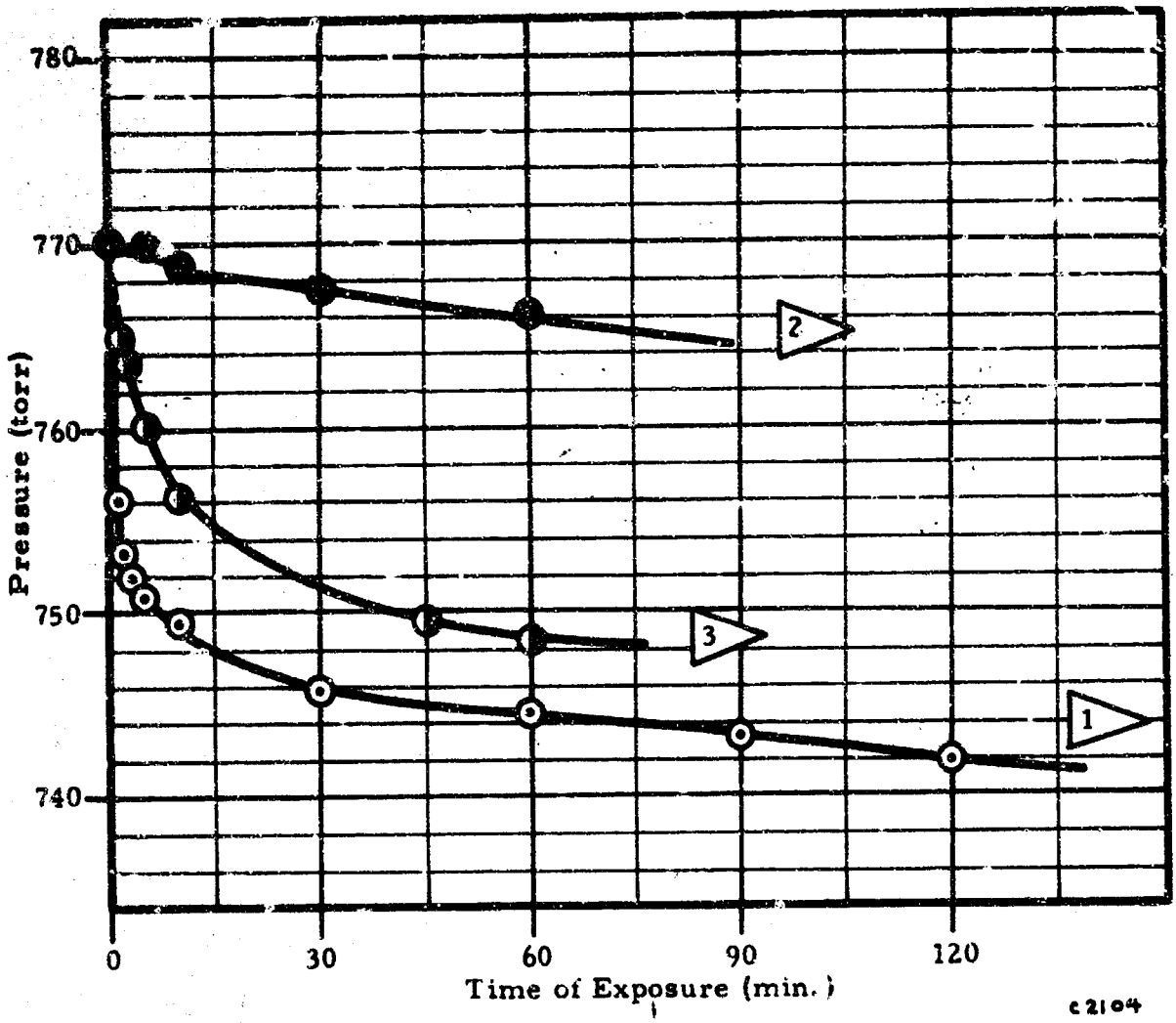

1 No prior passivation

2 Passivation in fluorine gas – 1 atm. – 1 hr. – 27°C (80°F)

3 Same as 2 except followed by exposure to 50% relative humidity in air at 25°C (77°F) for 48 hours

Figure 27. Exposure of Monel Powder (100 g) to Fluorine – 27°C (80°F)

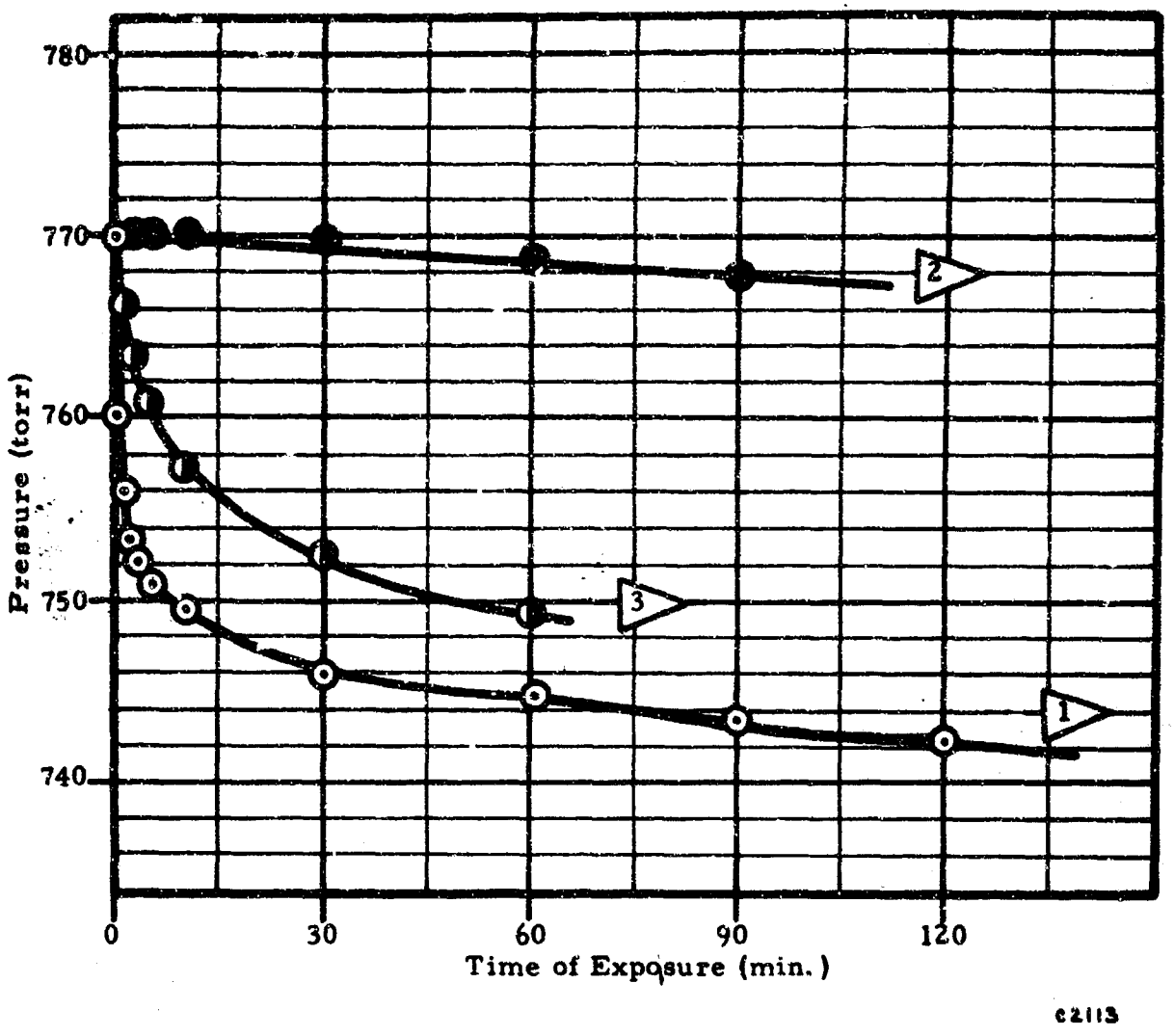

1 No prior passivation

2 Passivated in fluorine gas – 1 atm. – 1 hr. – following incremental build-up of pressure (see text for details)

3 Same as 2 except followed by exposure to 50% relative humidity in air at 25°C (77°F) for 48 hours

Figure 28. Exposure of Monel Powder (100 g) to Fluorine – 27°C (80°F)

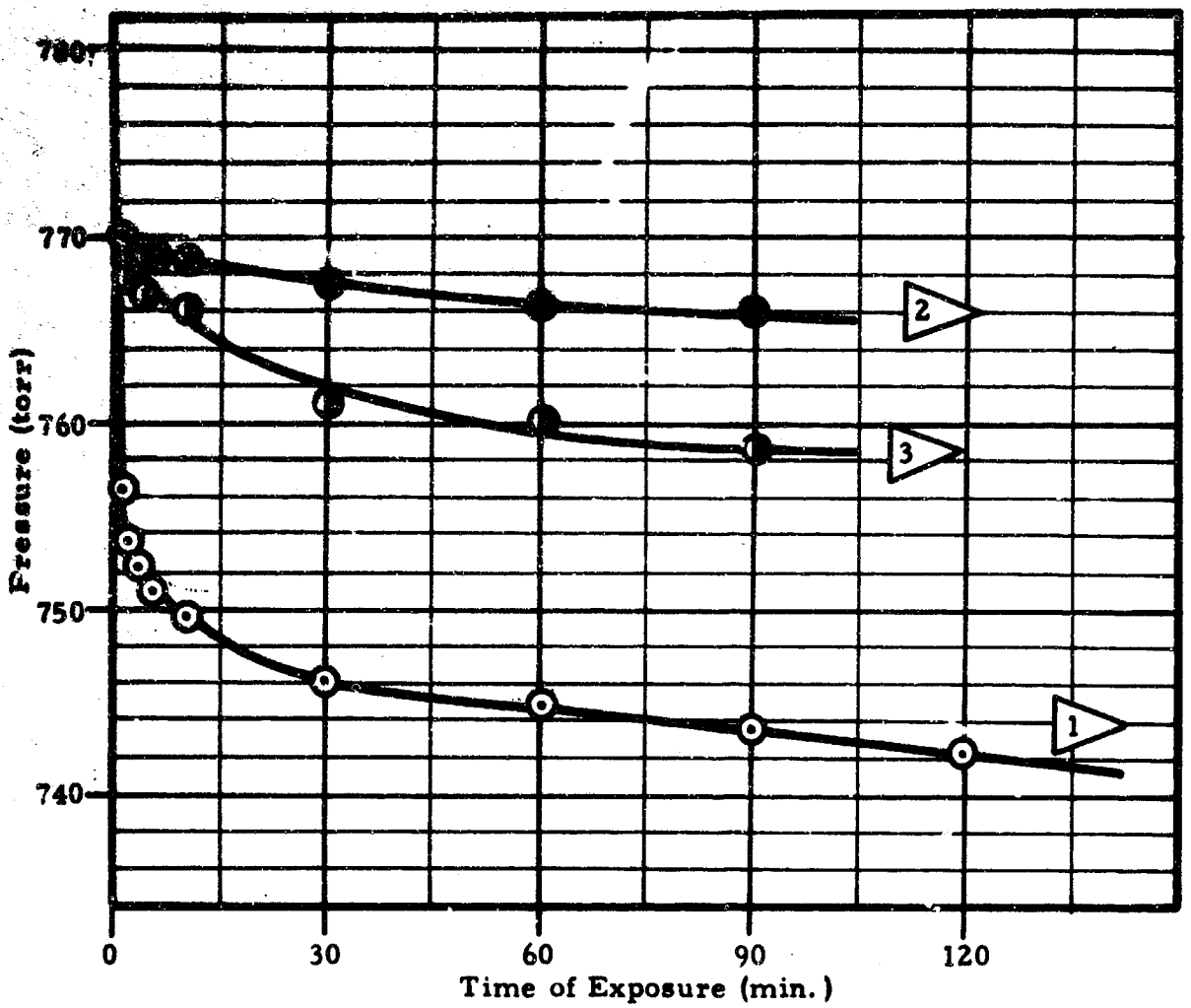

1 No prior passivation

2 Passivated in fluorine gas – 0.1 atm. – 1 hr. – 27°C (80°F)

3 Same as 2 except followed by exposure to 50% relative humidity in air at 25°C (77°F) for 48 hours

Figure 29. Exposure of Monel Powder (100 g) to Fluorine – 27°C (80°F)

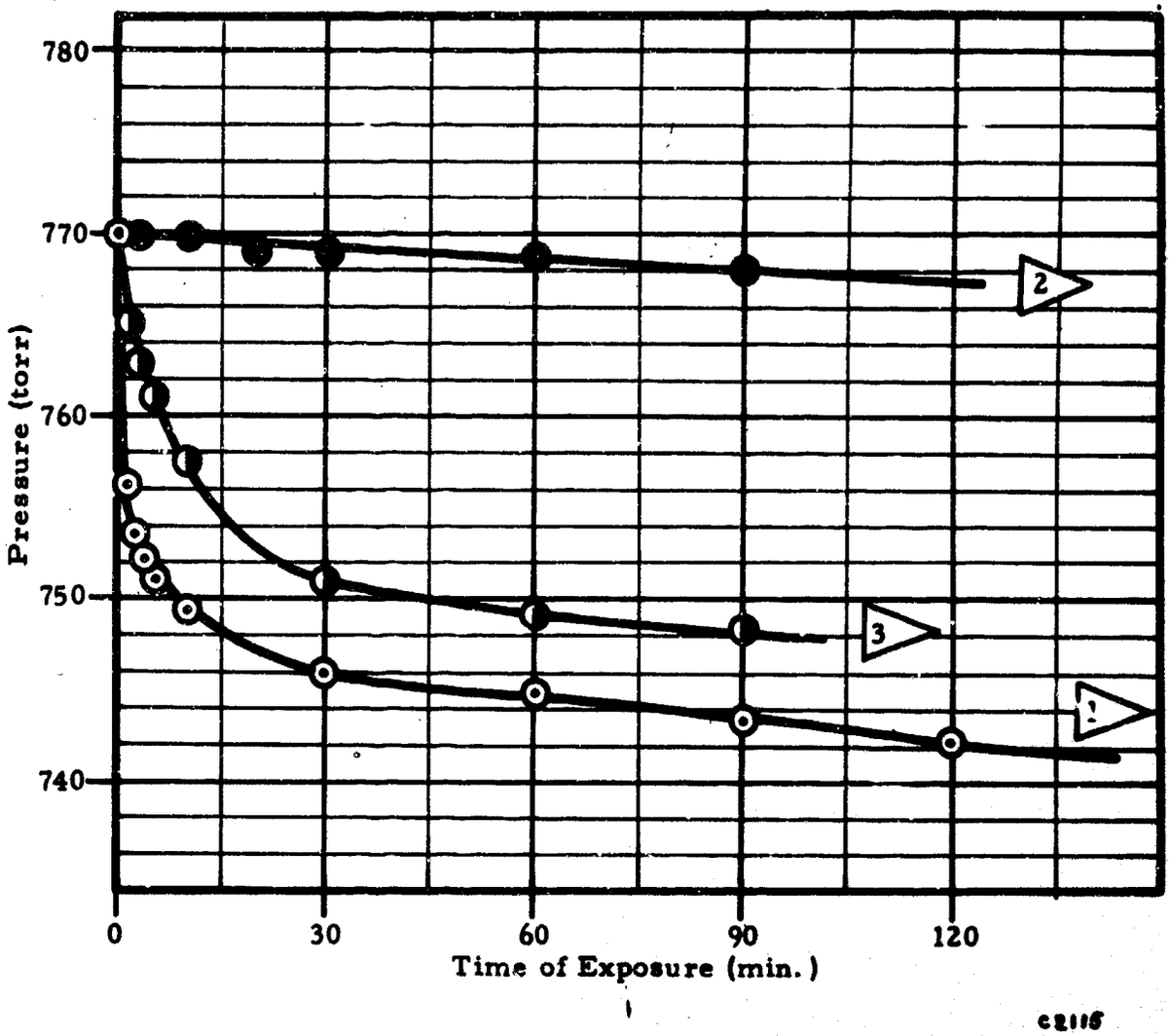

1 No prior passivation

2 Passivated in Compound A vapor – 1 atm. – 1 hr. – 27°C (80°F)

3 Same as 2 except followed by exposure to 50% relative humidity in air at 25°C (77°F) for 48 hours

Figure 30. Exposure of Monel Powder (100 g) to Fluorine – 27°C (80°F)

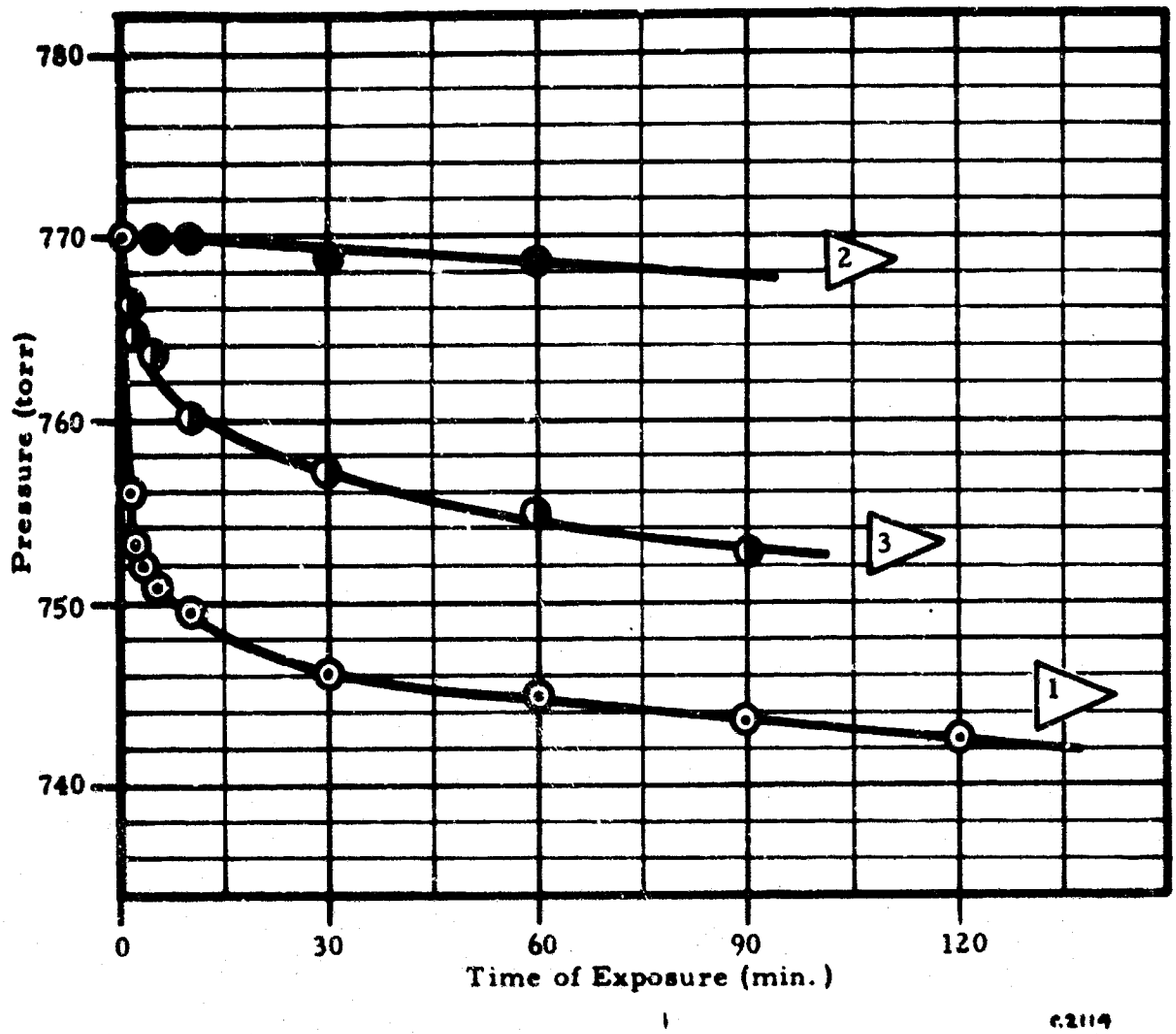

1 No prior passivation

2 Passivated in chlorine trifluoride vapor – 1 atm. – 1 hr. – 27°C (80°F)

3 Same as 2 except followed by exposure to 50% relative humidity in air at 25°C (77°F) for 48 hours

Figure 31. Exposure of Monel Powder (100 g) to Fluorine – 27°C (80°F)

d. Studies With 2024 Aluminum

The following results are reported for 2024 aluminum powder. Twenty gram samples were used. Previous results indicate that a fluoride film thickness of 8.4 Å is formed in one hour exposure to fluorine at one atmosphere pressure at 27°C (80°F).

The experimental data are plotted in Figure 32. Curve 1 is the normal change in system pressure due to reaction of fluorine with a fresh, unpassivated 20 gram sample. The upper curve is obtained after prior passivation in fluorine gas at one atmosphere pressure for one hour at 27°C (80°F). The sample, following this passivation treatment, takes up essentially no additional fluorine gas except a very small amount which might be attributed to an adsorption effect. After passivation, followed by exposure to 50% relative humidity in air, the same curve was obtained. Curve 2 and 3 are superimposable. On the basis of these observations, exposure of the aluminum alloy to moisture does not affect it insofar as any subsequent reaction with fluorine is concerned.

The same results were observed for 2024 aluminum samples which were passivated in chlorine pentafluoride and chlorine trifluoride vapor at one atmosphere for one hour at 27°C (80°F). The data are not plotted because the curves are identical to those given in Figure 32.

e. Studies With Nickel 200

The results in this section are reported for 80 gram samples of nickel 200 powder. A fluoride film thickness of approximately 22 Å should be formed by exposure to fluorine gas for one hour at one atmosphere and 27°C (80°F).

The data presented in Figures 33, 34, 35, and 36 cover passivations in chlorine trifluoride, fluorine (0.1 and one atmosphere pressure) and chlorine pentafluoride. In all passivations a moderate sensitivity to moisture is evident. Approximately 10 to 20 per cent as much fluorine reacts as in the initial passivation.

f. Studies With Copper

Data were obtained for 60 gram samples of copper powder. Copper exposed to fluorine gas for one hour at one atmosphere pressure and at 27°C (80°F) has an estimated equivalent fluoride film thickness of 13.1 Å although the method of calculation is open to question inasmuch as the exact reaction is not known.

Figure 37 covers data for passivation in fluorine at 27°C (80°F). Curve 3 shows that the fluoride film is very sensitive to moisture. A sample which was passivated in fluorine then exposed to 50% relative humidity in air took up additional fluorine as shown in Curve 3. An initial rapid reaction is followed by an extended linear portion.

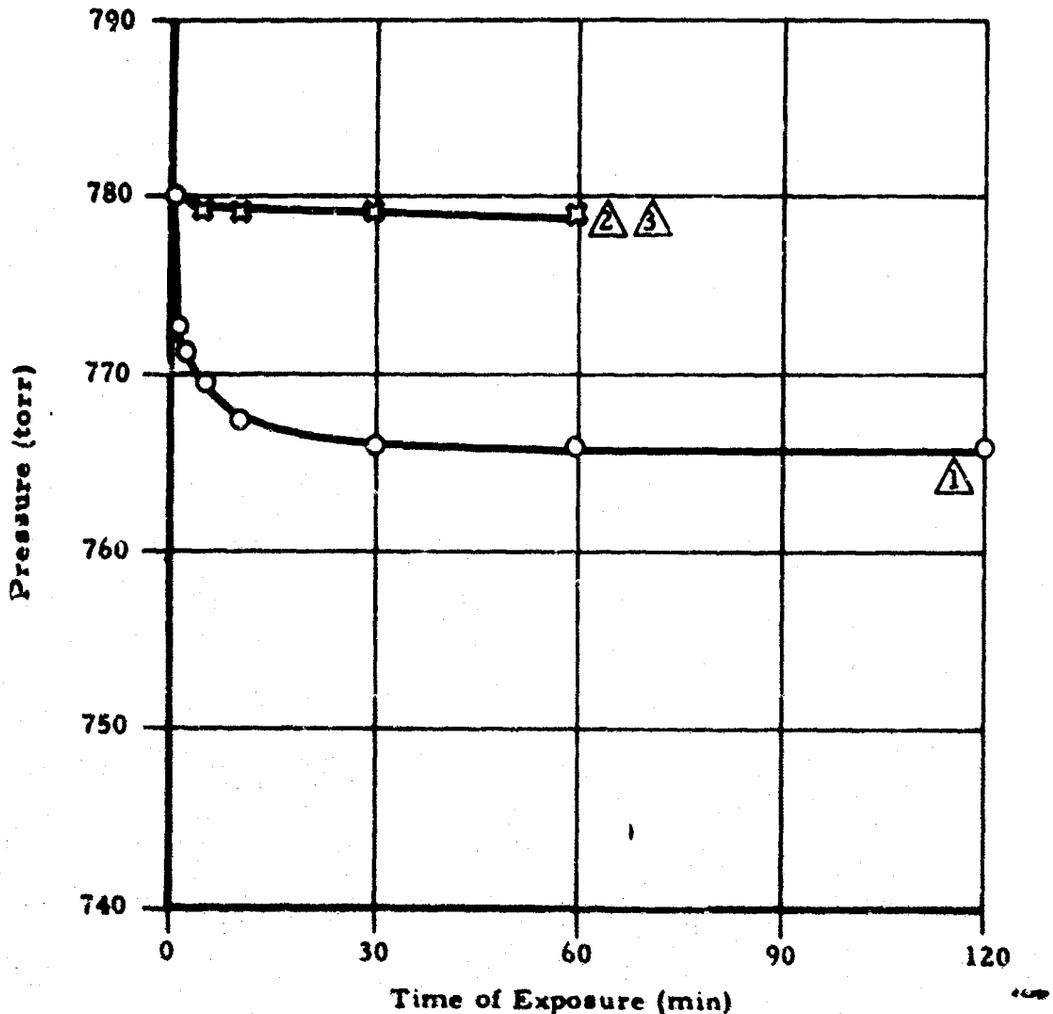

1 No Prior Passivation
2 Passivated in Fluorine - 1 hr - 1 atm 27°C (80°F)
3 Same as 2 except exposed to 50% R. H. in air at 25°C for 48 hours

Figure 32. Exposure of 2024 Al Powder (20g) to Fluorine at 27°C (80°F)

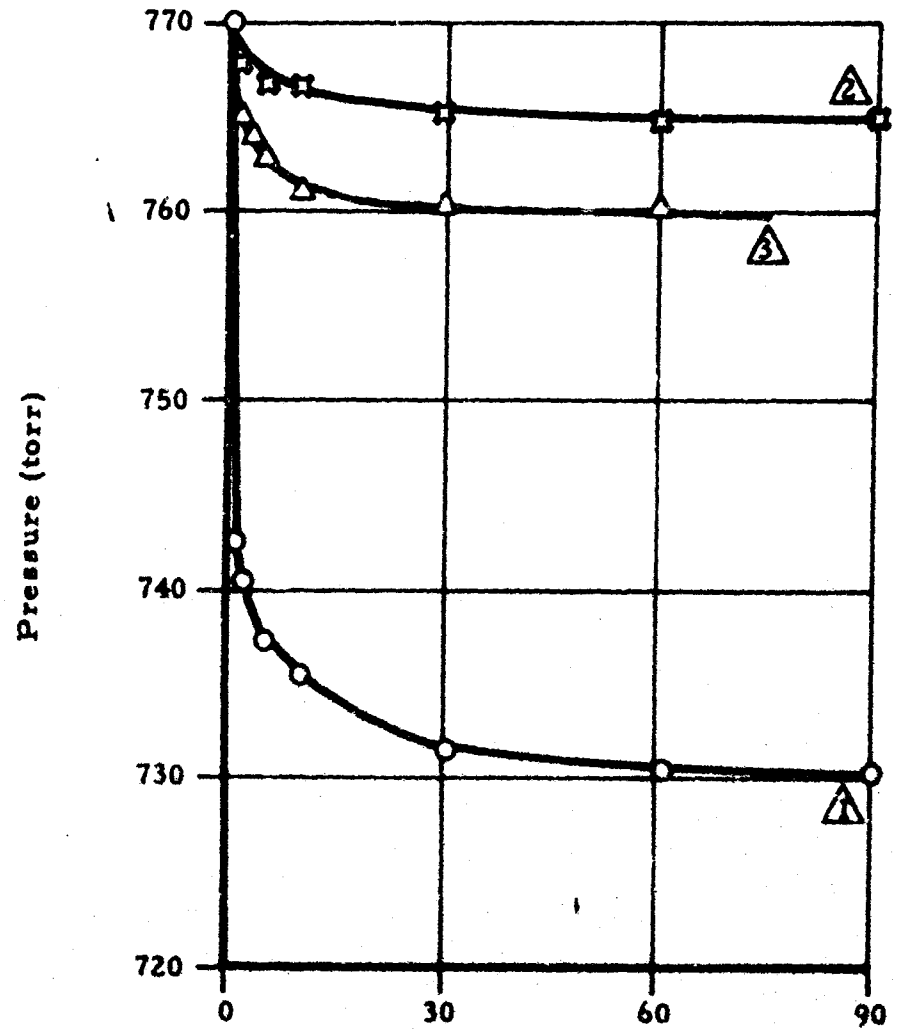

1 No Prior Passivation

2 Passivated in Chlorine Trifluoride - 1 hr - 1 atm - 27°C(80°F)

3 Same as 2 except exposed to 50% R. H. in air at 25°C (77°F) for 48 hours

Figure 33. Exposure of Nickel 200 Powder (80g) to Fluorine at 27°C (80°F)

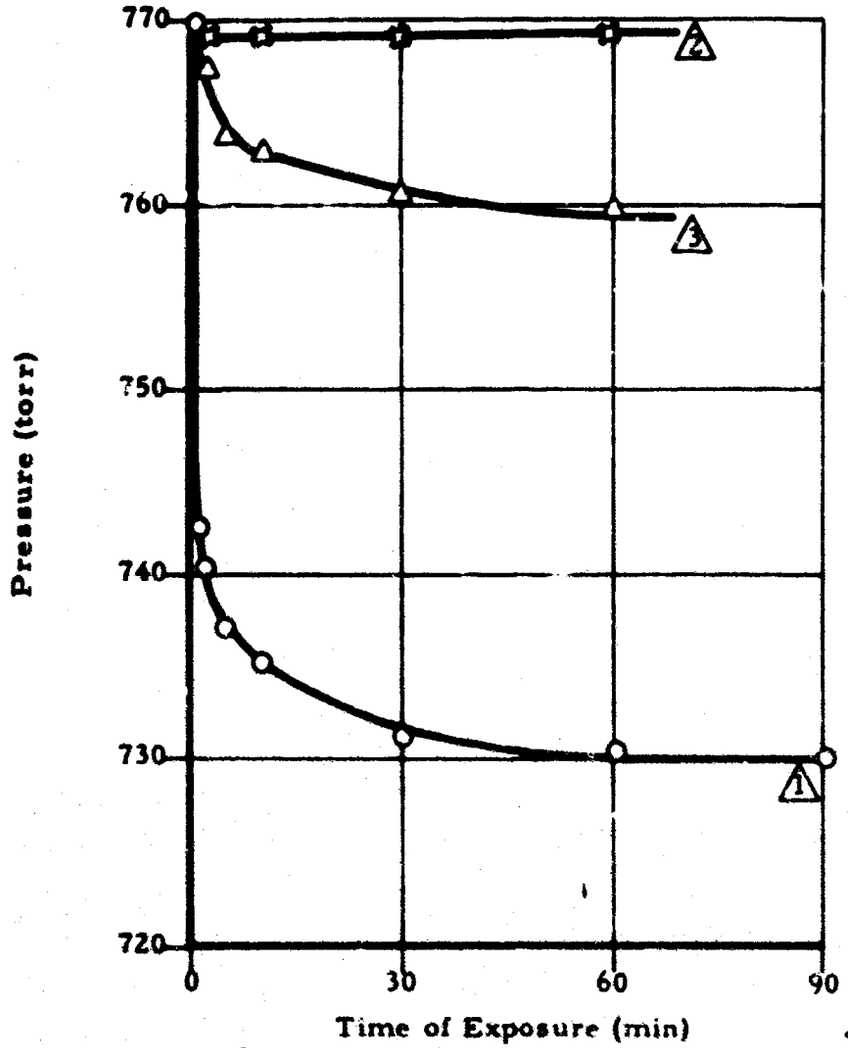

1 No Prior Passivation

2 Passivated with Fluorine - 0.1 atm - 1 hr - 27°C (80°F)

3 Same as 2 except exposed to 50% R.H. in air at 25°C(77°F) for 48 hours

Figure 34. Exposure of Nickel 200 Powder (80g) to Fluorine at 27°C(80°)

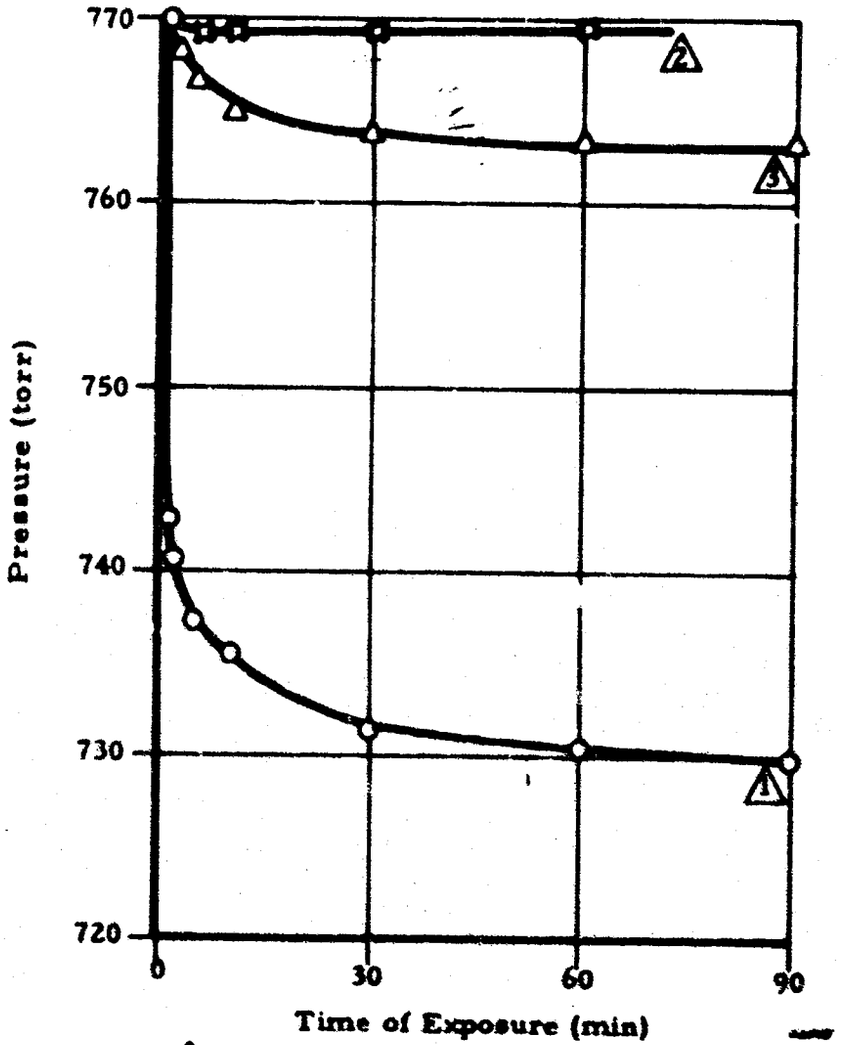

1 No Prior Passivation

2 Passivated in Fluorine - 1 hr - 1 atm - 27°C (80°F)

3 Same as 2 except exposed to 50% R. H. - in air at 25°C (77°F) for 48 hours

Figure 35. Exposure of Nickel 200 Powder (80g) to Fluorine at 27°C (80°F)

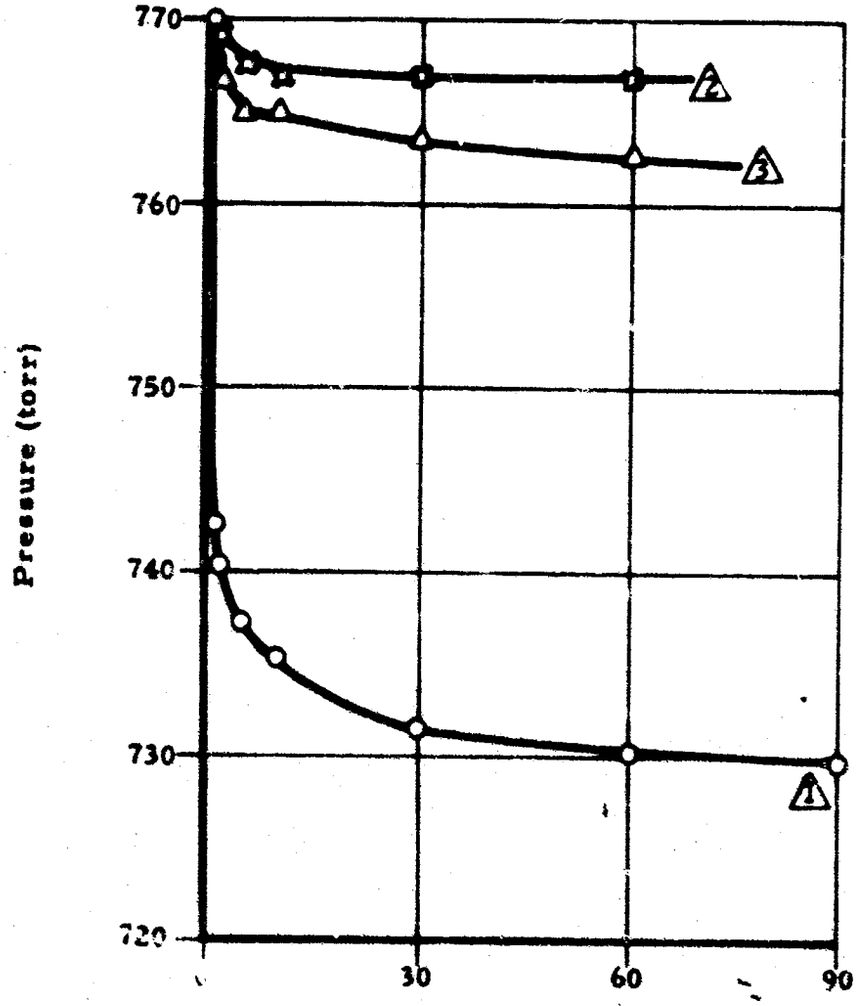

1 No Prior Passivation

2 Passivated in Comp. "A" Vapor - 1 hr - 1 atm - 27°C(80°F)

3 Same as 2 except exposed to 50% R. H. in air at 25°C(77°F) for 48 hours

Figure 36. Exposure of Nickel 200 Powder (80g) to Fluorine at 27°C(80°F)

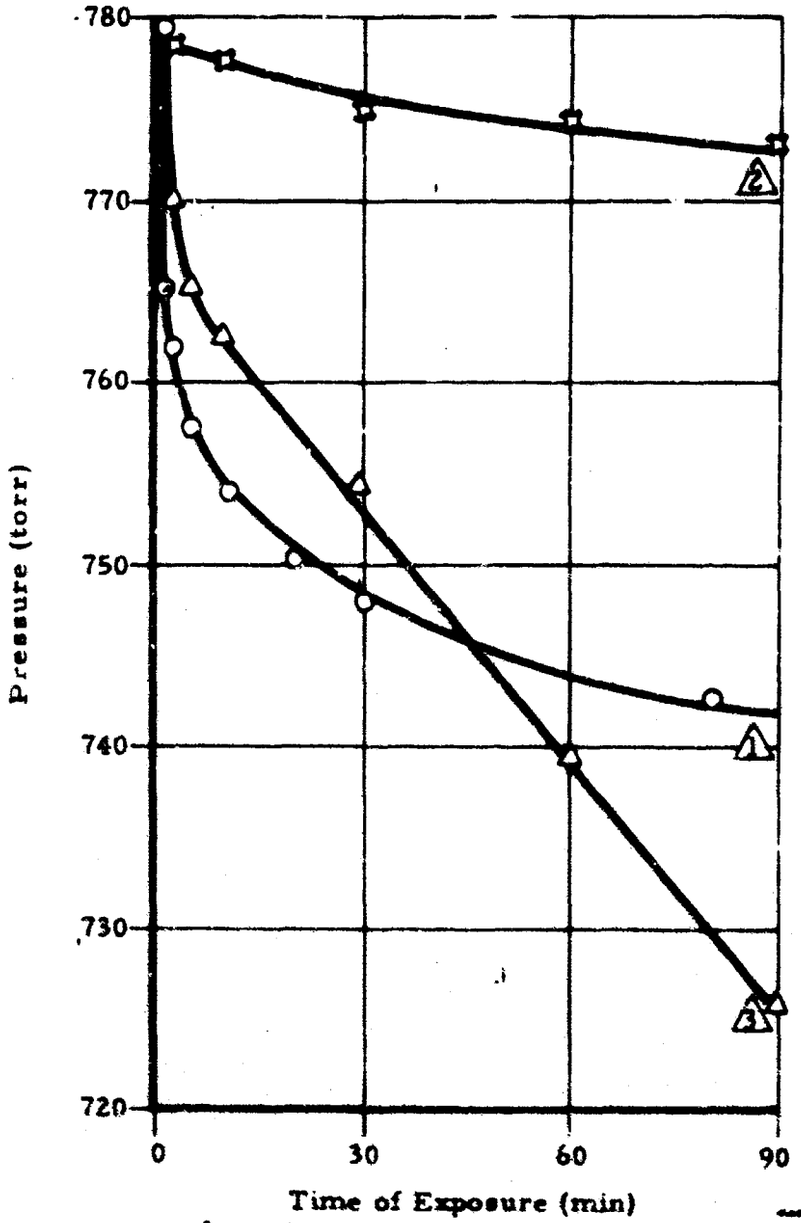

1 No Prior Passivation

2 Passivated in Fluorine - 1 hr - 1 atm - 27°C (80°F)

3 Same as 2 except exposed to 50% R. H. in air at 25°C (77°F) for 48 hours

Figure 37. Exposure of Copper (60g) to Fluorine at 27°C (80°F)

The same general trend is noted with the copper sample passivated in fluorine at 0.1 atmosphere pressure, as shown by the plots in Figure 38, although the extended linear portion of the curve has a different slope than shown in the preceding Figure 37. Of all the materials tested, copper shows the greatest corrosion after exposure of the fluoride film to moisture.

g. General Comments

The secondary corrosion of materials which have been passivated, exposed to moisture, then exposed to fluorine again is seen to vary greatly. For 2024 aluminum there is no detectable secondary corrosion. Copper suffers almost a catastrophic secondary corrosion. Nickel 200, 316 stainless steel and Monel 400 are intermediate and fall approximately in the order given for decreasing resistance to secondary corrosion.

The rates of secondary corrosion generally do not appear to be the same as the initial rates of fluoride film formation, the former generally having a lower rate. This implies that a completely different mechanism is operative.

6. ELECTROCHEMICAL STUDIES

Several electrode polarization experiments have been conducted using the apparatus shown in Figure 4. The most noteworthy observation has been the marked difference between the anodic current for a fresh nickel electrode and one which has been passivated in fluorine gas for 24 hours. A freshly prepared nickel 200 working electrode was rinsed in concentrated hydrochloric acid, then in distilled water, and dried. It was polarized in bromine trifluoride at +3.00 volts with respect to the platinum reference electrode. The anodic current between the nickel working electrode and the platinum counter electrode was measured as a function of time of immersion of the electrodes. The anodic current was observed to fall, rapidly at first and then more slowly, from an initial value in excess of 3 ma/cm^2 to reach a limiting current density of about 0.3 ma/cm^2 in approximately one hour. The data are plotted in Figure 39, Curve I.

The same nickel electrode was rewashed in acid and water, dried and again returned to the cell, and the polarization repeated. The second set of data gave Curve II, in general agreement with the first curve except that final current density was somewhat smaller.

The working electrode was again subjected to the same preparatory procedure as before, returned to the cell, and exposed to fluorine gas at one atmosphere at room temperature for 24 hours. Upon repeating the current density-time experiment, the maximum current density was only slightly over 0.03 ma/cm^2, and it fell rapidly in only six to eight minutes to reach a limiting current density of about 0.007 ma/cm^2. Therefore, the fluorine-passivated electrode yielded an anodic current of only a few per cent of that of an unpassivated electrode under the same polarizing voltage. The data are shown in Curve III.

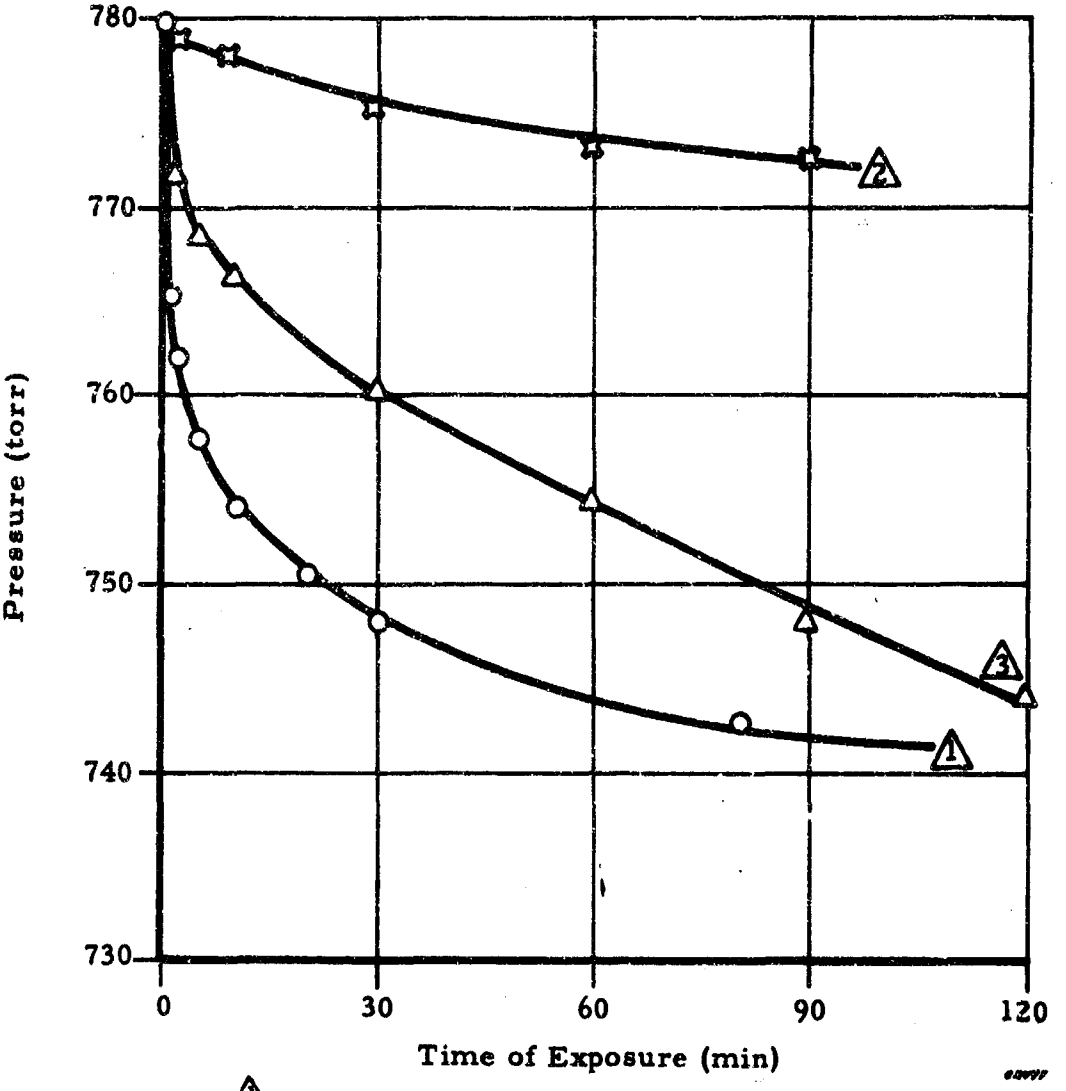

1 No Prior Passivation

2 Passivated in Fluorine - 1 hr - 0.1 atm - 27°C (80°F)

3 Same as 2 except exposed to 50% R.H. in air at 25°C (77°F) for 48 hours

Figure 38. Exposure of Copper Powder (60g) to Fluorine at 27°C (80°F)

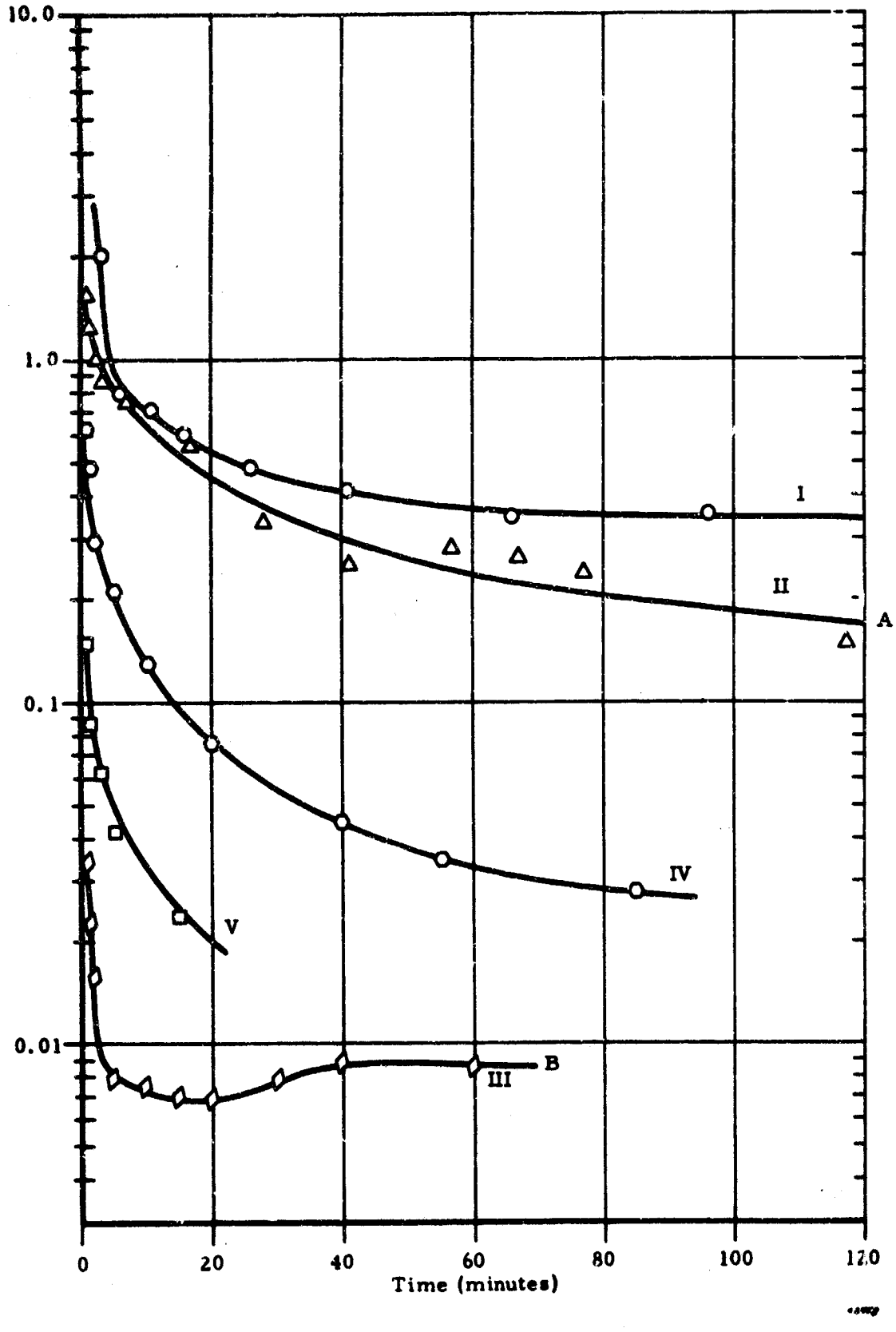

Figure 39. Anodic Current Density Curves for Nickel Electrodes in BrF_3

To test the effect of subsequent treatment on a passive surface, the working electrode was removed from the cell, rinsed copiously with distilled water, vacuum dried, and returned to the cell. The current density-time data following this treatment are shown on Curve IV. Although the magnitude of the current density is different from Curves I and II, the shape of the curves are similar.

The same electrode was then given an HCl rinse, followed by a water rinse, in the expectation that the electrode would return to a condition near that revealed by Curves I or II. However, the observed current density-time curve is shown at Curve V. Unfortunately due to time limitations, the limiting current density was not reached.

It is evident from the data that the initial as well as the approximately limiting current densities vary considerably depending on the surface treatment and history of the electrode. The results with the fluorine treated nickel electrode seem to be unique, however, in that the decrease in current density is very fast.

A similar procedure was applied to 316 stainless steel and Monel. Test electrodes (10 x 10 mm) were etched in hydrochloric acid, rinsed and dried. They were polarized in bromine trifluoride at +3.00 volts with respect to a platinum reference electrode, with a platinum counter electrode of a size identical to the test electrode spaced 5 mm away. The anodic current was measured as a function of time. The experiment was repeated with a chemically passivated test electrode.

Figure 40 shows the data for stainless steel 316 electrodes. The upper curve is for an unpassivated electrode, and the lower curve was obtained for an electrode passivated for 18 hours in chlorine trifluoride vapor at one atmosphere pressure and room temperature.

Figure 41 gives data obtained for Monel electrodes under similar circumstances, except that one Monel electrode was passivated in fluorine for 18 hours at one atmosphere total pressure at room temperature. The curves are very similar. The passivated electrode actually yielded a slightly greater current density.

In addition to the experiment in which the anodic current was measured as a function of time at a constant polarising voltage, polarisation curves were run on the working electrodes. Tests with nickel were on electrodes in conditions indicated at points marked A and B in Figure 39. The polarization curves are given in Figure 42. Curve A was obtained on the unpassivated nickel electrode following the two hours of constant polarization along Curve II of Figure 39, while Curve B was obtained following one hour of polarization along Curve III of Figure 39. Anodic polarization experiments were conducted on 316 stainless steel and Monel 400 in BrF_3 at 25°C. The data are plotted in Figures 43, 44, and 45. These experiments revealed electrochemical reactions occurring on the electrode materials. The polarization test subjects a metal electrode to a constant potential,

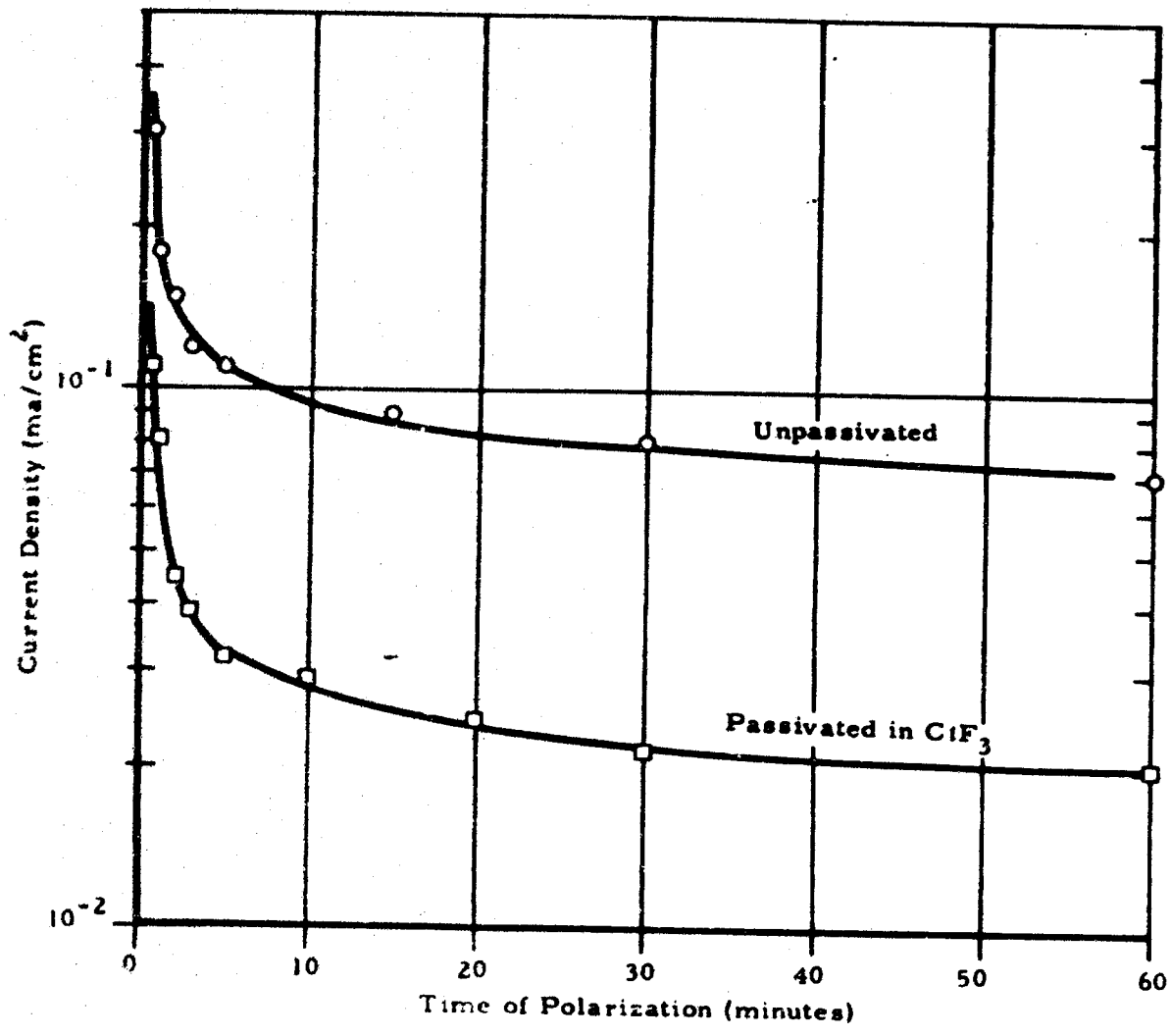

Figure 40. Anodic Current Density Curves for Stainless Steel 316 in BrF_3 – 25°C (77°F), Constant Polarization at +3.00 Volts

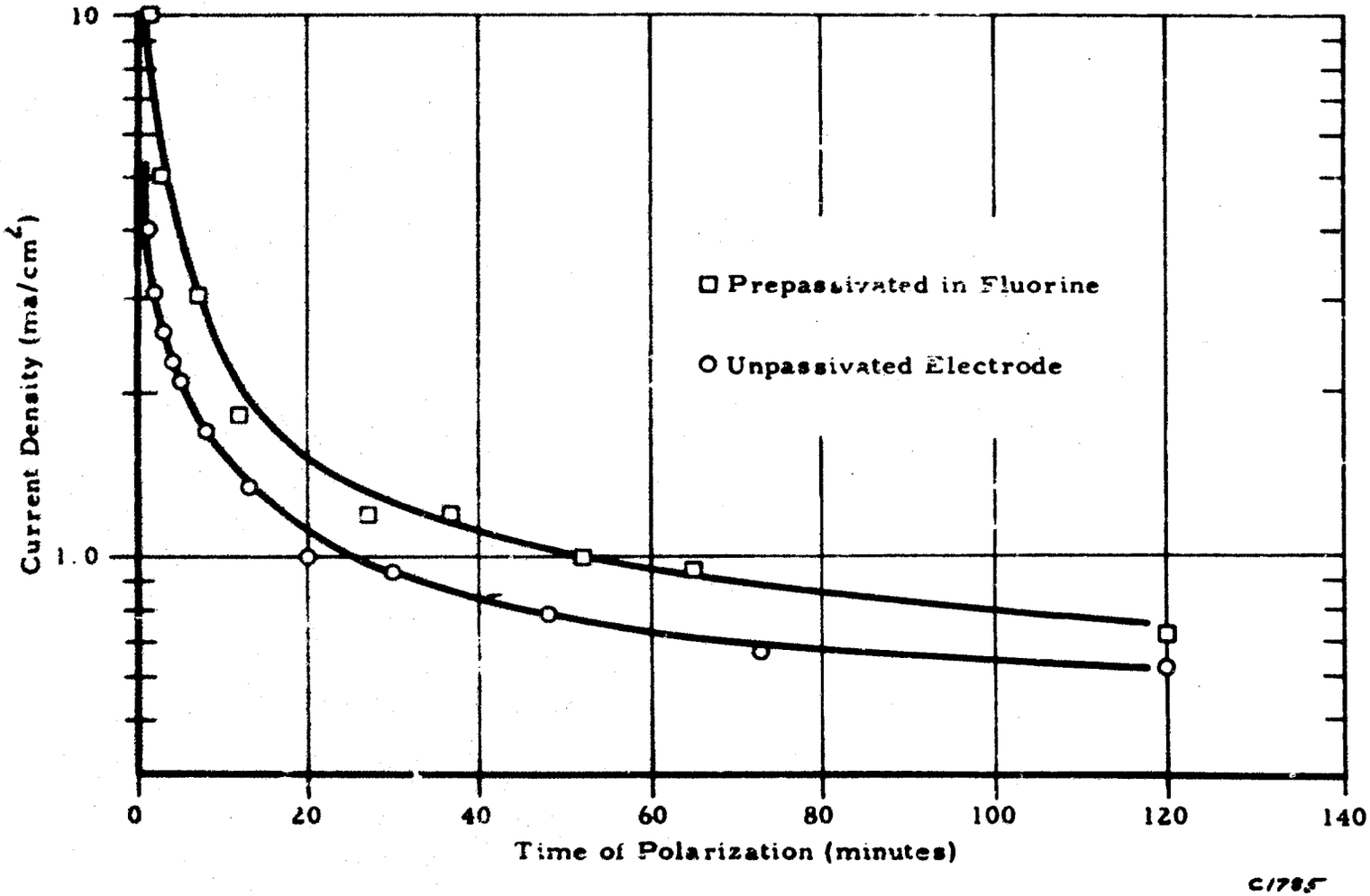

Figure 41. Anodic Current Density Curves for Monel in BrF_3 -- 25°C (77°F), Constant Polarizing at +3.00 Volts

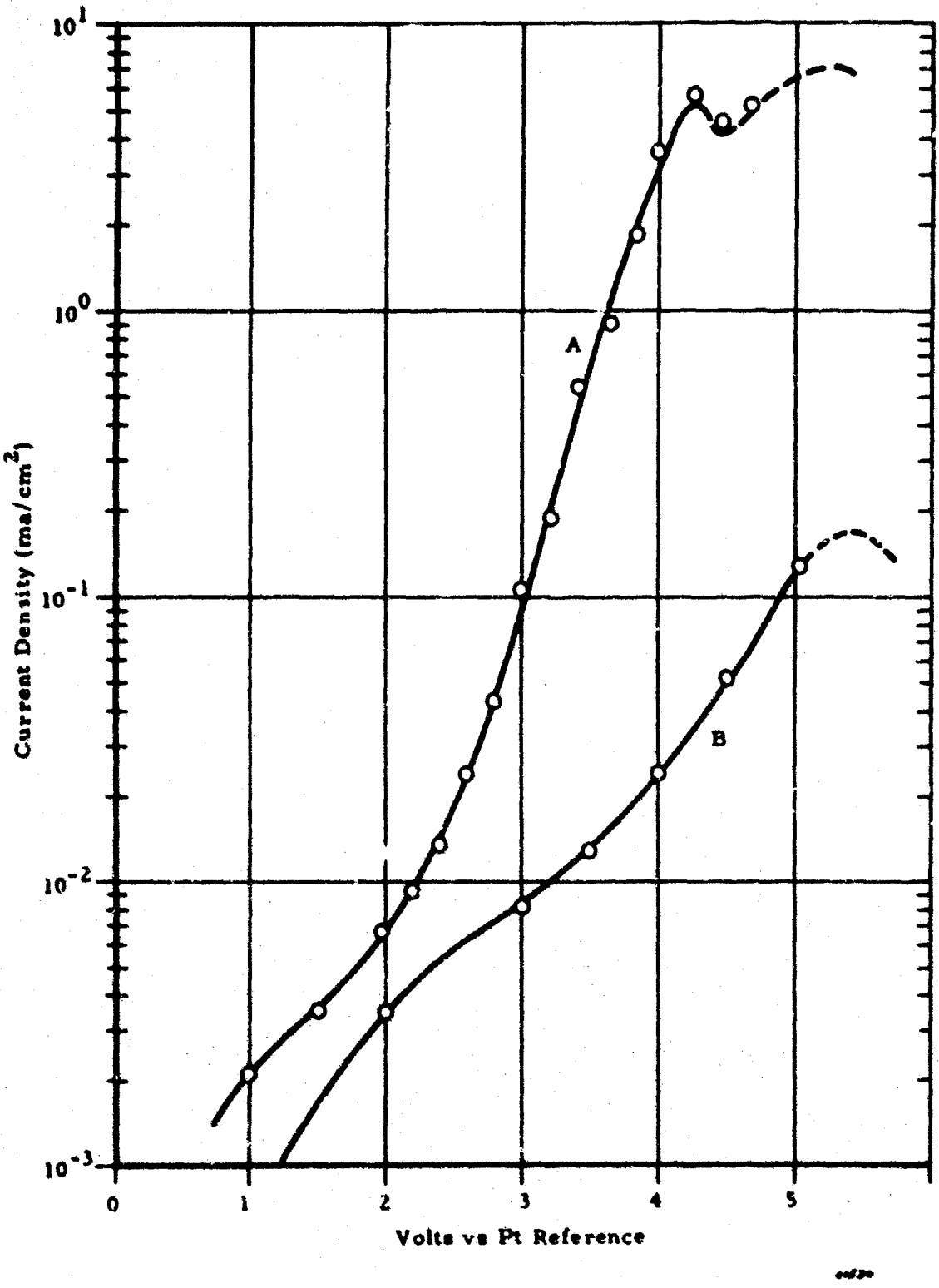

Figure 42. Polarization Curves of Passivated Nickel Electrodes in BrF_3

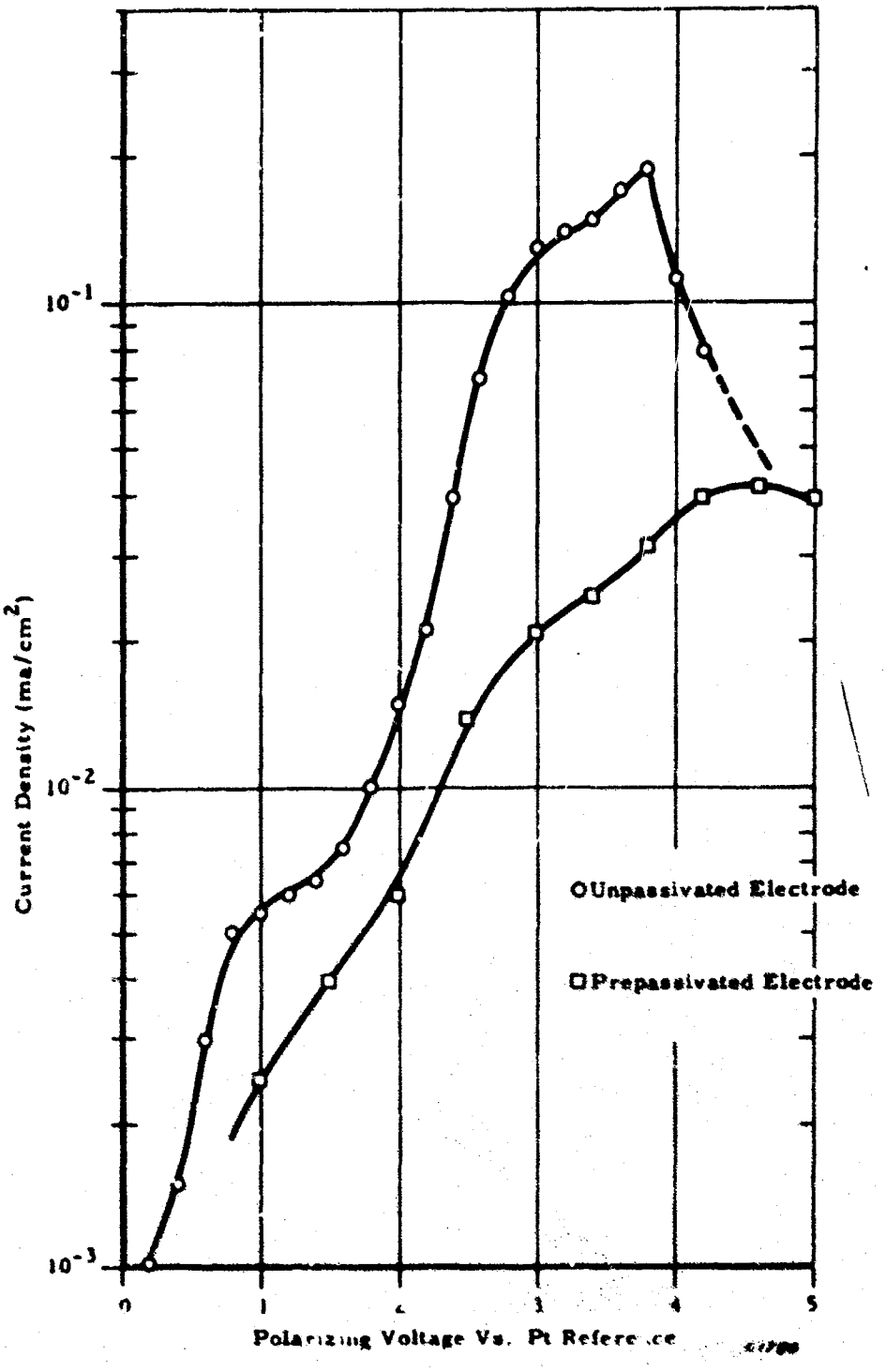

Figure 43. Polarization Curves for Stainless Steel 316 – BrF_3 at 45°C (77°F)

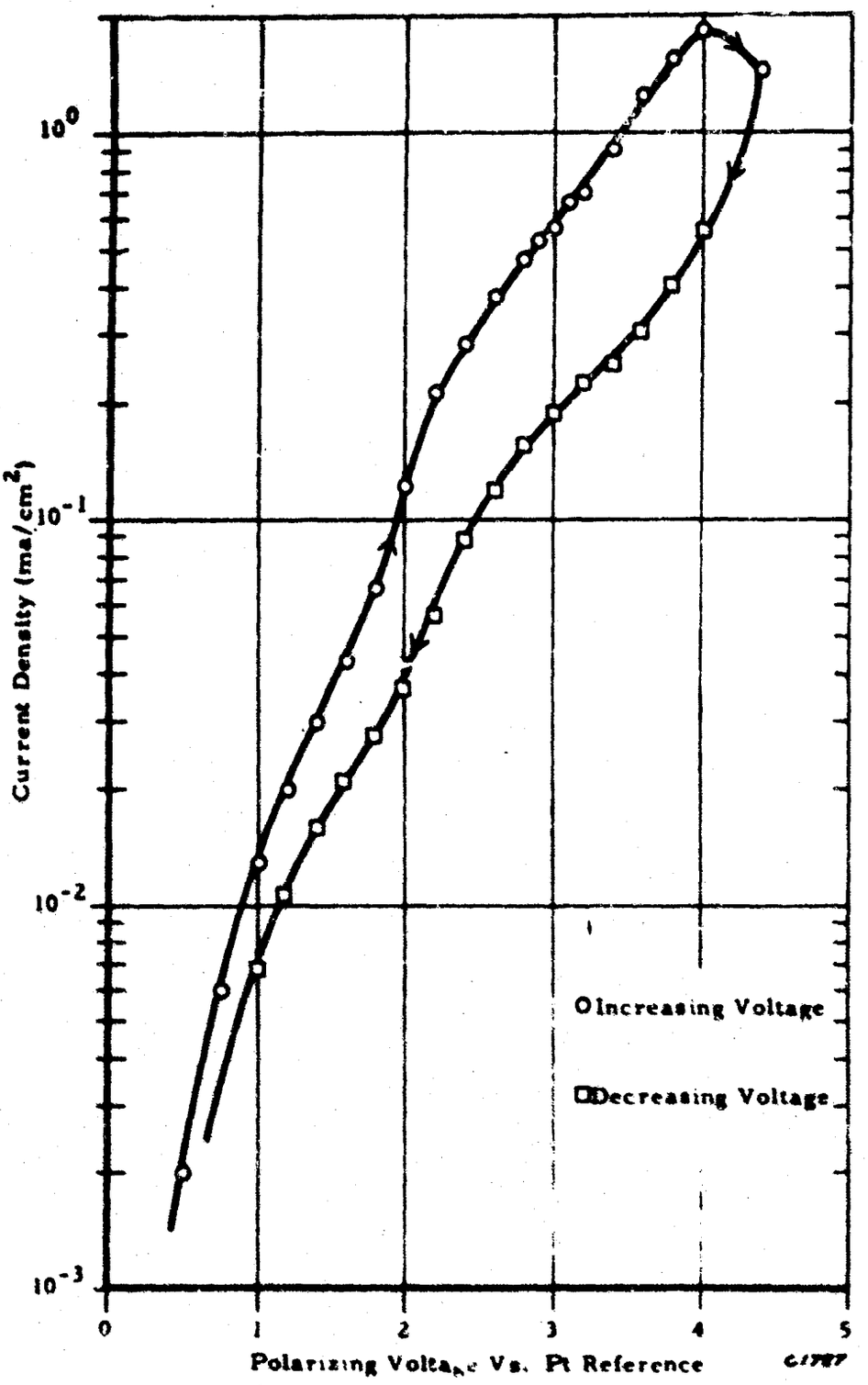

Figure 44. Polarization Curve for Monel – BrF_3, 25°C (77°F). Unpassivated Electrode

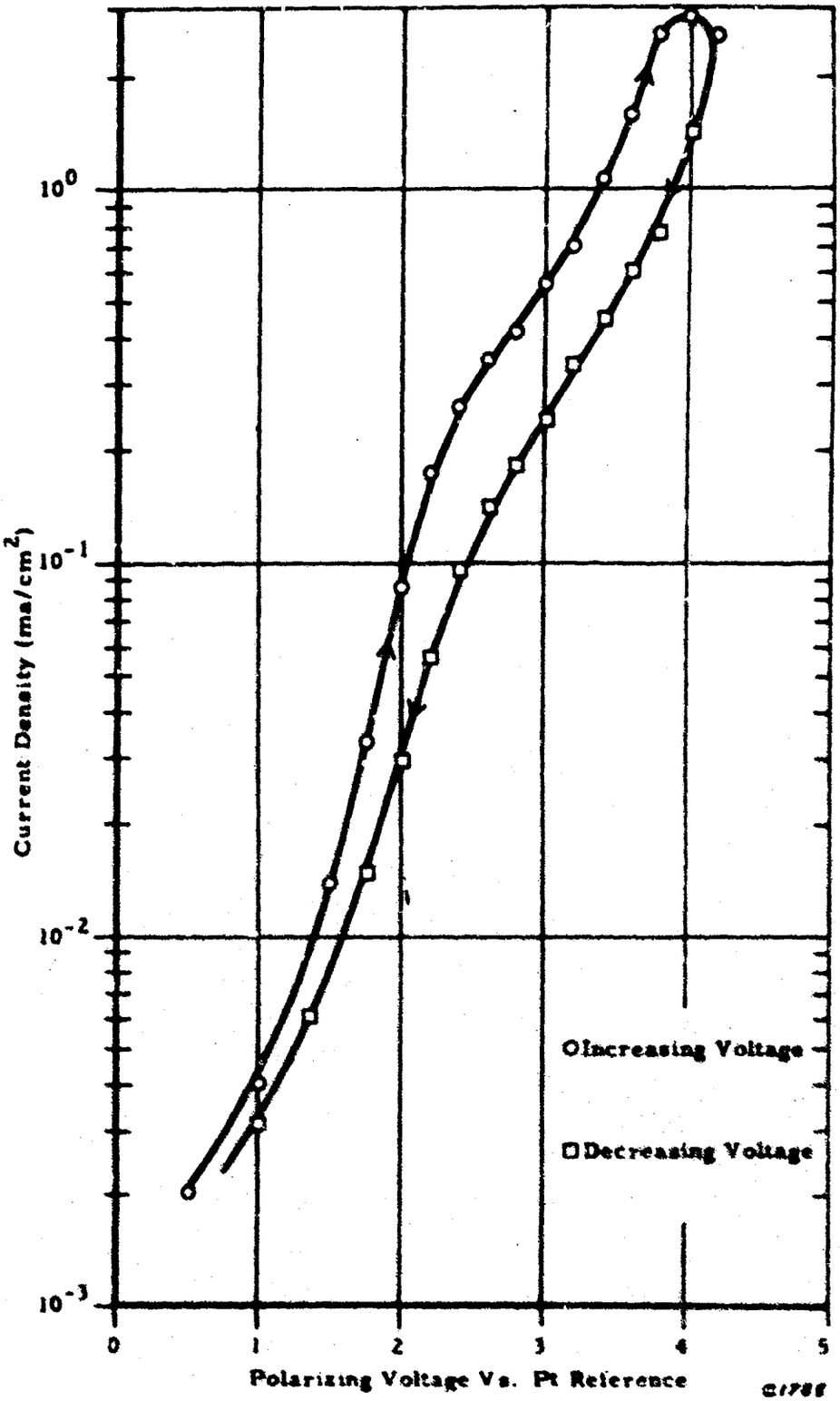

Figure 45. Polarization Curve for Monel in BrF_3. 25°C (77°F). Passivated Electrode

then the current is measured after one or two minutes. Potential steps of 0.20 volts are taken over the voltage range of interest. The apparent current density at each voltage, i, is calculated on the basis of the total electrode area. The anodic polarization curve of unpassivated 316 stainless steel reveals that two anodic reactions take place. They are represented by Tafel slopes, $b_1 = 0.90$, and $b_2 = 0.70$ (see Figure 46). This means the total current density I_D is equal to the sum of the anodic currents of two reactions.

$$I_D = i_1 + i_2$$

When 316 stainless steel is passivated by ClF_3, the anodic polarization curve is altered. The Tafel slope, $b_2 = 0.70$, is no longer observed. See the lower curve of Figure 43.

The passivation treatment has produced a more corrosion-resistant metal surface on which a different anodic reaction occurs. The Tafel slope for this polarization curve is not well defined. However, the current densities taken at 3.0 volts from the polarization curves for unpassivated and passivated 316 stainless steel agree with the limiting current densities reached with time according to Figure 40.

The Tafel slope, b_2, for unpassivated nickel 200 is the same as, b_2, for unpassivated 316 stainless steel. The polarization curve of F_2-passivated nickel behaves similarly to ClF_3-passivated 316 stainless steel. The Tafel slope, b_2, for unpassivated and F_2-passivated Monel 400 were the same and equal to 0.6 volt (Figures 44 and 45). Therefore, one does not expect a great difference in corrosion behavior between the untreated and surface-treated Monel 400 electrodes. The limiting current densities reached with time at 3.00 volts for the Monel 400 electrodes in BrF_3 were not too far apart (Figure 41). The polarization curves of both unpassivated and passivated Monel 400 suggest at least three anodic reactions — one below $i = 10^{-3}$ ma/cm^2, another between $i = 10^{-2}$ to 10^{-1} ma/cm^2, and the third above $i = 10^{-1}$ ma/cm^2 (see Figures 44 and 45). Two or more anodic reactions occurred on the metal electrodes investigated in BrF_3 in both unpassivated and passivated conditions. These electrode reactions have not been diagnosed, and interpretation of experimental data has to be based on simple reactions. It is possible that various slopes are related to the appearance or reaction of some other bromine fluoride species with electrode surfaces.

a. Electrode Flexing Experiments

It has been demonstrated above that there is a comparatively large difference in anodic current density between polarized nickel 200 electrodes before and after passivation in fluorine gas for 24 hours. For example, the current density when polarized in BrF_3 at +3.0 volts was approximately 30 to 50 times greater before passivation in fluorine.

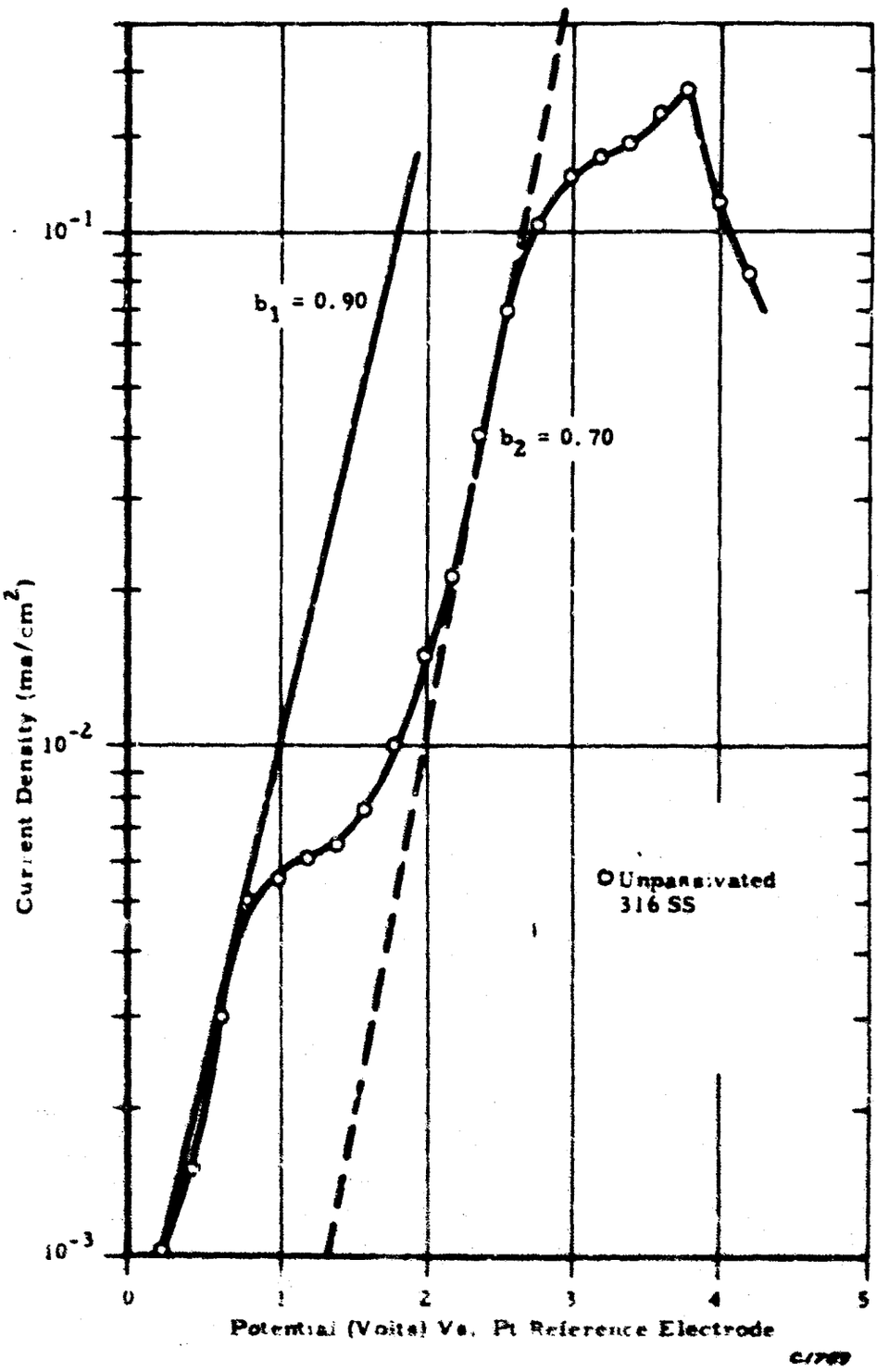

Figure 46. Tafel Slopes – Unpassivated Stainless Steel 316 Electrode

It was thought that use might be made of this observation in testing the stability of fluorine films on metal surfaces with respect to cracking and flaking away from the base metal. Accordingly, a nickel 200 foil strip 5 x 80 mm in size was formed into a tightly convoluted electrode as depicted in Figure 5 (Section 3). The electrode was passivated for 24 hours in fluorine, then the cell was filled with BrF_3 electrolyte. The electrode was polarized at +3.00 volts with respect to a platinum counter electrode as shown in the figure. After about one hour when the current density had stabilized at a low value, conforming to the lower curve of Figure 39, the electrode was extended, thus partially straightening out the loops of the convolutions. There was no evidence of any momentary or permanent increase in current density which would have been indicative of rupture or cracking of the passivation film. While the negative results is not conclusive, it implies that there was little disruption of the film, or that the involved area of the electrode was much too small for detection. It may be noted from Figure 39 that the initial current density of an unpassivated electrode can approach a value 200 to 300 times that of the current density at the time the electrode was flexed. The test was repeated with Monel 400 and copper electrodes with the same negative results.

7. ELECTRON DIFFRACTION ANALYSIS

Electron diffraction studies were carried out to characterize the fluoride films formed on metal surfaces by exposing the samples to fluorine gas or interhalogen compound only, or to fluorine gas followed by humid air. For each sample, 20 to 30 areas (approximately 7000 sq. micron) were selected for reflection diffraction analysis. The typical patterns observed are described below. It should be noted that a limited number of diffraction patterns were computed and slight variations in the relative amounts of components were observed because of surface heterogeneity.

a. Exposure to Fluorine

Metal samples were exposed to the following treatments:

1. Samples A: Samples exposed to fluorine gas at one atmosphere for one hour at 80°F, stored in vacuum before analysis (Copper Sample A_{Cu}, aluminum alloy 2024 Sample A_{Al}, nickel 200 Sample A_{Ni}, Monel 400 Sample A_M, Stainless Steel Type 316 Sample A_{ss}).

2. Samples B: Samples A exposed to air at 80°F, 50% relative humidity for two days (B_{Cu}, B_{Al}, B_{Ni}, B_M, and B_{SS}).

3. Samples C: Samples B re-exposed to fluorine gas at one atmosphere fo one hour at 80°F (C_{Cu}, C_{Al}, C_{Ni}, C_M and C_{SS}).

4. Samples D: Samples exposed to fluorine gas at one atmosphere for one hour at 200°F and stored at vacuum. (D_{Cu}, D_{Ni}, D_M)

(1) Copper Samples

When a copper sample was exposed to fluorine and never exposed to air (Sample A_{Cu}), a rather thin crystallized fluoride coating was found, as inferred from the fact that diffraction patterns of the copper substrate predominated and overshadowed the fluoride patterns. The prominence of the copper patterns increase during electron beam irradiation indicating that a non-crystalline fraction of the fluoride film was gradually decomposed or evaporated during the beam treatment. Diffraction of copper oxides, hydroxides, and the following fluorides was observed: $Cu(OH)F \cdot CuF_2$, $CuF_2 \cdot 2H_2O$ and occasionally CuF_2 (see Table XI and Figure 47). Insignificant changes were noted after exposure to dry air for 15 minutes. After two days exposure to air of 50% relative humidity (Sample B_{Cu}), fluoride patterns became less prominent and two additional diffraction rings were noted, indicating small crystals (less than 100 Å diameter) of Cu_2O and CuO (see Table XII and Figure 48). In certain samples exposed to moisture, thicker and non-uniform chemical films were noted as inferred by less prominent copper lines.

TABLE XI. COMPUTED DIFFRACTION PATTERN OF SAMPLE A_{Cu} AND REFERENCE LINES FOR THE COMPOUNDS IDENTIFIED (Principal Lines are Underlined)

Specimen			ASTM Reference Patterns					
1	2	3	Cu	$CuF_2 \cdot 2H_2O$	$Cu(OH)F \cdot CuF_2$	$Cu(OH)_2$	CuF_2	$6CuO \cdot Cu_2O$
5.14	5.14					5.30		
4.75	4.53	4.75		4.78				
4.32	4.32				4.22			
4.05	4.05							4.04
3.93	3.92							
	3.71	3.80		3.71	3.54	3.75		
3.50	3.47				3.45			
3.24	3.24			3.15			3.22	3.13
		2.95		2.98				2.90
2.71	2.71	2.71		2.71	2.71	2.64	2.82	
2.64					2.61		2.66	
	2.58	2.59		2.55	2.58	2.51	2.53	2.50
	2.49	2.43			2.47			2.47
2.36	2.40			2.35	2.34	2.36	2.39	
	2.21			2.29	2.25	2.26		
2.16	2.16	2.16		2.18	2.20		2.21	
2.00	2.09	2.02	2.09	2.02	2.10	2.08	2.04	2.05
1.83	1.89	1.88	1.81	1.85	1.87		1.82	1.88
1.73	1.70	1.63		1.70	1.72	1.73	1.77	
		1.58					1.69	1.58
1.54	1.45	1.43		1.43	1.43	1.45	1.51	
1.12	1.32		1.27			1.29	1.20	1.25
	0.90		0.90					

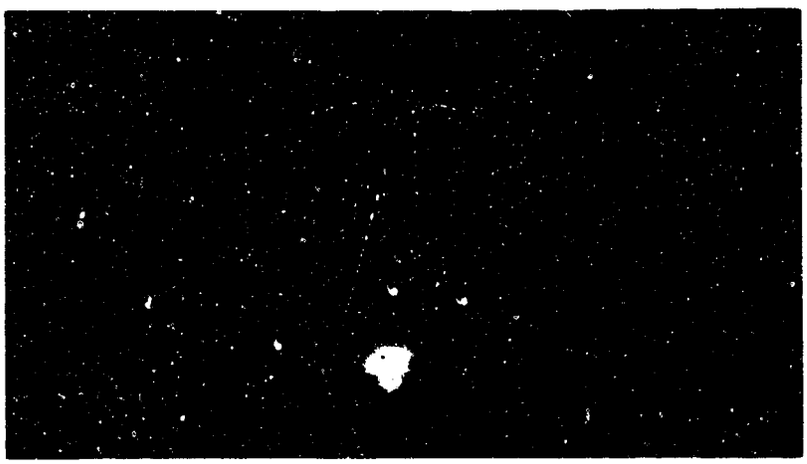

C2094

Figure 47. Reflection Diffraction Pattern of Sample A_{Cu} Note specimen shadow at the lower part of the Figure. Distinct rings originate from copper substrate. Spot pattern (marked by commas) inside the smallest circle show d-spacings characteristic of $CuF_2 \cdot 2H_2O$.

TABLE XII. COMPUTED DIFFRACTION PATTERNS OF SAMPLE B_{Cu} AND REFERENCE LINES FOR THE COMPOUNDS IDENTIFIED (Principal Lines are Underlined)

Specimen 1	ASTM Reference Patterns				
	Cu	Cu(OH)F	$6CuO \cdot Cu_2O$	Cu_2O	CuO
4.58		4.68			
3.07			3.13	3.02	
2.88			2.90		2.75
2.50		2.55	2.50	2.47	2.53
2.42		2.43	2.47		
2.09	2.09	1.97	2.05	2.13	1.96
1.83	1.81	1.83			
1.50		1.51	1.58	1.51	1.50

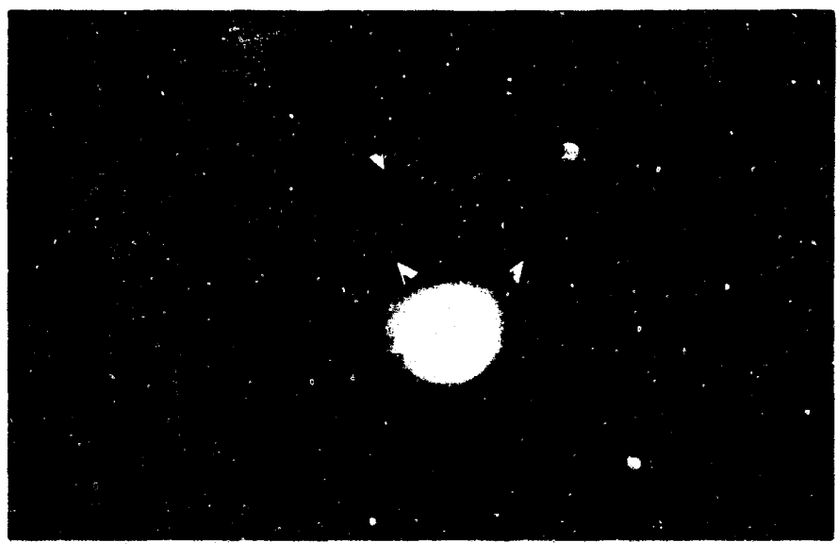

c2096

Figure 48. Reflection Diffraction From the Surface of Sample B_{Cu}. Note less prominent copper rings. Hydrolytic oxidation products of the copper fluorides are identified mainly as two new CuO and Cu_2O rings, pointed out by arrows, and disappearance of the $Cu(OH)F \cdot CuF_2$ pattern.

When the exposure to fluorine was carried out at higher temperatures (200°F, Sample D), the fluoride diffraction patterns consisted of spotty rings indicating a uniformly distributed copious amount of small crystals (see Figure 49). The major fraction of fluoride was identified as $Cu(OH)F \cdot CuF_2$. Some CuF_2 and also $Cu(OH)_2$ were found in certain areas (Table XIII).

When the sample exposed to fluorine and moist air was re-exposed to fluorine (Sample C_{Cu}), a thicker fluoride coating was formed, as inferred by disappearance of the copper substrate diffraction patterns and appearance of $CuF_2 \cdot 2H_2O$ and $Cu(OH)F \cdot CuF_2$ patterns with higher intensity (Figure 50 and Table XIV).

It was also found that sheet samples and powder samples exposed to fluorine and moist air exhibited diffraction patterns of similar composition. The copper sheet samples studied in detail showed that the formation of a passive film by fluorination of surface oxide and hydroxide coatings had not been completed in the period of exposure to fluorine. This is in agreement with the observations, in which it was noted that fluorine uptake by copper was not complete after one hour at room temperature and one atmosphere pressure of GF_2.

The increase in Cu_2O and CuO after exposure to humid air is in accord with the data from fluorine uptake experiments. It is interesting that the $Cu(OH)F$ pattern decreases as much or more than the $CuF_2 \cdot 2H_2O$.

(2) Aluminum Alloy, Nickel, Monel and Stainless Steel Samples

The electron diffraction patterns for aluminum alloy (Sample A_{Al}) exposed to fluorine gas and stored in vacuum are given in Table XV.

Aluminum metal, AlF_3, $Al(OH, F)_3$ and $AlF_3 \cdot 3H_2O$ were identified. Additional aluminum oxide (Al_2O_3) lines were found in Sample (B_{Al}) which was exposed to 50% humid air. Re-exposure of this sample to fluorine (Sample C_{Al}) did not significantly change the diffraction patterns except the Al_2O_3 patterns were not observed. Instead additional $Al(OH, F)_3 \cdot 6H_2O$ was found.

Nickel 200 samples exposed to fluorine gas and stored in vacuum (Sample A_{Ni}) exhibited Ni metal, NiO, and $NiF_2 \cdot 4H_2O$ patterns (see Table XVI). The fluoride films are not structurally homogeneous, and exhibit variations in crystal habit and composition. Figure 51 illustrates variations of diffraction patterns in different areas resulting from these inhomogeneities. Samples exposed to fluorine at 200°F (Sample D_{Ni}) exhibited some additional nickel hydroxide lines NiO (OH), $Ni(OH)_2$, $Ni_3O_2(OH)_4$ (see Table XVII). Exposure of the fluorine treated samples at room temperature to humid air produced additional lines of $Ni(OH)_2$ and NiO(OH). Re-exposure of these samples to fluorine appeared to eliminate hydroxide lines. The secondary reaction with additional fluorine following exposure of the passive surface to humid air produces prominent single crystals which

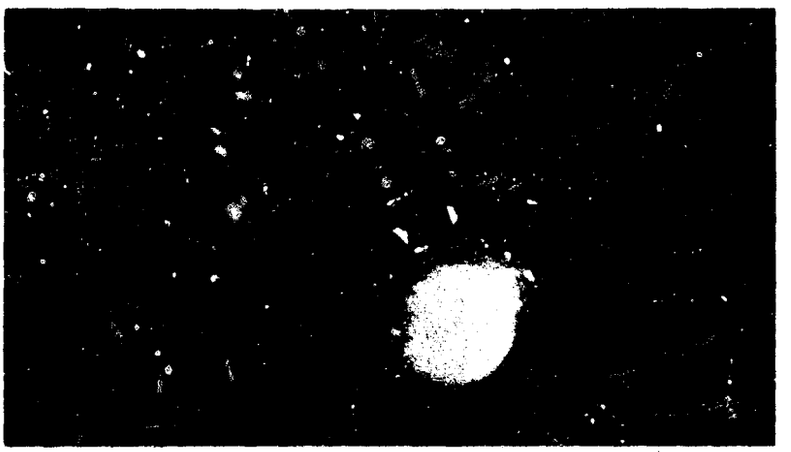

C2096

Figure 49. Reflection Diffraction From the Surface of Sample D_{Cu}, Fluorinated at 200°C. A prominent ring (marked by arrows) appears close to the center. The computed d-spacing indicates $Cu(OH)F \cdot CuF_2$; the intensity of the diffracted beam indicates copious amounts of the crystalline fraction.

TABLE XIII. COMPUTED DIFFRACTION PATTERNS OF SAMPLE D_{Cu} AND REFERENCE LINES FOR THE COMPOUNDS IDENTIFIED (Principal Lines are Underlined)

Specimen			ASTM Reference Patterns			
1	2	3	Cu	$CuF_2 \cdot 2H_2O$	$Cu(OH)F \cdot CuF_2$	$Cu(OH)_2$
4.80	4.75	4.70		4.78		
4.20	4.17	4.17			4.22	
		4.00				
		3.93				
3.65	3.76	3.70		3.71		3.75
3.50	3.50	3.50			3.54	
2.92				2.98		
2.70	2.73	2.88				2.86
	2.54	2.64		2.71	2.71	2.64
2.19	2.18	2.18		2.18	2.20	2.26
		2.06	2.09	2.02	2.10	2.08
	1.74	1.75	1.81	1.75	1.77	1.73

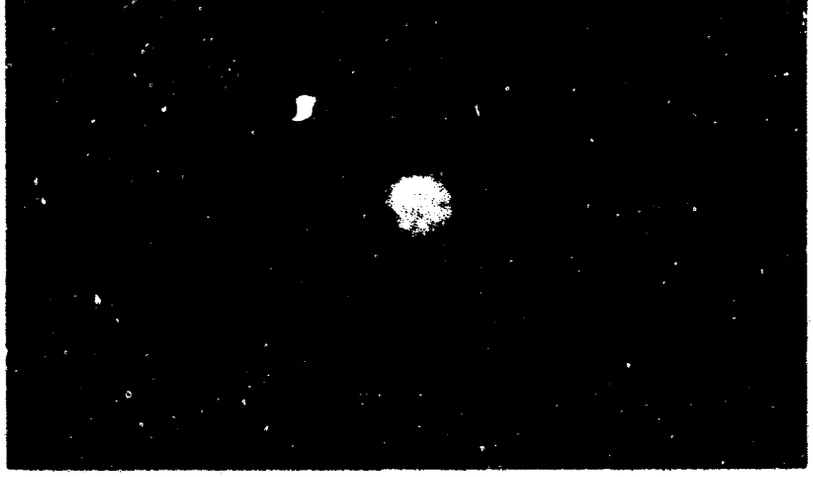

c2097

Figure 50. Reflection Diffraction of Sample C_{Cu}. Note the disappearance of copper patterns and the prominence of spot patterns of $CuF_2 \cdot 2H_2O$ and $Cu(OH)F \cdot CuF_2$.

TABLE XIV. COMPUTED DIFFRACTION PATTERNS OF SAMPLE C_{Cu} AND REFERENCE LINES FOR THE COMPOUNDS IDENTIFIED (Principal Lines are Underlined)

Specimen		ASTM Reference Patterns					
1	2	$CuF_2 \cdot 2H_2O$	$Cu(OH)F \cdot CuF_2$	$Cu(OH)_2$	$2CuO \cdot Cu_2O$	Cu_2O	CuO
4.75		4.78					
4.32			4.22				
4.17							
4.05					4.04		
3.90		3.71					
2.53	2.56	2.55	2.58	2.55	2.50		2.53
2.46	2.47		2.47		2.47		
2.40		2.35	2.34	2.34			2.32
2.16	2.20	2.16	2.20	2.14		2.12	
	2.10						
1.85	1.87	1.85	1.87	1.88	1.88		1.87
1.69	1.72	1.70	1.70				1.71
1.66			1.63				
1.56		1.55	1.55		1.55		1.55
1.50	1.51	1.52	1.51	1.49		1.51	1.50
1.48	1.49	1.43	1.43	1.44	1.48		
1.39	1.41		1.41		1.43		1.41
1.35				1.36			1.37
1.23				1.26	1.25	1.23	1.26
1.16				1.21	1.24		1.16
1.02					1.06	1.06	1.07
0.89					1.02	0.87	0.90

TABLE XV. COMPUTED DIFFRACTION PATTERN OF SAMPLE A_{Al} AND REFERENCE LINES FOR THE COMPOUNDS IDENTIFIED (PRINCIPAL LINES UNDERLINED)

Specimen						
1	2	3	Al	$Al(OH,F)_3.6H_2O$	$AlF_3.3H_2O$	AlF_3
		6.75	0.00			
	5.70			5.70		
5.15					5.45	
		4.45				
	4.30					
4.16					3.86	
		3.45			3.65	3.52
3.24					3.33	
				2.98	3.04	
				2.84		
2.63		2.70			2.73	
					2.65	
2.50	2.40	2.47		2.46	2.51	2.51
					2.44	
2.30	2.36	2.35	2.34	2.26		
2.22		2.15			2.19	
					2.11	2.12
2.12	2.05		2.02	2.01	2.03	
1.82		1.84		1.89	1.93	
					1.85	
1.70	1.79	1.77		1.74	1.78	1.76
	1.64			1.66	1.67	1.60
				1.55	1.56	1.56
1.48	1.47			1.48	1.52	
1.40	1.26	1.37	1.43	1.42	1.43	1.46
				1.38		1.36
1.30	1.30			1.28		1.26
1.26	1.21		1.22	1.23		1.23
1.21						1.18
	1.17		1.16			1.16
1.12	1.12	1.12				1.12
1.09	1.10					1.07
0.98	0.98	0.99	1.01			
0.84	0.86		0.90			

TABLE XVI. COMPUTED DIFFRACTION PATTERNS OF SAMPLE A_{Ni} AND REFERENCE LINES FOR THE COMPOUNDS IDENTIFIED (PRINCIPAL LINES UNDERSCORED)

Specimen									
1	2	3	4	5	6	NiO	$NiF_2 \cdot 4H_2O$	NiF_2	Ni
	5.25								
			5.0						
			4.9						
4.8	4.8						4.85		
	4.07						4.10		
3.97		3.97	4.0		4.0		3.98		
			3.33					3.31	
3.19	3.18								
				3.07	3.0		2.98		
2.76	2.71		2.70	2.66			2.75		
2.58		2.57	2.67					2.56	
		2.43	2.45	2.52	2.47	2.41			
	2.33		2.35	2.35			2.31		
2.23					2.18		2.22	2.23	
2.03		2.06	2.0	2.10		2.09	2.00		2.03
1.90	1.92	1.94		1.86	1.91		1.88		
		1.83	1.81						
1.75	1.65	1.75	1.67	1.67	1.67			1.72	1.76
	1.61		1.60	1.57	1.60		1.59	1.65	
	1.55	1.52			1.57	1.48	1.49	1.52	
1.46		1.46	1.45	1.44			1.44		
1.37		1.36		1.33	1.31		1.31	1.39	
		1.21			1.25	1.26	1.26	1.26	1.25
1.19		1.18		1.17	1.17		1.19		
1.14		1.13	1.14						
1.09		1.10	1.11	1.09	1.12		1.12	1.12	1.06
1.04		1.01	1.02		1.02				1.017
1.02									
0.95			0.98	0.98	0.97	0.96			
						0.93			0.88

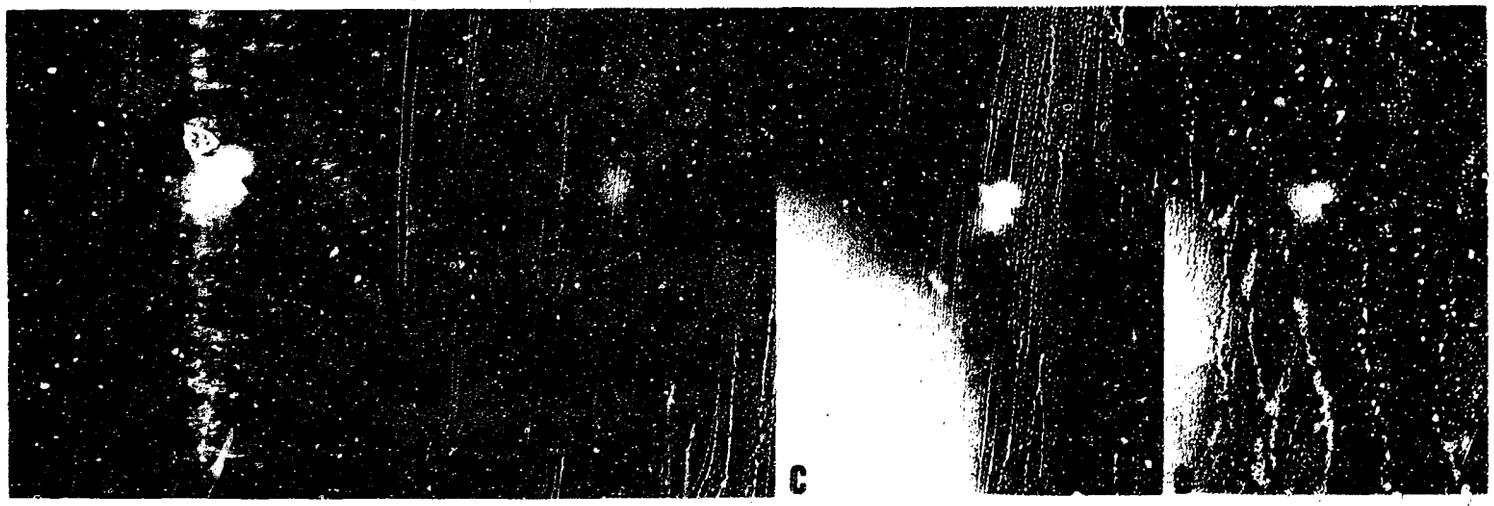

Figure 51. Reflection Diffraction from the Surface of Sample A_{Ni} in Four Areas of 7000 Sq. Micron. Note prominent single crystal pattern in A with a diffuse ring pattern in the background. B shows both ring patterns, characterized by randomly distributed crystals, and characteristic single crystal spot patterns. C and D depict rows of diffraction spots indicating whisker type crystals.

TABLE XVII. COMPUTED DIFFRACTION PATTERNS OF SAMPLE D_{Ni} AND REFERENCE LINES FOR THE COMPOUNDS IDENTIFIED (Principal Lines Underlined)

Specimen						Ni	NiF_2	$4Ni(OH)_2 \cdot NiO(OH)$	$NiF_2 \cdot 4H_2O$	NiO	$Ni(OH)_2$	γNiO(OH)	βNiO(OH)	$Ni_3O_2(OH)_4$
1	2	3	4	5	6									
								7.7				6.90		
									4.85				4.83	4.7
4.48		4.44									4.53			
	4.33		4.32											
	4.06	4.11	4.19	4.11					4.10					
3.80			3.82	3.82				3.85						
	3.71	3.42							3.78					
3.0	3.33			3.23			3.31					3.43		
3.23	3.25								3.11					
	2.83			2.96					2.98					
2.75									2.75					
								2.67			2.68			2.63
2.55	2.55	2.50	2.50	2.55			2.56	2.56	2.53					
2.32	2.31	2.36	2.30	2.34					2.44					
					2.32			2.31	2.31	2.41		2.42	2.41	2.42
							2.23		2.22		2.32	2.37		
2.13	2.13	2 13							2.15					
	2.09	2.07				2.03		2.09				2.19		
2.00	2.02	2.09						2.03	2.00	2.09		2.09		
	1.86	1.96							1.88					
1.78	1.82			1.81	1.71	1.76		1.75	1.78			1.86		1.90
1.74	1.73		1.72	1.69			1.72		1.74	1.0		1.77		
1.66	1.62	1.58	1.62				1.65	1.66	1.69-		1.75			
									1.65					
									1.59		1.56	1.57		1.52
1.51	1.51	1.51	1.54	1.51			1.52	1.53	1.49					
								1.50	1.46-44	1.48	1.48	1.47		
1.41	1.47			1.41			1.39	1.42	1.40			1.41	1.40	1.41
1.33	1.33		1.37	1.35				1.32	1.37		1.35	1.37		
1.28	1.30	1.30	1.27	1.30				1.28	1.31		1.33	1.32		
1.20	1.21	1.24		1.24	1.18	1.25	1.26		1.22		1.30	1.30		
1.13	1.10	1.13	1.15	1.11			1.12		1.17	1.26		1.21		
1.11										1.206	1.17	1.17		
1.09	1.08			1.09		1.06			1.16					
									1.12	0.96				
1.01	1.05					1.017				0.93				
0.92		0.96	0.90			0.88				0.85				
						0.81				0.80				
						0.79								

frequently grow away from the surface (see Figure 52).

NiF_2, CuF_2, CuOHF, CuOHF · CuF_2, and $Cu(OH)_2$ were identified on the Monel samples (A_M) after fluorine exposure (see Table XVIII). Figure 53 illustrates the diffraction patterns of a sample treated with fluorine gas without exposure to air. Samples exposed to humid air exhibited additional lines of $Ni(OH)_2$ and eliminated CuOHF · CuF_2 lines. Re-exposure of these air exposed samples to fluorine showed no $Ni(OH)_2$ nor $Cu(OH)_2$ lines but $NiF_2 \cdot 4H_2O$ and Cu(OH)F · CuF_2 lines were observed. Monel samples exposed to fluorine at 200°F indicated NiF_2, Cu(OH)F · CuF_2, $NiF_2 \cdot 4H_2O$, $Cu(OH)_2$ and $CuF_2 \cdot 2H_2O$ (see Table XIX).

Samples of stainless steel Type 316 exhibited FeF_3, $Fe_3F_5 \cdot 3H_2O$, CrF_3, $CrF_3 \cdot 3H_2O$, Ni, $NiF_2 \cdot 4H_2O$, $Ni(OH)_2$ and NiO(OH) lines (see Table XX). $Fe_3F_5 \cdot 7H_2O$ replaced the $3H_2O$ fluoride in the sample exposed to humid air after fluorination.

b. Exposure to Chlorine Pentafluoride and Chlorine Trifluoride

Copper samples (Cu_i) were exposed to ClF_5 for one hour at 80°F at one atmosphere, pumped down at 160°F under vacuum for 30 minutes, sealed off under vacuum and analyzed by reflection diffraction method without exposure to air. The diffraction patterns (Table XXI) indicated the presence of $CuF_2 \cdot 2H_2O$, CuCl and $CuCl_2 \cdot 2H_2O$ on the treated surface.

When the ClF_5 treated sample was exposed to air, 50% relative humidity for 48 hours, reflection electron diffraction analysis showed $Cu(OH)F_2 \cdot CuF_2$, $CuF_2 \cdot 2H_2O$, $Cu_2(OH)_3Cl$ (two crystallographic varieties), $CuCl_2 \cdot 2H_2O$ and CuCl. The incorporation of OH groups into the crystal lattice is noticeable.

Copper samples (Cu_{ii}) also were exposed to ClF_3 gas at 80°F for one hour at one atmosphere, pumped down at 160°F under vacuum for 30 minutes, sealed off under vacuum, and analyzed by reflection diffraction method without exposure to air. $CuF_2 \cdot 2H_2O$ patterns were identified (Table XXII and Figure 54).

When Sample Cu_{ii} was exposed to air of 50% relative humidity for 48 hours at 80°F, formation of blue crystals was noted on the surface (Figure 55). The diffraction pattern was identified as $CuF_2 \cdot 2H_2O$ by selected area electron diffraction (see Table XXIII). These smaller $CuF_2 \cdot 2H_2O$ crystals were randomly distributed over the entire surface. The main fraction of the passivating film consisted of a brown material that was identified as CuF_2 by selected area electron diffraction (Figure 46). The coating film was easily removed by slight mechanical attack, exposing a bright copper surface underneath.

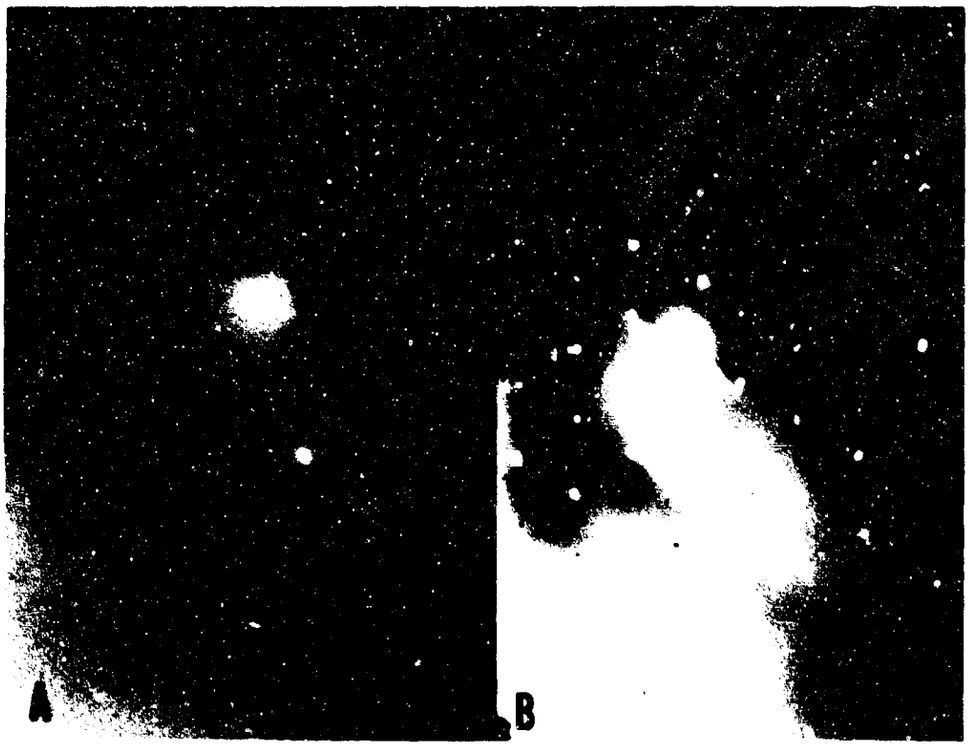

Figure 52. Reflection Diffraction from the Surface of Sample C_{Ni}. The reflection rings are larger in diameter than those in Sample A_{Ni}. Note prominence of diffraction spots from a single crystal and also electron shadow indicating crystals growing away from the surface.

TABLE XVIII. COMPUTED DIFFRACTION PATTERNS OF SAMPLE A_M AND REFERENCE LINES OF COMPOUNDS IDENTIFIED (PRINCIPAL LINES UNDERSCORED)

Specimen				$Cu(OH)_2$	$CuF_2.2H_2O$	NiF_2	CuOHF	$CuOHF.CuF_2$
1	2	3	4					
5.15			5.0	5.30				
4.70	4.70	4.68			4.78		4.68	
								4.22
3.80			3.80	3.75	3.71			
	3.68	3.70						
			3.60					3.54
3.35					3.15	3.31		3.45
		3.20	3.25		3.10			
		3.0			2.98			
		2.94	2.72	2.86	2.71		2.65	2.71
2.58		2.58	2.58	2.51	2.55	2.56	2.55	2.58
	2.45	2.35	2.35		2.35	2.73	2.34	2.34
2.25			2.15		2.18		2.14	2.10
2.10	2.06	2.10	2.10					
	1.96	1.97	2.0		2.02		1.97	1.99
1.89	1.92		1.88		1.96		1.88	1.87
1.78		1.78			1.75	1.72		1.72
1.70	1.62	1.70	1.66		1.70	1.65	1.63	1.70
1.60		1.59	1.58		1.60		1.59	1.63
1.48	1.	1.49		1.48	1.53	1.52	1.51	1.55
1.41		1.46						1.51
1.35	1.34	1.40	1.39			1.39	1.43	1.43
1.25	1.22	1.22	1.30			1.26	1.26	
	1.07	1.10	1.07					
1.04	1.06	1.04				1.12		
0.98	1.0							

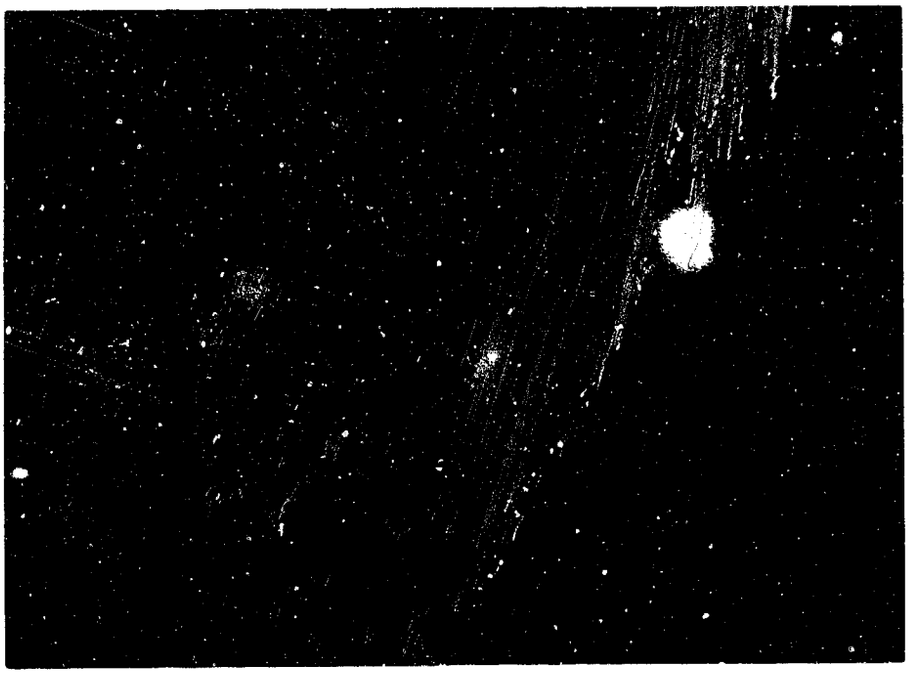

Figure 53. Reflection Diffraction from the Surface of Monel Sample A_M. Note ring patterns as an indication of random distribution of small crystallites in (A) and single crystal diffraction pattern originating from a larger crystal (B). The diffraction spots close to the central beam indicate hydrated compounds with long d-spacings.

TABLE XIX. COMPUTED DIFFRACTION PATTERNS OF SAMPLE D_M AND REFERENCE LINES OF COMPOUNDS IDENTIFIED (Principal Lines Underlined)

Specimen					NiF_2	$Cu(OH)F.CuF_2$	$NiF_2.4H_2O$	$Cu(OH)_2$	$CuF_2.2H_2O$
1	2	3	4	5					
		(6.50)							
				5.40				5.30	
			5.10						
			4.70	4.70			4.85		4.78
	4.30		4.30	4.33		4.22			
			4.05				4.10		
		3.90							
		3.70		3.70			3.78	3.75	3.71
						3.54			
	3.45	3.45				3.45			
	3.20	3.25	3.32	3.32	3.31				
3.08				3.10			3.11		3.10
							2.98	2.86	2.98
2 78			2.86	2.80		2.71	2.75		2.71
2.58	2.58		2.61	2.58	2.56	2.58	2.53	2.64	
2.35			2.45			2.34	2.31		2.35
2.25	2.24	2.30	2.27	2.24	2.23	2.25	2.22	2.26	
	2.14	2.05	2.15	2.15		2.10	2.15		
	2.03	2.0		1.98			2.0		
1.92	1.93	1 93	1.87	1.94			1.88		
		1.82	1.83				1.78		
	1.75	1.75	1.70	1..74	1.72	1.72	1.74		
1.60	1.61	1.66	1.66	1.64	1.65		1.69-1.65		
1.55		1.50	1.58	1.49	1.52		1.49	1.48	1.53
1.44			1.48			1.43	1.46		
1.36	1.38	1.34	1.35	1.38	1.39				
1.27	1.32	1.27	1.26	1.26	1.26		1.31		
1.22			1.22	1.24			1.22		
1.20			1.20				1.17		
1.15	1.12	1.11	1.15		1.12		1.16		
							1.12		
1.05			1.05	1.02					
1.00				1.00					
0.98			0.96	0.95					
	0.93	0.84							

TABLE XX. COMPUTED DIFFRACTION PATTERNS OF SAMPLE A_{88} AND REFERENCE LINES OF COMPOUNDS IDENTIFIED (Principal Lines Underlined)

Specimen						$NiF_2 \cdot 4H_2O$	FeF_3	$Fe_3F_5 \cdot 3H_2O$	$Ni(OH)_2$	NiO(OH)	Ni	$CrF_3 \cdot 3H_2O$	CrF_3
1	2	3	4	5	6								
						4.85	4.82						
				4.70				4.69				4.70	
4.47									4.53				
			4.10			4.10						4.09	4.00
			3.35	3.80		3.78	3.70	3.71					
3.60													3.62
	3.51			3.45						3.43			
3.21	3.21		3.19				3.18	3.22					
				3.10		3.11		3.16				3.09	
				3.0		2.98		2.97					
				2.76		2.75							
							2.66		2.68				
				2.58		2.53						2.59	
2.36	2.30		2.33						2.32	2.37			
				2.25	2.25	2.22							
	2.15				2.17					2.19			
			2.05		2.06		2.07	2.08		2.09		2.04	
2.01			1.96	1.95	2.0	2.0							
1.90	1.90		1.88		1.95	1.88	1.86	1.83		1.88		1.87	
1.78	1.78	1.80	1.76	1.78		1.75	1.75	1.74	1.75	1.77	1.76	1.77	
1.64	1.58		1.60	1.65		1.69	1.65	1.68	1.56	1.57		1.63	1.65
						1.59	1.60	1.61				1.56	
1.49			1.51	1.50		1.49	1.45	1.45	1.48	1.47		1.49	
			1.37									1.46	
1.34		1.36	1.35	1.38		1.37	1.41	1.42	1.35	1.37			
1.29		1.28	1.33			1.31	1.31		1.30	1.32	1.25	1.30	
1.20	1.20		1.20	1.20		1.17			1.17	1.17			
	1.11	1.14			1.15								
1.08	1.08	1.05	1.06	1.06	1.10						1.06		

TABLE XXI. COMPUTED DIFFRACTION PATTERNS FROM SAMPLE Cu_i AND REFERENCE LINES FOR COMPOUNDS IDENTIFIED (Principal Lines Are Underlined)

Specimen				$CuCl_2 \cdot 2H_2O$	$CuF_2 \cdot 2H_2O$	CuCl
1	2	3	4			
5.18				5.4		
		4.70	4.70		4.78	
4.45						
				4.03		
				3.73	3.71	
3.30	3.40		3.26	3.33		3.40
		3.16			3.15	3.21
3.05	3.04			3.08		
	2.94	2.98	2.87		2.98	
2.70				2.72	2.71	
2.59			2.58	2.63	2.55	
2.44		2.45		2.52		
2.30			2.35		2.25	
2.16		2.15	2.27	2.20		
2.06	2.05		2.03			
1.93	1.94	1.96	1.92			1.95
		1.94	1.80	1.85	1.85	
1.72			1.72	1.81	1.75	
1.66	1.67	1.67			1.70	
1.58	1.60	1.64	1.63		1.65	
1.52			1.52		1.55	
1.48			1.46		1.43	
1.42						
1.36		1.32	1.35			
1.13	1.18	1.20	1.18			
1.10		1.12				
1.02	1.05		1.05			
0.98	1.01		1.01			
0.94	0.94	0.86	0.86			

TABLE XXII. COMPUTED DIFFRACTION PATTERNS OF SAMPLE Cu_{11} AND REFERENCE LINES OF COMPOUNDS IDENTIFIED (Principal Lines are Underlined)

Specimen				$Cu(OH, F).CuF_2$	$CuCl_2$	$CuCl_2.2H_2O$	$CuF_2.2H_2O$	$Cu(OH)F.CuF_2$	CuCl
1	2	3	4						
	6.50								
	4.96		5.45		5.70	5.4	(4.82) 4.78		5.4
4.30	4.30	4.55 / 4.25	4.30	4.22				4.31	
						4.03			
	3.27		3.45		3.42	3.73	3.71	3.46	
	3.08		3.15			3.33	3.15		3.33
2.90					2.90	3.08	2.98	2.82	3.00
2.66	2.61	2.58	2.70		2.62	2.72 / 2.63	2.71		2.72 / 2.67
2.48						2.52	2.55	2.56	
		2.44	2.45	2.47				2.49	
2.42					2.36	2.20	2.35	2.34	2.36
								2.14	
1.90	1.95	1.96	1.93	1.87	1.86	1.85	1.85	1.89	1.88
	1.77	1.76			1.80	1.81	1.75	1.79	
1.63		1.70			1.70		1.70	1.72	1.73
			1.66	1.63	1.64		1.65		1.66
1.56	1.53	1.59	1.56		1.58		1.55		
1.53			1.51	1.51	1.49		1.53	1.47	
1.50		1.49		1.43			1.43	1.44	
1.37		1.39	1.38						
1.35	1.3	1.30	1.32						
1.32	1.32								
1.26	1.29	1.29							
1.22	1.27	1.24							
	1.18								
1.13	1.12	1.10	1.14						
1.07	1.08	1.02							
1.03									
0.98		0.99	0.97						
0.96		0.89							

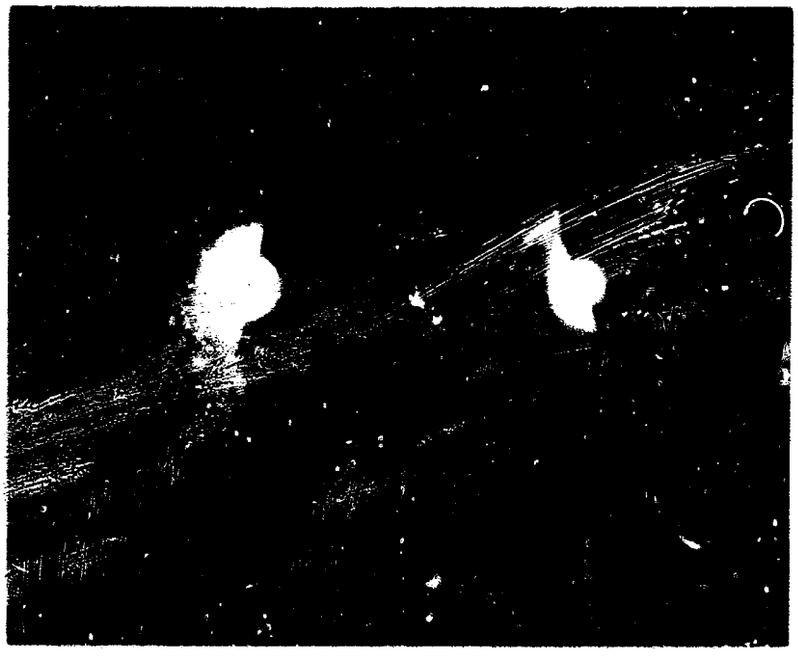

Figure 54. Reflection Diffraction from the Surface of Sample Cu_{ii}. Note superposition of two distinctly different diffraction patterns of materials of submicroscopic crystallite size. The difference in particle size in the two fractions is apparent. $CuF_2 \cdot 2H_2O$ and $CuCl_2 \cdot 2H_2O$ were identified.

Figure 55. Photomicrographs with polarized light of $CuF_2 \cdot 2H_2O$ crystals on the surface of sample Cu_{ii} after exposure to air, 50% relative humidity for 2 days. Magnification 100X.

TABLE XXIII. COMPUTED DIFFRACTION PATTERNS OF SAMPLE Cu$_{ii}$ EXPOSED TO AIR AND REFERENCE LINES FOR COMPOUNDS IDENTIFIED (Principal Lines are Underlined)

Green-Blue Crystals	$CuF_2 \cdot 2H_2O$	Brown Surface Coating		CuF_2
		Sample		
4.65	4.78	1	2	
4.20		3.25	3.22	3.22
3.72	3.71			
3.05	2.98		2.82	2.82
2.70	2.71		2.66	2.66
2.40	2.35		2.53	
			2.39	2.39
2.24	2.18			
			2.21	
2.0	2.02			
		1.91	2.04	2.04
1.8	1.85			
			1.82	1.82
1.7				
			1.77	
1.58	1.60			
1.53	1.58	1.63	1.69	1.69
1.48				
			1.51	1.51
1.42	1.40			
1.24		1.24	1.20	1.20
		1.20		
1.15		1.09		
		0.72		

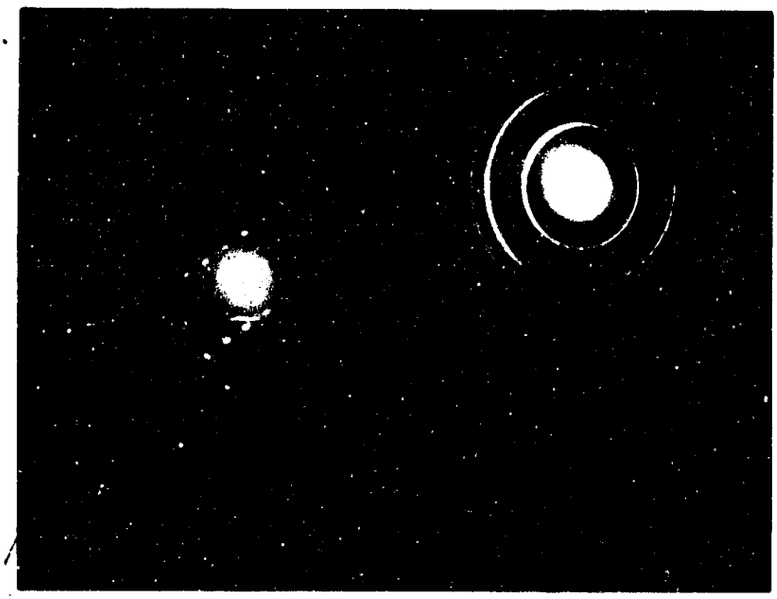

Figure 56. Selected Area Electron Diffraction from Isolated Particles Shown in Figure 55. A indicates $CuF_2 \cdot 2H_2O$ single crystals, and B high degree of crystallinity in the brown matrix film consisting of 100 to 200 Å particles of CuF_2.

SECTION V

SUMMARY AND CONCLUSIONS

The rates of reaction of gaseous fluorine with ten powdered alloys have been determined at 27°C (80°F) by a manometric method. Fluoride film thickness as a function of time up to 4 hours was calculated for each of the alloys, assuming that the reaction takes place between fluorine and the normal oxide film on the metal surface. The fluorination reaction conforms to a logarithmic rate law for all metals investigated, at least in the early stages of the reaction. At longer times of reaction, the fluorination-time curves for aluminum alloys seem to be asymptotic. After reaching an apparent film thickness of about 10 Å, the film ceases to grow. Copper and Monel tend to exceed a logarithmic rate at long exposure times and the film continues to grow linearly at a slow rate of about 1 Å per hour.

The pressure dependence of reaction rate has been investigated for Nickel 200 over the range of fluorine pressure from about 100 to 1100 torr. The reaction rate varies approximately as the cube root of fluorine pressure.

Fluoride film thicknesses formed on the metal powders range from about 6 to 30 Å for exposure times of one hour near one atmosphere and 27°C (80°F). Analysis of the rate date indicate that the mechanism of fluorine attack is consistent with a quantum-mechanical tunneling effect acting as the rate determining factor. The fluoride film is believed to grow at the expense of the oxide film.

The reaction rates of chlorine trifluoride and chlorine pentafluoride with alloy powders were studied by a gravimetric method. Although the data are quite scattered due to experimental difficulties, in general the rates of reaction and fluoride film thicknesses are comparable to those observed with fluorine gas at the same temperature and pressure.

The effect of humid atmosphere exposure on fluoride films was investigated. Powder metal samples were passivated, then exposed to 50% relative humidity in air at 25°C (77°F) for 48 hours. After evacuation, the samples were re-exposed to fluorine and the amount reacting determined manometrically. The effect of moisture on the fluoride films was seen to vary greatly. For 2024 aluminum, there was no detectable secondary fluorination. At the other extreme, copper was observed to take up a very large amount, exceeding that required for the initial passivation of the surface. Nickel 200, 316 stainless steel, and Monel 400 are intermediate and fall in the order shown for increasing secondary corrosion in fluorine. The rate of the secondary attack of fluorine is generally much slower than the rate of initial fluorination, implying a different reaction mechanism.

Electrode polarization studies carried out with Nickel 200 and 316 stainless steel electrodes show that there is a considerable difference in anodic polarization curves before and after passivation. However, polarization curves for Monel before and after fluorine passivation were nearly identical.

Nickel 200, Monel 400, and copper electrodes which had been previously passivated in gaseous fluorine were mechanically flexed while being anodically polarized in bromine trifluoride. There was no detectable increase in anodic current which would have been indicative of a cracking or rupture of the fluoride film.

Reflection electron diffraction analyses of fluorinated metal surfaces have been carried out to identify the composition of various fluoride films formed under different exposure conditions. The surfaces examined have included metal coupons exposed to fluorine gas and vacuum sealed as well as metal coupons passivated in fluorine and then exposed to humid air and also re-exposed to fluorine. Metal coupons (particularly copper) exposed to fluorine and never exposed to air exhibited basic metal fluorides as well as hydrated metal fluorides suggesting that the basic oxides, existing on metal surfaces prior to fluorine exposure, enter into the fluorination reactions. Exposure of passivated surfaces to humid air in general produced additional hydrated metal fluorides. These hydrates appeared to be the cause of secondary fluorination reaction which occurred when air exposure is followed by re-exposure to fluorine. The fluoride films formed by exposure to chlorine trifluoride and chlorine pentafluoride contained metal chloride species, and were more susceptible to hydrated fluoride formation by exposure to humid air.

Reflection electron diffraction analysis also showed that the fluoride films formed on powdered metals and on sheet stock of the same composition were essentially identical. This lends greater weight to contention that the data obtained on powdered metals are comparable to data for bulk or sheet metal specimens.

The following conclusions can be drawn from the observations discussed in detail in Section 4 and summarized above.

1. Passive films formed on metals by exposure to fluorine are more resistant to attack by humid air than films formed by the reaction of halogen fluorides. Thus, fluorine is the most effective agent for passivation of metals.

2. Adequate passive films are formed at all pressures in the range 100 torr to 1100 torr (0.12 to 1.45 atmospheres). Passivation of metal systems at low fluorine pressure is, therefore, economically advantageous provided the system can withstand vacuum. Passivation should be carried out at atmospheric pressure for unevacuable structures.

3. The fluorination reaction to produce a passive fluoride film on metals is generally sufficiently complete in 15 minutes at room temperature. Additional exposure does not improve the protective properties of the film. Passivation procedures should provide a minimum of 15 minutes and maximum of 30 minutes of exposure to fluorine for the most inaccessible portions of a system; inaccessibility being dependent on geometry and diffusion rate of fluorine gas.

4. Copper which has been exposed to fluorine, then to moist air, and then re-exposed to fluorine a second time, reacts at an increased rate with the fluorine and in the exposure times investigated, this rapid rate shows no sign of decreasing. Copper is not desirable in fluorine systems. When it is used, it must be treated to remove the fluoride film and repassivated whenever the fluorinated surface is exposed to moisture.

5. Passive films on stainless steel and nickel, after exposure to humid air, were found to react with fluorine in a typical passivation reaction that was less extensive than the original passivation and which reached completion in a shorter time. Stainless steel and nickel surfaces should be repassivated after exposure to moisture.

6. Passive films on aluminum alloys after exposure to moisture, were inert toward fluorine. Passive aluminum alloy surfaces need not be repassivated after exposure to humid air.

7. Copper and Monel 400 continued to react with fluorine gas over an extended period of time and the apparent film thickness continues to increase slowly. Although no specific investigation was made, there is a possibility that these materials may eventually form thick scales. Additional investigation of this point is needed.

8. A significant difference in anodic polarization behavior of passivated and unpassivated nickel 200 and 316 stainless steel electrodes was demonstrated. This phenomenon might be utilized as a criterion for assessing the quality of passivated surfaces.

9. On the basis of a study of anodic current densities of convoluted nickel 200, Monel 400 and copper electrodes in BrF_3 when flexed, there is no evidence that fluoride films are readily peeled or flaked off the metal during flexure. Repassivation is not necessary when passive metals are subjected to mild physical deformations.

10. Metals in several sizes of subdivision, from bulk solids to powders finer than 300 mesh, were abruptly exposed to fluorine and interhalogen gases at pressures in excess of 1 atmosphere. No ignition reactions were ever observed. This implies that spontaneous ignition of metals of the compositions covered in this investigation is unlikely unless triggered by impurities or impact energy. 100% fluorine can be used for passivation of thoroughly cleaned metal systems. Stepwise increase in concentration is unnecessary.

REFERENCES

1. P. T. Landsberg, J. Chem. Phys., 23, 1955, p. 1079.
2. U. R. Evans, "Pittsburg International Conference on Surface Reactions," 1948, p. 71.
3. U. R. Evans, J. Electrochem. Soc., 91, 1947, p. 547.
4. N. Cabrera and N. F. Mott, Rep. Prog. Phys., 12, 1948-1949, p. 163.
5. P. E. Brown, J. M. Crabtree and T. F. Duncan, J. Inorg. and Nuclear Chem., 1, 1955, p. 202.
6. U. R. Evans, Trans. Electrochem. Soc., 83, 1943, p. 335.
7. P. M. O'Donnell and A. E. Spatkowski, J. Electrochemistry Soc., 111, 1964, p. 633.
8. H. M. Haendler, et al, J. Am. Chem. Soc., 74, 1952, p. 3167; 76, 1954, p. 2177; 76, 1954, p. 2178.
9. S. Kleinberg and J. F. Tompkins, The Compatability of Various Metals with Liquid Fluorine, ADS-TDR-62-250, Air Products and Chemicals, Inc., March 1962.
10. P. M. O'Donnell, Kinetics of the Fluorination of Iron, NASA TN D-3575, August 1966.
11. R. L. Jarry, J. Fischer, and W. H. Gunther, J. Electrochem. Soc., 110, 1963, p. 346.
12. R. L. Ritter and H. A. Smith, J. Phys. Chem., 70, 1966, p. 805.
13. H. J. Emeleus and A. A. Woolf, J. Chem. Soc., 1950, p. 164.
14. R. L. Farrar, Jr. and H. A. Smith, J. Phys. Chem., 69, 1955, p. 763.
15. O. Kubaschewski and B. E. Hopkins, Oxidation of Metals and Alloys. 2nd ed., Academic Press, Inc., New York, N. Y., 1962, pp. 168-179.
16. M. S. Toy, W. A. Cannon and W. D. English, Solution and Conductivity Studies of Fluorine-Containing Oxidizers and Ionic Fluoride Compounds, Douglas Report SM-49121(144F), DA-31-124-ARO(D)-115, Dec. 1965.

17. A. J. Rosenberg, J. Am. Chem. Soc., 78, 1956, p. 2929.

18. O. Kubaschewski and B. E. Hopkins, Oxidation of Metals and Alloys. 2nd ed., Academic Press, Inc., New York, N. Y., 1962, pp. 56-59.

ACKNOWLEDGEMENT OF DISTRIBUTION

This report has been distributed in accordance with the CPIA distribution list dated 10 January 1966.

UNCLASSIFIED
Security Classification

DOCUMENT CONTROL DATA - R&D
(Security classification of title, body of abstract and indexing annotation must be entered when the overall report is classified)

1. ORIGINATING ACTIVITY (Corporate author)
Astropower Laboratory
Missile and Space Systems Division
A Division of Douglas Aircraft Company, Inc.
Newport Beach, California

2a. REPORT SECURITY CLASSIFICATION
UNCLASSIFIED

2b. GROUP

3. REPORT TITLE
Halogen Passivation Studies

4. DESCRIPTIVE NOTES (Type of report and inclusive dates)
Final Report - 1 November 1965 through 31 October 1966

5. AUTHOR(S) (Last name, first name, initial)
W. A. Cannon, W. D. English, S. K. Asunmaa, S. M. Toy, and N. A. Tiner

6. REPORT DATE	7a. TOTAL NO. OF PAGES	7b. NO. OF REFS
November 1966	123	18

8a. CONTRACT OR GRANT NO. AF04(611)-10932
b. PROJECT NO. 3148
c. BPSN 623148
d. Program Structure No. 750G

9a. ORIGINATOR'S REPORT NUMBER(S)
AFRPL-TR-66-330

9b. OTHER REPORT NO(S) (Any other numbers that may be assigned this report)

10. AVAILABILITY/LIMITATION NOTICES
This document is subject to special export controls and each transmittal to foreign governments or foreign nationals may be made only with prior approval of AFRPL (RPPR-STINFO), Edwards, California 93523.

11. SUPPLEMENTARY NOTES

12. SPONSORING MILITARY ACTIVITY
Air Force Rocket Propulsion Laboratory
Research and Technology Division
Air Force Systems Command
Edwards Air Force Base, California 93523

13. ABSTRACT

This report includes data on the nature of passivation of metal surfaces with fluorine and fluorine compounds, the composition of passive films formed, and the deleterious effect of atmospheric moisture on passive surfaces. Fluorination reactions reach completion on stainless steel, nickel and aluminum alloy surfaces very rapidly. The surface films formed range from 5 to 20 Å in thickness and grow at the expense of the oxide films. The apparent film thickness on copper and Monel surfaces continues to increase slowly over an extended period of time. Exposure of passive films to a humid atmosphere produces hydrated metal fluorides which cause secondary fluorination reactions upon reexposure of the surfaces to fluorine. The passive films formed by exposure to chlorine trifluoride and chlorine pentafluoride were comparable in thickness to the films formed by fluorine gas, contained metal chloride species, and were less resistant to humid air attack. Fluorine gas appears to be the most effective agent for passivation of metals. Adequate passive films are formed at all pressures within 0.1 to 1.4 atmospheres for a period of 15 to 30 minutes. Stepwise increase in concentration is unnecessary for passivation of metals, and slight deformation of metal surfaces does not destroy the passive films.

DD FORM 1 JAN 64 1473

UNCLASSIFIED
Security Classification

14 KEY WORDS	LINK A		LINK B		LINK C	
	ROLE	WT	ROLE	WT	ROLE	WT
Fluorine						
Passivation						
Fluorinating Agents						
Fluoride Films, formation						
Fluoride Films, characteristics						
Structural Materials						
Halogen Fluorides						
Aluminum Alloys						
Stainless Steel						
Nickel Alloys						
Copper						
Metal Powders, surface area						
Electrode Polarization, bromine trifluoride						
Electron Diffraction						

INSTRUCTIONS

1. ORIGINATING ACTIVITY: Enter the name and address of the contractor, subcontractor, grantee, Department of Defense activity or other organization *(corporate author)* issuing the report.

2a. REPORT SECURITY CLASSIFICATION: Enter the overall security classification of the report. Indicate whether "Restricted Data" is included. Marking is to be in accordance with appropriate security regulations.

2b. GROUP: Automatic downgrading is specified in DoD Directive 5200.10 and Armed Forces Industrial Manual. Enter the group number. Also, when applicable, show that optional markings have been used for Group 3 and Group 4 as authorized.

3. REPORT TITLE: Enter the complete report title in all capital letters. Titles in all cases should be unclassified. If a meaningful title cannot be selected without classification, show title classification in all capitals in parenthesis immediately following the title.

4. DESCRIPTIVE NOTES: If appropriate, enter the type of report, e.g., interim, progress, summary, annual, or final. Give the inclusive dates when a specific reporting period is covered.

5. AUTHOR(S): Enter the name(s) of author(s) as shown on or in the report. Enter last name, first name, middle initial. If military, show rank and branch of service. The name of the principal author is an absolute minimum requirement.

6. REPORT DATE: Enter the date of the report as day, month, year, or month, year. If more than one date appears on the report, use date of publication.

7a. TOTAL NUMBER OF PAGES: The total page count should follow normal pagination procedures, i.e., enter the number of pages containing information.

7b. NUMBER OF REFERENCES: Enter the total number of references cited in the report.

8a. CONTRACT OR GRANT NUMBER: If appropriate, enter the applicable number of the contract or grant under which the report was written.

8b, 8c, & 8d. PROJECT NUMBER: Enter the appropriate military department identification, such as project number, subproject number, system numbers, task number, etc.

9a. ORIGINATOR'S REPORT NUMBER(S): Enter the official report number by which the document will be identified and controlled by the originating activity. This number must be unique to this report.

9b. OTHER REPORT NUMBER(S): If the report has been assigned any other report numbers *(either by the originator or by the sponsor)*, also enter this number(s).

10. AVAILABILITY/LIMITATION NOTICES: Enter any limitations on further dissemination of the report, other than those imposed by security classification, using standard statements such as:

(1) "Qualified requesters may obtain copies of this report from DDC."

(2) "Foreign announcement and dissemination of this report by DDC is not authorized."

(3) "U. S. Government agencies may obtain copies of this report directly from DDC. Other qualified DDC users shall request through _____."

(4) "U. S. military agencies may obtain copies of this report directly from DDC. Other qualified users shall request through _____."

(5) "All distribution of this report is controlled. Qualified DDC users shall request through _____."

If the report has been furnished to the Office of Technical Services, Department of Commerce, for sale to the public, indicate this fact and enter the price, if known.

11. SUPPLEMENTARY NOTES: Use for additional explanatory notes.

12. SPONSORING MILITARY ACTIVITY: Enter the name of the departmental project office or laboratory sponsoring *(paying for)* the research and development. Include address.

13. ABSTRACT: Enter an abstract giving a brief and factual summary of the document indicative of the report, even though it may also appear elsewhere in the body of the technical report. If additional space is required, a continuation sheet shall be attached.

It is highly desirable that the abstract of classified reports be unclassified. Each paragraph of the abstract shall end with an indication of the military security classification of the information in the paragraph, represented as *(TS)*, *(S)*, *(C)*, or *(U)*.

There is no limitation on the length of the abstract. However, the suggested length is from 150 to 225 words.

14. KEY WORDS: Key words are technically meaningful terms or short phrases that characterize a report and may be used as index entries for cataloging the report. Key words must be selected so that no security classification is required. Identifiers, such as equipment model designation, trade name, military project code name, geographic location, may be used as key words but will be followed by an indication of technical context. The assignment of links, rules, and weights is optional.